UNIVERSITY OF GHANA

IMPACT OF WAVE DYNAMICS ON THE COAST OF GHANA

BY

TRINITY MENSAH-SENOO XORSE

(10203247)

THIS THESIS IS SUBMITTED TO THE UNIVERSITY OF GHANA, LEGON IN PARTIAL FULFILLMENT OF THE REQUIREMENT FOR THE AWARD OF MPHIL OCEANOGRAPHY DEGREE

JUNE 2013

DECLARATION

I Trinity Mensah-Senoo Xorse hereby declare that this thesis, except for the references to other people's work, which have been duly acknowledged, is the result of my own research work in the Marine and Fisheries Sciences Department of the University of Ghana under the supervision of Dr. Kwasi Appeaning Addo and Dr. George Wiafe and has not been presented in whole or in part for another degree elsewhere.

Sign …….. Date ……

Trinity Mensah-Senoo Xorse

(Student)

Sign …….. Date ……

Dr. Kwasi Appeaning Addo

(Principal Supervisor)

Sign …….. Date ……

Dr. George Wiafe

(Supervisor)

DEDICATION

This is solely dedicated to my lovely mum, Frederica Amenyra.

ACKNOWLEDGEMENT

My first thanks goes to the Almighty God for seeing me through my M.Phil. studies.

I am very grateful to my supervisors, Dr. Kwasi Appeaning Addo and Dr. George Wiafe for their patience and guidance through this work.

I also thank my mum, dad, siblings, Joana Dzaba and Mr. Richard Powel for their support.

My heartfelt gratitude also goes to Dr. Elvis Nyarko and all lecturers in the department and research assistants, Sowah Laryea, Donatus Bapentire, Kwame Agyekum and Emmanuel Klubi.

I also thank Thomas Lippmann from The Center for Coastal and Ocean Mapping of the University of New Hampshire.

To all who contributed directly or indirectly to the success of this work God Richly bless you all.

TABLE OF CONTENTS

Pages

LIST OF TABLES

Pages

LIST OF FIGURES

Pages

LIST OF ABBREVIATIONS

CERC	Coastal Engineering Research Centre
EPA	Environmental Protection Agency
IPCC	Intergovernmental Panel on Climate change
ITCZ	Intertropical Convergence Zone
NOAA	National Oceanic and Atmospheric Administration
SLR	Sea Level Rise
SST	Sea Surface Temperature
WAM	WAve prediction Model

ABSTRACT

Wave and wind dynamics are important in the estimation of beach erosion rates and sediment transport modelling. They are also important in modelling sea fatigue, oil spill transport and planning of coastal and marine activities. This work sought to quantify the magnitude of wave and wind parameters along the coast of Ghana as well as identify how these parameters varied across the year. A nine years wave and wind data from the National Oceanic and Atmospheric Administration (NOAA) global wave model and data from a Wave Rider Buoy were analysed for this purpose. Wave data analyses were based on long term and short term methods. Potential sediment transport rates were also calculated using the Soulsby-Van Rijn sediment transport equation. From the results, mean significant wave height was 1.39 m, mean period was 10.91 s and mean wind speed was 4.65 ms^{-1}. The results also revealed monthly trend of wave heights where wave heights increased gradually from January (1.00 m), the beginning of the year to a peak in August (1.73 m) and then began to decrease to a low in December (1.10 m). Wave periods also exhibited an almost similar trend but the highest wave period occurred in May (11.85 s). Wind speeds showed similar monthly variability and had the highest in July (5.61 ms^{-1}). Wave directions were mainly in the South (S) and South-South-West (SSW) direction with those in the SSW direction forming majority. Sediment volume transport were also determined where crosshore transports, 2.25E+08 m^3y^{-1}, were found to be higher than longshore transports1.82E+08 m^3y^{-1} (E+08= ×10^8; m^3y^{-1} = metre cube per year). The outcomes of this study are very relevant as it will aid in policy making for the monitoring and protection of the coastal environment and; serve as a guide for the construction of coastal and offshore structures.

CHAPTER ONE

INTRODUCTION

1.1 Background

Coastal erosion is a global problem and about 70% of the world's sandy beaches are reported to be recessional (Bird, 1985). The global erosion rate of land is estimated to be about 6 cm/thousand years resulting in a flux to the sea of 5×10^9 ton/year dissolved solids and 20×10^9 ton/year particulate solids (Schwartz, 2005). The coastline of Ghana, especially the eastern portion which is mainly sandy have been heavily ravaged by waves; carrying chunks of sediment away and destroying nearby properties (Oteng-Ababio *et al*., 2011).

Various studies along the coastline of Ghana have shown various degrees of erosion at various points along the entire coast. In Wiafe (2010), where the coastline was divided into four sections, erosion was found to be dominant along the eastern part of the coast. In other works, shoreline recession was estimated at an alarming rate of -22.9m/year at Kedzi a coastal town along the eastern coast of Ghana (Bapentire, 2011). Possible causes have been related to Sea Level Rise as a result of thermal expansion of the ocean; change in storm climate as a result of climate change; and the human factor (Zhang, Douglas, and Leatherman, 2004).

Indeed there is established evidence of Sea Level Rise (SLR) on all continents (IPCC, 2007). In Ghana for instance, in Appeaning Addo's findings in 2009, Ghana has a historic SLR of about 2mm/year. Climate change SLR models also predict a global rising trend of 0.18 to 0.59 m by 2100, depending on all six families of the Special Report on

Emissions Scenarios (IPCC, 2007). SLR impacts has also been enormous. They include shoreline erosion; coastal flooding, accompanied by; salt-water intrusion into estuaries and freshwater aquifers; altered tidal range in rivers and bays; changes in sedimentation patterns; and loss of some coastal flora and fauna (IPCC, 2001). These impacts have been exacerbated by frequent coastal storms and coastal human activities such as beach sand mining (Mensah, 1997).

It is true that the factors mentioned above are the causes of coastal erosion but taking a closer look will reveal that the main 'cause' here is 'wave action'. Take out the wave factor along the coast and we will realise there will be virtually no erosion though SLR may result in coastal inundation and probable loss of properties. Waves dislodge sediments as they break on the shore and transport them offshore with the generated ebb or rip current or elsewhere along the shore with the longshore current (Fredsoee and Deigaard, 1992). It has therefore become necessary to study the wave climate and dynamics and how it contributes to coastal erosion along the coast of Ghana.

Wave as defined by the physicist is a travelling disturbance or oscillation, moving through space and time impacting energy through the medium as it moves, often without a permanent displacement of the medium (Ostdiek and Bord, 2007). The particles of the medium only move about their equilibrium positions. Other types of wave like electromagnetic waves only displace or produce electric and magnetic fields of force as they travel. Such waves do not require a medium for their propagation while it is a necessity for the former (Ostdiek and Bord, 2007). Examples of such waves that require medium for propagation include heat, sound, and water waves which are of great importance here. Waves dominate the surface of water bodies and occur at varying scales. Ocean surface waves range from capillary waves, gravity waves, surges, tsunamis

and to large scale types like tides. Their period ranges from fractions of a second for capillary waves, about 30 seconds for gravity waves and up 24 hours for trans tidal waves. Energy carried by these waves also varies accordingly (Bouws *et al*., 1998) and are obvious when they impact objects like boats, buoys, ships and the coast where they often eventually end up. Ships and boats depending on orientation may topple upon impact. On the shore waves dislodge sediments as they break on the coast and carry them away with the generated water current.

Ocean surface waves are the result of forces acting on the ocean. The predominant natural forces are pressure or stress from the atmosphere (usually from winds), earthquakes, gravity of the Earth and celestial bodies (the Moon, the Sun), the Coriolis force (due to the Earth's rotation) and water surface tension (Bouws et al., 1998). The characteristics of the waves (often the speed, height and period) depend on the controlling forces (Massel, 1996). For example a wave will travel at an approximate speed of the wind that generated it. Tsunamis for instance are generated by under water or oceanic plate movements. Energy or force carried by the tsunami depends on the magnitude of the quake. The earthquake responsible for the series of tsunamis across Asia in December 2004, for instance was caused by the Indian plate slipping beneath the Eurasian plate thrusting the sea floor upwards, and creating massive amounts of energy that sent giant waves racing across the Indian Ocean (Edwards, 2005). By frequency of occurrence wind generated waves dominate the ocean surface. Unlike tsunamis which are relatively infrequent (Casale and Margottini, 2004) wind generated waves and tides are frequent or regular and are more predictable.

Waves impact activities at sea as well as activities on the coast. Impact at sea may not be as detrimental as on the coast except for extreme conditions, orientation and stationary

objects held in place like platforms. This follows the fact that the water particles do not travel with the wave but rather transmit the involved energy to nearby particles and rather perform an orbital motion (Garrison, 2009). So objects at the surface of the water tend to perform a relative bobbing up and down movement as the waves pass whereas stationary objects held in place like fixed platforms may suffer severe impact and may be dislodged. As deep water waves approach the shallow shore however, their speed get transformed into potential energy thus wave heights are increased and therefore approaching waves have high tendency of 'climbing' upland increasing their area of impact as they plunge or break (Garrison, 2009). This effect is evident in a storm surge where water tends to pile on the coast.

Waves play a major role in shaping shorelines by removing or depositing sediments (erosion or accretion). High energy waves dislodge sediments as they break on coasts and carry them away with the backwash or the generated longshore current. The rate of sediment removal by waves is dependent on several factors. These include the tidal range (vertical expanse of coast exposed to wave activity), sea level rise, sediment type/particle size, angle of shoreline orientation to incoming current and wave activity, slope and more importantly the wave climate (wave energy). A coast with a high tidal range will have wave action reaching far onshore. A steep sloping beach is susceptible to plunging waves thus more sediments are dislodged (Mangor, 2004); high energy waves will have more damaging effects on the coast; a coast which is more or less parallel to incoming waves may have little erosion.

The sea has immense uses such as construction of harbours, defence, extraction and exploration of resources and production of energy and power. Due to these countless reasons humans have decided to perfect the sea to the extent of predicting its behaviour.

The science of oceanography had not begun till mid nineteen century (Stewart, 2008). The importance of ocean wave prediction was first considered by the United States in early 1940's for the planning of naval fleet operations during the Second World War (Mandal and Prabaharan, 2010).

Information about wave climate has become a necessity for the planning and carrying out of activities on the ocean as well as the coast. Offshore oil exploration activities for instance are very much dependent on ocean surface conditions. Increased advances in technology has enabled more complex computations to be made and predictions are becoming more accurate. Ocean waves, state as well as sediment transport models can now be made (Janssen, 2008). Such advances will help coastal engineers, managers and policy makers to take more informed approaches and decisions in managing the coastal area. These high level approaches and researches are however now gaining grounds in the African community as little has been done in such areas.

The dynamic processes that occur within coastal zones produce diverse and productive ecosystems which are of great importance historically for human populations. Coastal margins make up only 8% of the worlds' surface area but provide 25% of global productivity (Small and Cohen, 2004). This zone also supports approximately 38% of the world's population (Al-Tahir and Ali, 2004; Small and Cohen, 2004). Two-thirds of the world's cities occur on the coast (Crooks and Turner, 1999). It is therefore important to investigate and offer protection to this important zone.

1.2 Aims and Objectives

This research aims at assessing the impact of wave activities along the Ghanaian coast through modelling techniques. The objectives were:

- To examine the offshore wave characteristics of Ghana from in situ and modelled data
- To ascertain the effect of wind on the propagation of waves
- To identify the energy regime of waves along the coast of Ghana
- To determine how waves impact the coast through sediment transport.

1.3 Justification

Ascertaining the effect of wind on wave propagation along the coast will help determine if waves are locally generated or are swells coming from distant. Determination of wave energy and direction will help to determine the magnitude of wave impact and resultant direction of sediment transport. This will help in making informed decisions on ways and types of beach management approaches to adapt. Amongst other importance of this study, companies in the marine sector have an increase need for wave information to control and plan their operations. Wave dynamics are needed for baseline design statistics and operational assistance for coastal projects. Knowledge of wave dynamics on the continental shelf is also important for defence. Offshore Oil industries need wave forecasts and wave climate to design sea states, fatigue analysis and operational planning. Wave data is also needed for operational assistance in coastal construction projects. There are limited documentations on volumetric sediment transport on the beaches of Ghana.

CHAPTER TWO

LITERATURE REVIEW

2.1 Introduction

Beach erosion has been a topical issue for the past decades. It has increased in importance in recent times as a result of sea level rise. Waves, wind and their associated currents are the sole drivers of sediment transport in the coastal region. This chapter seeks to review available literature on waves and their impact on coastal sediment transport. It also reviews sediment transport dynamics and quantification of their rate of transport using sediment transport model.

2.2 Wave and Wind Dynamics

Waves and winds play an important role in atmospheric, oceanic and coastal processes. The oceans' surface is governed by waves; capillary waves, gravity-capillary waves, gravity/wind generated waves, infra-gravity waves, long period waves (seiches, Tsunamis), tidal waves and trans-tidal waves with periods up to fractions of a second, a second, thirty seconds, five minutes, twelve hours and twenty-four hours respectively (Bouws *et al*., 1998). Amongst these, wind generated waves dominate. The size and speed of a wind generated wave depends on characteristics of the generating wind; that is speed (how fast it blows to create a turbulent situation), duration (how long it blows) and fetch (distance over which it blows). Once formed on the ocean surface, they are called windseas. Windseas then undergo sorting and leave their point of generation and are now called swells. Swells are fully developed waves and can travel far distances, over 20,000 km across the oceans and can keep a relatively constant energy over 2,000 km (Ardhuin

et al., 2009). Empirical data supports the idea that windseas and swells together account for more than half of the energy carried by all waves on the ocean surface, surpassing the contribution of tides, tsunamis, coastal surges etc. (Alves, 2006).

Swells dominate wave climates in the tropics and pose some draw backs to wave prediction in such areas (Ardhuin *et al*., 2009). A study by Young *et al*., (2011) has also shown that waves in the West African region poorly correlate with local wind speeds; stronger correlations only occur during storm events as local winds get stronger. Studies conducted over the last three decades have also revealed that the presence of swell affects several important processes at the air–sea interface, such as the modulation, blockage and suppression of short wind-generated waves (Alves, 2006). Swells in the tropical Atlantic are generated from the far North Atlantic Ocean and South Atlantic Ocean in the Antarctic region. The longest waves in the Atlantic Ocean occur along the coasts of Western Europe and West Africa. Those along the West African Coast are observed to have originated from the Antarctic region (Ardhuin *et al*., 2009). Tropical waves range from 0-3 m with the highest often occurring in the tropical Pacific (Short, 2012).

2.2.1 Wave Analysis and Prediction

Ocean wave analysis and prediction is an important activity in the meteorological and oceanographic services of many countries. Marine and coastal activities such as offshore oil drilling, coastal engineering works largely depend on wave climate (Khandekar, 1989). Wave data analysis may be done in two forms. These are Short-term or Long-term analysis (Kamphuis, 2000). Short-term analysis refers to analysis of waves that occur within one wave train or within one storm whereas Long-term analysis refers to the derivation of statistical distributions that cover many years. Data size required for such analyses vary accordingly; data for short-term analysis may range from about 30 seconds

to about 20 min whiles long-term analysis may require data spanning over several hours to several decades (Bouws *et al*., 1998). The complex nature of the sea surface tends to defy scientific analysis and therefore some assumptions and approximations will have to be made (Kamphuis, 2000). One example of assumptions made is that the waves are in stationary state. For swells, it is assumed propagation is well approximated by linear wave theory and that deep water swell propagation exclusively follow great circle paths (Alves, 2006).

Wave prediction is a necessity as it is expensive and quite impossible to place wave buoys or wave recorders at every point in the oceans. Ocean wave prediction is often done using models and the first models were based on simple empirical formulations (Bouws *et al*., 1998). Wave prediction models have evolved since; from first generation models, second generation wave models and the current third generation models. An example of such third generation model is the WAM (WAve prediction Model) by the Wave Modelling Group. WAM forms a basis for other several third generation models. An example of such is the WAVE WATCH III by NOAA (National Oceanic and Atmospheric Administration) which is a global wave model and is being adapted to predict waves in shallow waters (Tolman, 2008; Tolman *et al*., 2002). Wave analysis, modelling and prediction have been extensively treated in the World Meteorological Organisation's 'Guide to Wave Analysis and Forecasting', 1998 2nd edition (Bouws *et al*., 1998).

Wave prediction in the tropics however has some drawbacks since swells dominate in this region. Because swells are observed to propagate over long distances, their energy should be conserved or weakly dissipated, but little quantitative information is available on this topic. As a result, swell heights are relatively poorly predicted (Ardhuin *et al*.,

2009). Numerical wave models that neither account specifically for swell dissipation, nor assimilate wave measurements, invariably overestimate significant wave heights in the tropics. Typical biases in such models reach 45 cm or 25% of the mean observed wave height in the East Pacific (Rascle *et al*., 2008). Further, modelled peak periods along the North American west coast exceed those measured by open ocean buoys, on average by 0.8 s (Rascle *et al*., 2008), indicating an excess of long period swell energy. Theories proposed so far for nonlinear wave evolution or air-sea interactions, require order-of-magnitude empirical correction in order to produce realistic wave heights (Ardhuin *et al*., 2009; Tolman *et al*., 2002). Swell evolution over large scale is thus not understood. Some other studies attribute drawbacks to weather predictions in the tropics to the lack of in situ data (Krishnamurti et al., 1991). Thus unless thorough studies of swells are carried out in the region and efforts made in installations made to carry out in situ data collection, tropical coastal states like Ghana along the Atlantic ocean may have inaccurate wave and weather predictions.

2.2.2 Wind Speed and Sea State Determination

Winds vary considerably in time and space, and so do waves and because of short-term predictability in the winds, there is an associated predictability for wind waves, enabling operational fore-casts to be made (Bouws *et al*., 1998). Sea state is often described as the general condition of the free surface on a large body of water (with respect to wind waves and swell), at a certain location and moment. This is statistically represented by the wave height, period and power spectrum. Two empirical scales are used to describe wind and wave conditions at sea. The Beaufort scale (Table 2.1) relates wind speed to the physical appearance of the sea surface by considering such factors as apparent wave height and the prominence of breakers, whitecaps, foam and spray. It is the oldest method of judging

wind force (Allaby, 2002). The Beaufort Wind Scale has Beaufort numbers ranging from 0 – 12, corresponding to different wind speeds and conditions.

Table 2.1: Beaufort Wind Scale

Beaufort	**Wind speed (**ms^{-1}**)**	**Description**
0	<1	Calm
1	01-02	Light air
2	02-03	Light breeze
3	04-05	Gentle breeze
4	06-08	Moderate
5	09-11	Fresh breeze
6	11-14	Strong breeze
7	14-17	Near gale
8	17-21	Gale
9	21-24	Severe gale
10	25-28	Storm
11	29-32	Violent storm
12	33+	Hurricane

Adapted from Schwartz (2005)

The Beaufort scale is a formalized relationship between sea state and wind speed, and it can be used to obtain an estimate of waves in the open sea when wind speed is known. The Beaufort Wind Scale is often used together with the Douglas Sea State Scale (Table 2.2). The Douglas Sea State Scale has been a standard for estimating ocean surface roughness numerically or descriptively (Ward *et al*., 2006). These scales can be used to describe local wave and wind climate of a region. For instance, sea state along the Ghanaian coast could be described as ‘Slight’ to ‘Moderate’ as significant height of the waves generally lies between 0.9 m and 1.4 m and rarely attains 2.5 m or more (TGL, 2009).

Table 2.2: Douglas Sea Scale

Sea State			Swell	
Code	**Height (m)**	**Description**	**Code**	**Description**
0	no wave	Calm (Glassy)	0	No swell
1	0 - 0.10	Calm (Rippled)	1	Very low (short and low wave)
2	0.10 - 0.50	Smooth	2	Low (long and low wave)
3	0.50 - 1.25	Slight	3	Light (short and moderate wave)
4	1.25 - 2.50	Moderate	4	Moderate (average and moderate wave)
5	2.50 - 4.00	Rough	5	Moderate rough (long and moderate wave)
6	4.00 - 6.00	Very Rough	6	Rough (short and heavy wave)
7	6.00 - 9.00	High	7	High (average and heavy wave)
8	9.00 - 14.00	Very High	8	Very high (long and heavy wave)
9	14.00+	Phenomenal	9	Confused (wave length and height indefinable)

Adapted from Bouws *et al*., (1998), MetOffice, (n.d.) and Schwartz, (2005).

Wind speed measured at 11 m (36 feet) above sea surface is usually applied to the scale. The wave heights are approximate and represent fully arisen sea state. As with any subjective judgment method, the Beaufort Wind Scale and the Douglas Sea State Scale are far from perfect. They are often modified by institutions or organisations to suit their operations.

2.3 Storm Surges

A storm surge is a dome of increased sea level height in association with the approach of an intense cyclone (Needham and Keim, 2011). Persistent onshore winds, in conjunction with reduced air pressure, force water levels to rise, especially in shallow water of impacted coasts (Needham and Keim, 2011). In some cases surges can last for several

days and cause flooding in coastal low lands and sometimes cause loss of life and properties in severe cases. Tropical cyclone-generated storm surges create natural disasters that are among the most deadly and costly global catastrophes. Individual disasters have inflicted hundreds of thousands of fatalities and billions of dollars in damage (Needham and Keim, 2011). In 1970, a tropical cyclone in the Bay of Bengal generated a 9.1-meter surge which killed approximately 300,000 people in Bangladesh. Also in 1991, a storm surge killed approximately 140,000 people in Bangladesh (Dube *et al*., 1997). Storm surge heights are often calculated by multiplying the ratio of stress of the acting wind and the water density, by the ratio of fetch and water depth (Kelly, 2003).

A study by Appeaning Addo (2010), suggested that the significant difference in wind speed as winds approach shore probably explains why storms and storm surge are not common along the Accra coast (Appeaning Addo, 2010). There have however been some cases of water surge along the eastern and western coasts of Ghana. The event of SLR also suggest probable coastal storm surges (Armah, 2005; Bapentire, 2011). The damage wrought by rising sea levels is amplified by increasingly violent tropical storms, which can create sea surges up to 3 m (10 feet) high in the West African Region. In August 2007, a storm originating about 5,000 km off the coast of Lagos destroyed protective beach barriers, highlighting the vulnerability of Africa's west coast (Mustapha, 2011).

Several important processes influence storm surges. These include: Ekman transport by winds parallel to the coast that transport water toward the coast causing a rise in sea level; winds blowing toward the coast that push water directly toward the coast; wave run-up and other wave interactions which transport water toward the coast adding to the first two processes; edge waves generated by the wind that travels along the coast; the low pressure inside the storm raises sea level by one centimetre for each millibar decrease in

pressure through the inverted-barometer effect; Finally, the storm surge adds to the tides, and high tides can change a relative weak surge into a much more dangerous one (Dean and Dalrymple, 2001; Needham and Keim, 2009). In coastal areas with strong tides, tides are an important factor affecting storm surges and ocean circulations. A study by Tang *et al*. (1996), demonstrated that a nonlinear interaction between storm surge and tides affects strongly the prediction of coastal sea levels and is predominantly caused by the quadratic bottom friction. The slope of the pile of water on the coast is proportional to the wind stress (Stewart, 2008). Storm surge frequencies have increased in recent times with the phenomena of climate change and sea level rise (Forces, 2011; Pérez *et al*,, 2011; Titus *et al*., 2009).

2.4 Climate Change and its Impact on the Coastal Environment

Climate change is a significant and lasting change in the statistical distribution of weather patterns over periods ranging from decades to millions of years. Climate change is now widely recognized as the major environmental problem facing the globe (UNEP, 2008). Three main factors have been identified to cause climate change and they are volcanic forcing, solar forcing and anthropogenic forcing (Crowley, 2000). Current climate change conditions has been widely described as human induced as it has been attributed to increased concentration of greenhouse gases in the earth's atmosphere due to human activities (Houghton and Change, 1996; Schellnhuber and Cramer, 2006). Greenhouse gases found in the Earth's atmosphere include: water vapor, carbon dioxide, methane, nitrous oxide, and ozone. These gases tend to trap heat and help control the earth's temperature. Carbon dioxide alone, is reported to have increased by 35% during the industrial age (IPCC, 2007). One of the major impacts of the increase in concentration of

the greenhouse gases is global warming with its associated irregular weather patterns and increased storminess. Global warming results in increase evaporation, excess precipitation (Fowler and Hennessy, 1995), melting of the cryosphere and thermal expansion of the oceans. The later has been found to cause Sea Level Rise (SLR) (IPCC, 2001). Two major outcomes of climate change that had been found to impact the coastal environment are SLR and Increased Storminess (Zhang, Douglas, and Leatherman, 2004).

When discussing impacts of SLR, it is very important to distinguish inundation from erosion (e.g. Zhang, Douglas, and Leatherman, 2004). With SLR, the high water line migrates landward in proportion to the slope of the coastal area. In some areas the slope is gradual, and the impact from sea level rise can be severe. For example, in low-lying regions such as salt marshes, an increase in the rate of sea level rise much beyond a few mm per year can result in marsh destruction because the plants there cannot respond rapidly enough to the increasing water level. SLR is evident on all the continents and global SLR models predict a global rising trend of 0.18 to 0.59 m by 2100 (IPCC, 2007). Wetland losses due to SLR are expected to be in the order of 17% along the Atlantic coasts, 31-100% along the Mediterranean coast and 84-98% along the Baltic coast (IPCC, 2001). Greater defence of these coastlines to prevent coastal flooding will lead to additional loss of coastal habitats (IPCC, 1990). Offshore structures and installations for hydrocarbon extraction and renewable energy will also be at greater risk. Studies on impacts of inundation of a coastal town, Dansoman, near Accra Ghana, predicts a coastline recession of about 202.06 m with the loss of about 0.78 km^2 of land to permanent inundation considering worse scenario by 2100 due to SLR (Appeaning *et al.*, 2011). According to the study, in Mustapha (2011), for every one metre rise in sea level,

Ghana will lose at least 110 square km of land to the ocean. The study further explains that even where urban areas are spared, rising seas pose a challenge to the water supply as salty sea water can contaminate fresh water sources and underground water reserves. Increasing salinity will make the ground water both undrinkable and unsuitable for agriculture, leading to food and water insecurity.

Storm surges due to coastal storms cause a local rise in water level that tends to pile up water on the coast. From the Marine Board Series (2007), it is reported that increased storminess will exacerbate the effect of SLR in coastal systems because of the higher frequency of storm surges and extreme wave action (Anadón *et al*., 2007). Most climate change models predict an increase in precipitation with an average maximum increase of 6% by 2100, but do not have a good agreement of increase in storminess with a warming earth (Cubasch *et al*., 2001). Studies in the United States also conclude there is no significant increase in storminess in this century (Zhang *et al*., 1997, 2000). A study in South Africa also shows a relative increase in wind and wave climate and an increase of 0.5 m in storminess over a 14 year period (Rossouw and Theron, 2009).

2.4.1 Impact of Climate Change on Oceanic Wave Heights

Various climate change models predict rise in oceanic significant wave height in various oceans. The rate and sign of the projected future wave height changes are not constant throughout the century; and in some regions, these appear to be quite dependant on the forcing conditions. The rate of change appears to have a positive relationship with the rate of increase in the greenhouse gas forcing (Wang *et al*., 2004). There is however an appreciable level of uncertainties amongst models. The North Sea projections for instance had uncertainties in extreme significant wave heights which ranged up to 0.7 m south of the Norwegian coast. For extreme wind speeds, highest uncertainties were up to 0.9 m s^{-1}

off the Danish coast (Grabemann and Weisse, 2008). The smallest model-related uncertainties in the climate change signals of extreme wave height and wind speed are about 0.1 m and 0.2-0.4 m s^{-1} respectively, and occur in the southwestern part of the model domain towards the English Channel (Grabemann and Weisse, 2008). The existence of these various sources of uncertainty requires characterization of the uncertainties, to evaluate the level of confidence in "regional" climate change simulations (Wang and Swail, 2006).

Modelling on the Dutch coast however projects an unchanged significant wave height with reduced annual period maxima 0.3–0.6 s (Winter *et al*., 2012). Modelling scenarios in the northeast Atlantic also projected to have increases in both winter and fall seasonal means and extremes of significant wave height in the twenty-first century (Winter *et al*., 2012). These increases were generally accompanied by decreases in the midlatitudes of North Atlantic and increases in the southwest North Atlantic. The generalised extreme value analysis showed that global warming may result in changes in the location parameter of the distribution of wave height extremes, eventually leading to changes in the size and frequency of extreme wave height events. For example, in the Norwegian Sea, an extreme wave height event that occurs on average once every 20-yr period in fall in the present-day (1990s) climate (base line), is expected to occur on average once every 4–12 years in the climate projected for year 2080 (Wang *et al*., 2004).

Significant increases in significant wave heights were projected for the Antarctic area for the April-May-June and July-August-September seasons with decreases in the region between 40°S and 60°S. Such a pattern of changes was also projected for the October-November-December season (Wang and Swail, 2006). The Gulf of Guinea which experiences swells originating from the Antarctic region (Ardhuin *et al*., 2009) will

therefore consequentially experience higher significant wave height according to the projections.

2.5 Impact of Waves and Winds on the Coastal Environment

Waves and winds are the main forces that drive oceanic and coastal processes. These processes include atmosphere-ocean surface interactions, influencing sea surface temperature (SST), mixing and aeration, generation of currents and sediment transport. Waves impact coastal habitats by their direct effect on benthic vegetation, as well as indirectly by shaping the bottom sediment characteristics in coastal areas. In coastal and shelf regions, tides, storm surges, wind waves and oceanic circulation are the main processes that determine the physical environment of the region and are major components of marine forecasts (Moon, 2005).

Waves play an important role by acting as a significant barrier to the exchange of heat and gases between ocean and atmosphere. Forcing enters the surface wave fields first and is transmitted to the surface current field mainly by wave breaking. The wave breaking enhances turbulent kinetic energy that is responsible for mixing the momentum down through the water column (Drennan *et al*., 1992). Wave breaking hence has a considerable effect on the near-surface distributions of oceanic mixed layer properties, such as velocity, temperature, and salinity, affecting ocean circulation modelling (Moon, 2005). Surface waves are also responsible for producing Langmuir circulations, which are formed due to the interaction of the wind-driven surface shear with the Stokes drift of the surface waves (Kantha and Clayson, 2004). Langmuir circulations are responsible for ocean surface vertical mixing and thereby destroying the surface thermal stratification in shallow diurnal mixed layers (Kantha and Clayson, 2004).

Waves and currents can induce large forces and stresses on and near hydraulic structures. This hydrodynamic load is responsible for unwanted effects such as vibrations and fatigue, damage to the revetment of both structures and their base, and scour around structures offshore and along coasts. Offshore constructions and sea vessels will also have to contend with such forces (Bea *et al*., 1999). Elsewhere where these forces are blocked along the shore by structures like sea defences, these are likely to be transferred elsewhere along the shore. An example is the impact of the Keta Sea Defence on the eastern coast of Ghana on the down drift coast (Bapentire, 2011). Variations in wave direction patterns could also change beach evolution trends (Casas-Prat and Sierra, 2012).

Studies by Smith et al., (2009) on the impact of wave parameters on cross-shore and longshore sediment transport at various sections in the nearshore yielded significant impact. In their studies, the cross-shore distribution of longshore sediment flux indicated three distinct zones of transport: the incipient breaker zone, the inner surf zone, and the swash zone. A peak in transport occurred for plunging waves in the incipient breaker zone, indicating that this breaker type suspends more sediment for transport at wave breaking. Transport in the inner surf zone indicated that wave height was the dominating factor and independent of wave period. Swash zone transport, which accounted for a significant percentage of the total transport, especially under low-wave energy conditions, showed a dependence on wave height, period, and beach slope (Smith *et al*., 2009).

A significant amount of turbulence and diapycnal mixing that occurs within the ocean is generated via the interaction of internal waves with topographic features. Specifically, when an internal wave in a continuously stratified fluid encounters topography in which the slope matches the angle of the internal wave group velocity vector, breaking occurs as

a result of focusing of internal wave energy along the slope (Finkl and Bruun, 1998; Müller and Briscoe, 1998).

Waves play major role in shaping coastlines. Waves destabilize, resuspend particles and influence longshore circulation as they break. Waves carry two forms of energy; kinetic energy, by virtue of the wave's displacement and potential energy by virtue of wave's height. These energies are often in equal proportions and this is termed as the equipartition of energy (Bouws *et al*., 1998). As the waves enter shallow waters the waves interact with the bottom, some energy is lost through friction and most of the kinetic energy is transformed into potential energy resulting in an increase in wave height (Edge, 2011). When this transformation is quick enough, wave heights increase rapidly, reaching maximum heights (high energy) forming surfs. This occurs where the shore slope is steep or becomes steep suddenly with rapid decrease in water depth. On the other hand when the transformation is rather slow, waves may never reach appreciable heights and the energy is gradually dissipated. This occurs on gently sloping shores.

As the waves break they impact their energy to the shore. The energy with which waves impact the coast can also be influenced by aeration with the release of shock pressure at impact depending on the level of air present in the wave or trapped between the wave and the object of impact (example beach or sea defence structures) (Bullock *et al*., 2001). In the calculation of the total energy of waves, waves are assumed to be simple linear waves. The total energy is a relationship between the wave height, the water density and gravity (Bouws et al., 1998).

Winds also play an important role in coastal sediment transport especially in arid regions. For example in Mauritania and Senegal, Saharan sands are driven seawards by the *irifi*, a

hot easterly wind, to form the great red draas and superimposed barchans that trend obliquely across the Mauritanian coast between Cape Blanc and the Senegal River, notably in the Azefal and Akchar ergs (Kocurek *et al*., 1991). The Sahara now contributes 13×10^6 m^3 of quartz sand to the continental shelf annually, but this amount may have been much larger in the past (Schwartz, 2005). Sand transport by wind is the primary source of sediment supply for the building of foredunes on sandy beaches and thus a major component of sediment budget calculations for both the beach (the source) and the dune (the sink) (Davidson-Arnott *et al*., 2005). Coastal dunes often constitute the final defence line against high waves and water levels during severe storms. If they are overtopped or breached, serious damage due to flooding and direct wave attack could occur, resulting in loss of life and property (Larson *et al*., 2004). Sediment transport by wind (aeolian transport) can remove sand from beach systems and move it into large dunes that can either remain stationary or migrate a considerable distance inland. In some cases, migrating sand dunes can pose a hazard by threatening burial of buildings, highways, roads and even villages (Dean and Dalrymple, 2004). In some cases this migration is caused by wave action; evidence of which can be seen in some coastal communities, example Totope along the eastern coast of Ghana.

2.5.1 Coastal Erosion

Coastal erosion is a global problem since about 70% of the world's sandy beaches are reported to be recessional (Zhang, Douglas, and Leatherman, 2004). The main cause of coastal erosion is wave action. This is aggravated by the current situation of SLR which affords wave action assess to sediments back beach and inland. Studies have also shown that there is a likely increase in wave heights as a result of climate change (Wang and Swail, 2006). The coastal zone though makes up only 8% of the worlds' surface area, it

provides about 25% of global productivity (Al-Tahir and Ali, 2004). This zone also supports approximately 38% of the world's population (Small and Cohen, 2004). Two-thirds of the world's cities are located in this zone (Crooks and Turner, 1999). There are glaring evidences of coastal erosion along the entire coast of Ghana (Wiafe, 2010). Ghana's Environmental Protection Agency estimated that the ocean is encroaching inland by 1.5 to 2 metres along the country's 539 km shoreline annually EPA, 2006. The most risky areas were identified as Ada Foah, Azizanya and eastern parts of Keta, which are recording an average loss of 4 metres per year (Mustapha, 2011). Waves have ravaged the eastern coastline of Ghana especially the Ada and Keta area (Oteng-Ababio et al., 2011) removing chunks of sediment, eroding coastal transport links and buildings.

2.6 Sediment Transport and Deposition

Sediment transport is the essential link between the waves and currents and the morphological changes (Roelvink and Reniers, 2011). It is a strong and non-linear function of the current velocity and orbital motion, the sediment properties such as grain diameter and density and small-scale bed features often lumped together in the parameter 'bed roughness' (Roelvink and Reniers, 2011). The main hydrodynamic parameter that controls erosion, suspension and deposition of muds and sands in estuaries and coastal waters, is the bed shear-stress which is the frictional force exerted by the flow per unit area of bed (Soulsby and Clarke, 2005).

Natural coastal processes are the result of the energetics of waves and tidal motion. The latter tend to be dominant in estuaries, the former along the open coast. However, they often combine to produce distinctive coastal landforms and are responsible for the movement of sediment along-shore and on- and off-shore (RESPONSE, 2006).

Longshore sediment transport and its rate is dependent on wave energy and the angle at which waves strike the coast (an angle of about 30° being the most effective), (CoastalProcesses, n.d.). The overall significance of longshore sediment transport depends on whether it occurs along coasts of free or impeded transport. Impeded transport is characteristic of coasts with irregular configurations, the amount of longshore transport being limited by the trapping of sediment against headlands or coastal engineering structures such as sea defence systems.

Rip currents generated by waves have long been recognised as a major mechanism for offshore sediment transport (Short, 1985). Unfortunately, there is no quantitative information available to examine sediment exchange within evolving rip systems and most existing studies reveal little about the nature of basic sediment transport processes and patterns operating within rip channels (Brander, 1999). However, recent studies of offshore transport both within and outside the surf zone, have dealt almost exclusively with oscillatory motions, lower frequency oscillations, far-infragravity frequencies, and bed return flow or undertow as mechanisms for offshore sediment transport (Nielsen, 1992). Research by Brander, (1999) revealed that transport in the rip channels is also affected by tidal levels in that, transport rates increase at low tide and gradually reduce towards high tide. Brander concluded that the waves were responsible in entraining sediments but transport is mainly by currents. Ruessink *et al*., also share the same view in their research where oscillatory motions were responsible for suspending sediments whiles sediments were transported offshore by undertow (Ruessink *et al*., 1998).

Sediment transport is affected by the sediment type (size). Packed sediments have a dissipative capacity as a result of hydraulic conductivity, and this tends to increase with increasing sediment size. Hydraulic conductivity is however affected by the beach profile

and ground water. Dissipative capacity is also compromised with mixed sediment composition. Mixed beaches with considerable amount of sand will behave just like complete sand beaches under moderate to high wave action (Mason and Coates, 2001).

Researches indicate increases in sediment transport with decrease in temperature (Héquette and Tremblay, 2009; Xu *et al*., 2002) winter measurements accounting for more than 90% of annual transport in some cases (Xu *et al*., 2002). Significant increase in bedload sediment transport in cold water is interpreted to be the result of temperature-induced variations in fluid viscosity that affect turbulence and boundary layer dynamics as well as bed configuration (Héquette and Tremblay, 2009). This suggests similar trends in the tropics like the Gulf of Guinea during the upwelling months where SST decreases.

Sediment transport during uprush and backwash after a wave break suggests that the uprush is a more efficient transporter of sediment than the backwash, because of a larger friction factor during the uprush causing larger bed shear stresses for a given free-stream velocity. This increased transport competency of the uprush is necessary for maintaining the beach, otherwise the comparable strength and greater duration of the backwash would progressively remove sediment from the beach (Masselink *et al*., 2005).

Some other sediment transport mechanisms described by Elfrink and Baldock (2002) include sediment transport through suspended load, bed load, advection and convection. The complexities of sediment transport are staggering but there are some general trends that are robust and lead to unambiguous morphological effects. Sand tends to go in the direction of the near-bed current. If the current increases, the transport increases by some power greater than 1. On a sloping bed transport tends to be diverted downslope. The orbital motion stirs up more sediment – convective transport (Elfrink and Baldock, 2002)

- and thus increases the transport magnitude. In shallow water, the wave motion becomes asymmetric in various ways which leads to a net transport term in the direction of wave propagation or opposed to it (Roelvink and Reniers, 2011).

2.7 Other Influences on Coastal Sediment Transport

Other causal factors influencing coastal sediment transport include coastal geomorphology, shoreface morphology, shoreline orientation (Backstrom *et al*., 2008), and bathymetry. An understanding of both the geomorphology and geology of the coastline is fundamental to the understanding of its past evolution and is an indicator of its likely future response. The geological formations underlying the coast may fundamentally control both the present morphology and the nature/rate of future response to environmental forcing. The broad outline of the coastline owes much to the variety of rocks and large-scale geological structures, which have different levels of resistance to erosion (May and Hansom, 2003). Coastal areas underlain by very resistant rock types have not changed measurably in the historic past and are not expected to significantly change within the next 100 years despite predicted changes in relative sea level or wave energy. However, even within very resistant rock types, rapid changes can occur due to cliff failure along joint or fault planes. Weaker rock types provide less resistance to erosion but may provide much of the sediment supply to beaches and barriers. The composition and nature of sediment supply is determined by the lithology of the eroding geological formations (RESPONSE, 2006).

The West African coastline has a narrow shelf, less than 30 km (Schwartz, 2005). This means that higher-energy waves reach the shore, destabilising the shore and influencing

sediment transport rates (Brink and Robinson, 2005; Schwartz, 2005). This has been responsible for the phenomenal erosion rates along the West African shore (UNEP, 1985).

Apart from the genetic and morphological classifications of coasts, (Engineers, 2002), coasts can also be classified by the angle of the prevailing waves (Mangor, 2004), Figure 2.1. Thus the coast is classified according to the angle of the prevailing wave to the coastline. There are 5 main types of coasts defined by the angle of incidence of the prevailing waves.

1. Type 1: Perpendicular wave approach, the angle of incidence is close to zero, and there is relatively zero net transport
2. Type 2: Nearly perpendicular wave approach, angle of incidence is 1^o - 10^o, net transport is small to moderate
3. Type 3: Moderate oblique wave approach, angle of incidence is 10^o - 50^o, there is large net transport
4. Type 4: Very oblique wave approach, angle of incidence is 50^o - 85^o, net transport is large
5. Type 5: Nearly coast-parallel wave approach, angle of incidence is $>85^o$, net transport is near zero

The angle of incidence is measured with respect to the normal to the coastline. This angle of incidence between the coast orientation and the prevailing waves can also be expressed as the angle between the present coastline and the coastline orientation of net zero transport. The magnitude of the sediment transport is also dependent on whether the coast is exposed, moderately protected or protected. The coast is described as protected when the "once per year event" of significant wave height with a duration of 12 hours/year

($Hs_{12h/y}$), < 1 m ; moderately exposed, 1 m < $Hs_{12h/y}$ < 3m; and exposed, having $Hs_{12h/y}$ > 3 m (Figure 2.1) (Mangor, 2004).

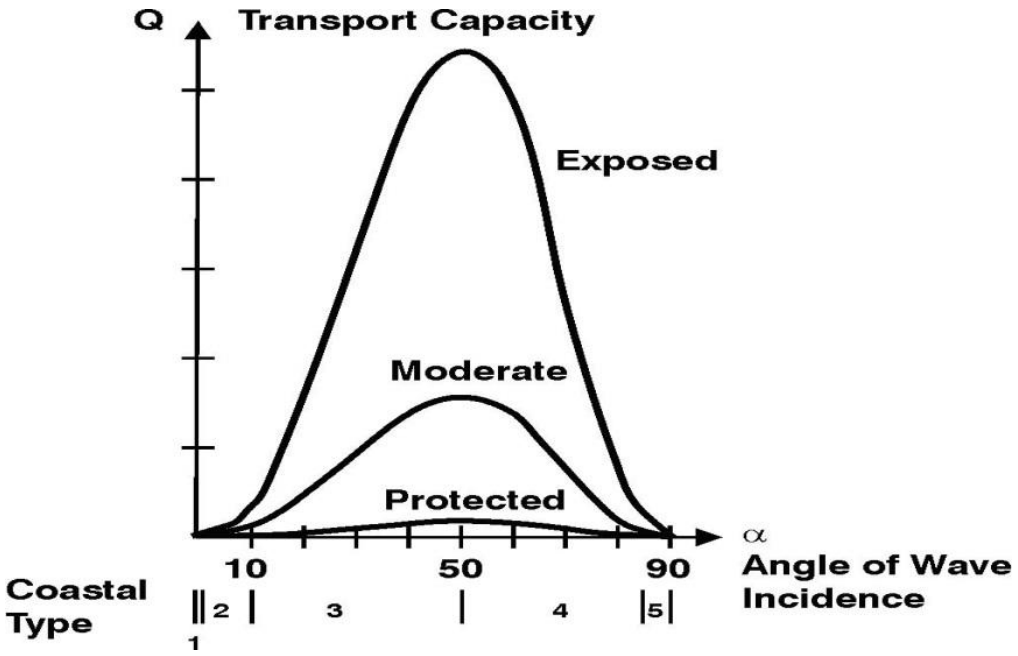

Figure 2.1: Littoral transport Q as a function of the angle of wave incidence and wave exposure (Mangor, 2004).

Directly or indirectly, climate affects most processes shaping the coast. As elsewhere, Africa's coastal climates reflect the impact of seasonal changes in Earth–Sun relations on the Intertropical Convergence Zone (ITCZ), air masses, and wind regimes. Seasonal climate changes affect the wave regime and aeolian sediment transport systems which are well known for helping in the formation of coastal dunes (Lynch et al., 2013; Schwartz, 2005). Exceptional waves generated by submarine landslides or earthquakes may also lead to significant beach erosion. These events generate destructive high-energy waves that remove the beach sediments and transport them far offshore. Sea level rise has also been one profound influence on coastal sediment transport. Sea level rise results in an increase in both horizontal and vertical sea water access to beach sediments, making them

vulnerable to crossshore and longshore sediment transport (Schwartz, 2005). Apart from the increased water level, sea level rise together with climate change has resulted in increased wave heights and thereby increase in wave energy and its eventual impact on the shore (Schwartz, 2005; Wang and Swail, 2006).

Many forces intersect and interact in the surf and swash zones of the coastal ocean, pushing sand and water up, down, and along the coast. Variations in the height and direction of waves, as well as the shape of the seafloor, drives currents that feed back and rearrange the system (Raubenheimer, 2004). Location of sand bars for instance can increase wave impact or reduce it. The location of sandbars can protect or endanger the face of the beach. As undertow drives sandbars away from the shoreline and further out to sea, waves break further from the shore. When sandbars are pushed closer to shore, waves break closer and run further up the beach (Raubenheimer, 2004).

The type of breaker as a result of beach slope may also modify the sediment transport regime. The predominant type of wave break, ε depends on wave steepness and beach slope expressed through the surf scaling parameter as $\varepsilon = \frac{\pi H}{Tgtan2\beta}$. Where: H is wave height, T is wave period, g is the acceleration of gravity and β is the beach slope. With spilling breakers, $\varepsilon > 20$, plunging occurs for $2.5 < \varepsilon < 20$ and surging breakers predominate when $\varepsilon < 2.5$ (Mangor, 2004). Thus, the higher the period, the lower ε and the higher the impact of wave on the shore.

2.8 Anthropogenic Influences on Coastal Sediment Transport

On coasts with a strong net sand transport in one direction, any interruption of the sand transport will lead to new patterns of sedimentation and erosion. The beach will start to

change, adjusting to the new conditions. If left alone long enough, a new near equilibrium situation will eventually develop (Bird, 2011). A typical example of such disturbance is the dredging of a coastal inlet, and the construction of jetties to prevent littoral sediment from filling up the channel too fast; the sediment will accumulate on one side, where the jetty is built, and make the beach accrete until it reaches the end of the pier where the littoral sediment begins get into the channel. On the other side the sand transport capacity exceeds the sand input, so the beach will erode (Lindorm, 2007). Another man-made reason for coastal erosion is the decrease of sand supply to the shore from land, due to the regulation of rivers; example the creation of the Akosombo Dam has led to substantial decrease in sediment supply to the eastern coast of Ghana (Ly, 1980). The sand gets trapped in reservoirs behind dams instead of reaching the beach. (Lindorm, 2007).

Beach erosion problems have been tackled by engineering projects such as those based on the construction of seawalls and groynes. It is currently believed that these kind of remedies solve the problem locally but do not prevent, and may in some cases intensify, the erosion effects at some neighbouring places (Bapentire, 2011). Beach nourishment projects are a more natural solution to beach erosion problems, but these require a continuous supply of sediment. Sand mining taking place on the inner continental shelf, designed to nourish beaches and coastal dunes, may also have a negative environmental impact if it induces near shore coastal erosion (da Silva *et al*., 2006). Other anthropogenic activities such as sand winning and mining (Mensah, 1997), and mineral extraction from beaches also exacerbate sediment transport as these activities destabilise the sediment arrangement, making them vulnerable to wave action.

2.9 Sediment Volume Transport Estimation

Studies on sediment transport are currently one of the main issues in the marine coastal environment. The earliest equation is that of Du Boys in 1879, who assumed that sediment particles move along the bottom in layers of progressively decreasing velocities in a vertical downward direction (Charlier and De Meyer, 1998). The first empirical formula was presented by Meyer-Peter and Müller (1943). They performed flume experiments with uniform particles and with particle mixtures. Kalinske (1947), and Einstein (1950), introduced statistical methods to represent the turbulent behaviour of the flow. Kalinske (1947) assumed a normal distribution for the instantaneous fluid velocity at grain level. Einstein (1950) gave a detailed but complicated statistical description of the particle motion in which the exchange probability of a particle is related to the hydrodynamic lift force and particle weight (Charlier and Meyer, 1998).

Total longshore sediment transport rate and its cross-shore distribution in the surf zone are essential to many coastal engineering and science studies (Smith and Zhang, 2003). Over the last decades, along many parts of coasts, a general retreat of shoreline associated with beach erosion has been observed. These morphological changes are often induced by changes in the sediment supply, caused by the construction of river dams, by the destruction of natural protections, such as dune systems, and due to modifications in the wave field and mean sea level caused by global climate changes (da Silva *et al*., 2006).

Calculating nearshore sediment transport is a challenge due to the complexity of the hydrodynamics and the variety of the governing phenomena. It is very difficult to estimate sediment fluxes on beaches due to the combination of steady flows (currents) and oscillatory flows (waves) (Camenen and Larroudé, 2003). Moreover, many other

effects should be integrated such as the variations in mean water level (tide, set-up, and set-down), breaking wave effects (turbulence and undertow), and topographic influence (mean slope and bed forms). Furthermore, these parameters induce different types of transport (bed load, suspended load, and sheet flow), with very different physical implications for the movement of sand (Camenen and Larroudé, 2003).

During the past three decades, numerous formulae and models for computing the sediment transport by waves and currents have been proposed, ranging from quasi-steady formulas based on the traction approach of Bijker, and the energetics approach of Bagnold, to complex numerical models involving higher-order turbulence closure schemes that attempt to resolve the flow field at small scale (Bayram *et al*., 2001). A probabilistic approach was also introduced by Einstein (1950). One limitation of sediment transport formulae is that authors have mainly compared and fitted their formulae only to a certain set of data (experimental or field data). For example, Bijker (1967), Bailard (1981), and Bailard and Inman (1981) mainly compared their formula to field data for littoral drift; Van Rijn (1984) compared his formula to a large variety of field data; Dibajnia and Watanabe (1992), Dibajnia, Ribberink (1998), and Ribberink and Al Salem (1994) compared and fitted their formula to experimental flume data and, Soulsby (1995) compared Bailard formula with data and models (Camenen and Larroudé, 2003). Another popular sediment transport formula is the CERC (Coastal Engineering Research Centre) formula that is widely used for longshore sediment transport estimation.

"The Wang *et al*., (1998) paper is significant because it provides one more basis for distrust of the CERC longshore transport equation. Given that our understanding of longshore transport processes is incomplete, that field measurement techniques are inaccurate and produce inconsistent results, and inherent problems with the CERC

formula exist, it is not even clear that we know what "realistic" transport rates are. The logical outcome should be a fundamental re-examination of longshore transport assumptions and predictive methods" (Stutz and Pilkey, 1999), in their conclusion on the discussion of Wang *et al*., (1998).

The Soulsby-Van Rijn equation is one of recent sediment volume transport formulae which is made up of a combination of the Soulsby and the Van Rijn sediment transport formulae. It is more useful as it has certain attractive features that take into account sediment transport mechanisms (Roelvink and Reniers, 2011). These features are that:

It is a very simple expression

It is easy to implement

It is reasonably close to Van Rijn's full formulations

It gives clear insight in mechanisms

It considers bed load and suspended load separately

It has combined current and wave effects

It has a critical velocity and

It has a bed slope effect

2.10 Sediment Transport Rate along the coast of Ghana

The coast of Ghana has sediment transport rates that exceed one million cubic yards (1 yard = 0.9144 m) thus about 764554.9 m^3 of longshore sediment transport in one year, as a result of the large waves on these exposed open ocean coasts (Hayes *et al*., 2008). However, not much work has been done in Ghana concerning quantification of coastal sediment volume transport rates. Most studies have been focused on beach erosion rates, for example (Addo, 2003; Appeaning *et al*., 2008; Ly, 1980) and sediment contribution

by inland fluvial systems to the coast (Akrasi, 2011; Boateng *et al*., 2012). These studies are important especially the later which reveals how much the sediment supply to the coast had been drastically reduced (from a little over $72\times10^6 m^3/a$ to about $8\times10^6 m^3$) as a result of anthropogenic activities (Boateng *et al*., 2012). This shows how much in deficit the coast is of sediment.

CHAPTER THREE

METHODOLOGY

3.1 Study Area

Ghana lies along the Gulf of Guinea in West Africa, 5.5 degrees north of the Equator, within longitudes 3°5' W and 1°10' E and Latitudes 4°35'N and 11° N (UNEP, 2007). The bordering countries are Cote D'Ivoire towards the West, Burkina Faso in the North and Togo towards the East. Ghana has a total land area of 238,533 km^2 with a coastline, the study area (Figure 3.1), of about 550km. Its southwards facing coastline forms part of the West African coast which is subject to strong longshore drift. The Gulf of Guinea has the strongest drift rates, sometimes exceeding 1 million m^3 a^{-1} of sand or gravel (Schwartz, 2005). Thus there is a net littoral transport in a particular direction and according to Wellens-Mensah *et al*., (2002), it is an eastwards drift along the coast. The coastal zone of Ghana may be defined as the area below the 30m contour representing about 7% of the land area. This portion of the land though small supports about 25% of the nation's total population (Boateng, 2009).

The coast of Ghana has been sub-divided into three major zones based on geomorphologic characteristics. They are Eastern, Central and Western coast (Boateng, 2009). The Eastern coast, is about 149km, stretches from Aflao (Togo Border) in the East to the Laloi lagoon west of Prampram (Boateng, 2009). This zone is a long stretch of eroding sandy beach and is a high-energy beach with wave heights often exceeding 1 metre in the surf zone (Ly, 1980). Other features include barrier beaches and bars confining lagoons. The eastern zone has a major river, the Volta River that tends to influence the geomorphology of the zone (Wellens-Mensah in Boateng, 2009). The

surface geology of the area is made up of fluvial sediments delivered from the river as well as marine and fluvial-marine sediments. The barrier beaches, comprised of medium to coarse sand, rise steeply in elevation to about 2m above mean sea level.

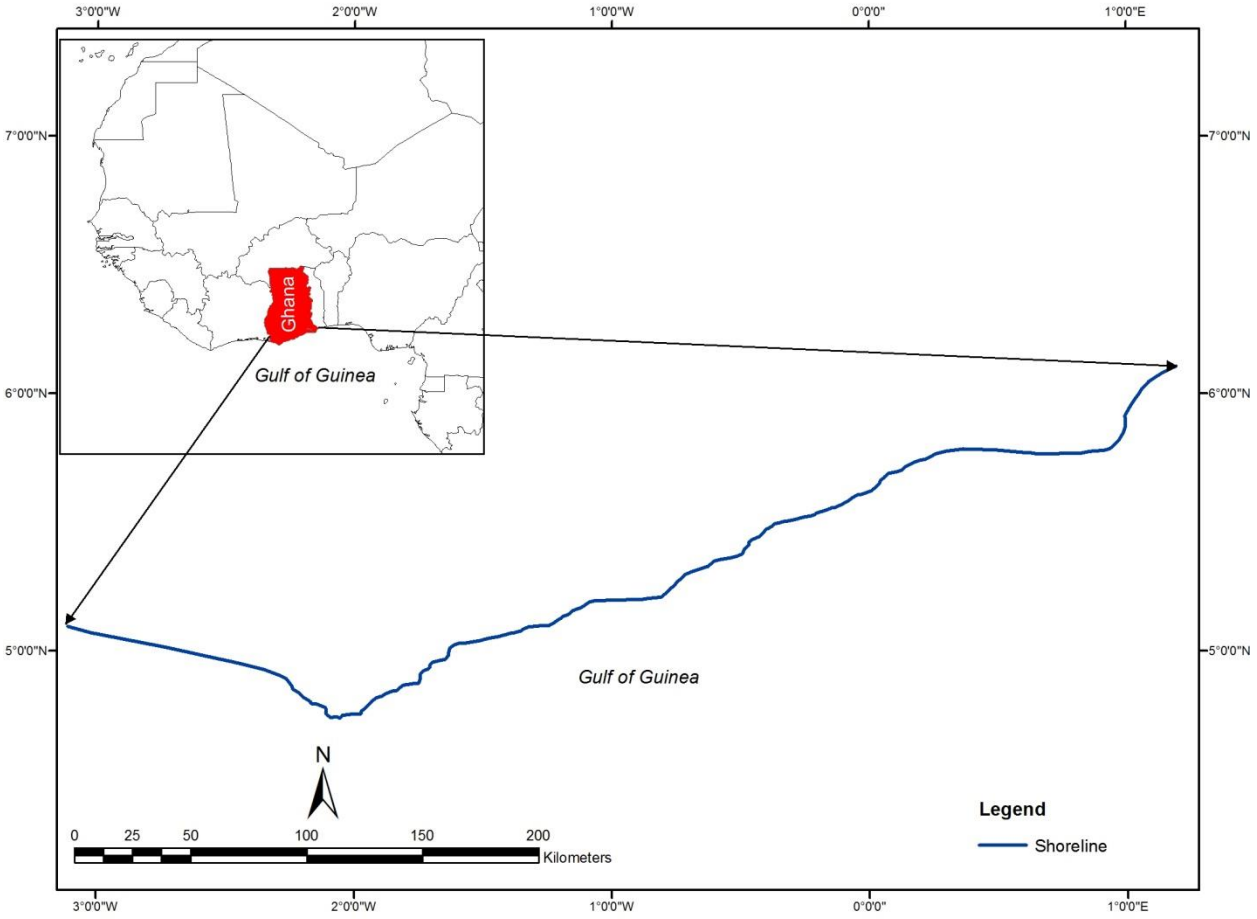

Figure 3.1: Map showing study area (Coastline of Ghana)

The Central coast represents a medium energy environment. It is an embayment coast of rocky headlands and sand bars with spits enclosing coastal lagoons. It consists of 321km of shoreline extending from Laloi Lagoon west of Prampram to the estuary of River Ankobra near Axim. The morphology of this coast is influenced by sediment delivered from a series of north to south draining rivers including the Densu River on the West of Accra, Ayensu River on the West of Winneba (Boateng, 2006). Others include River

Nakwa East of Cape Coast, River Pra East of Shama and Ankobra River West of Axim. Sediments tend to be confined within embayments between rocky headlands and promontories. The beaches along certain sections of this coast are thought to be fairly stable (Armah and Amlalo, 1998).

The Western coast covers 95km of shoreline and it is a relatively low energy beach. It consists of a flat and wide beach backed by a coastal lagoon. The coast extends from the estuary of the Ankobra River to the border with La Cote d'Ivoire. This coast comprises gently sloping fine sandy beaches backed by coastal lagoons. Sediments forming these beaches are likely to be derived from the Ankobra and the Tano Rivers. Figure 3.2 and 3.3a and 3.3b show major coastal geology adapted from Agyei Duodu *et al*., (2009) and bathymetry along the West African coastline and point of deployment of wave rider buoy respectively.

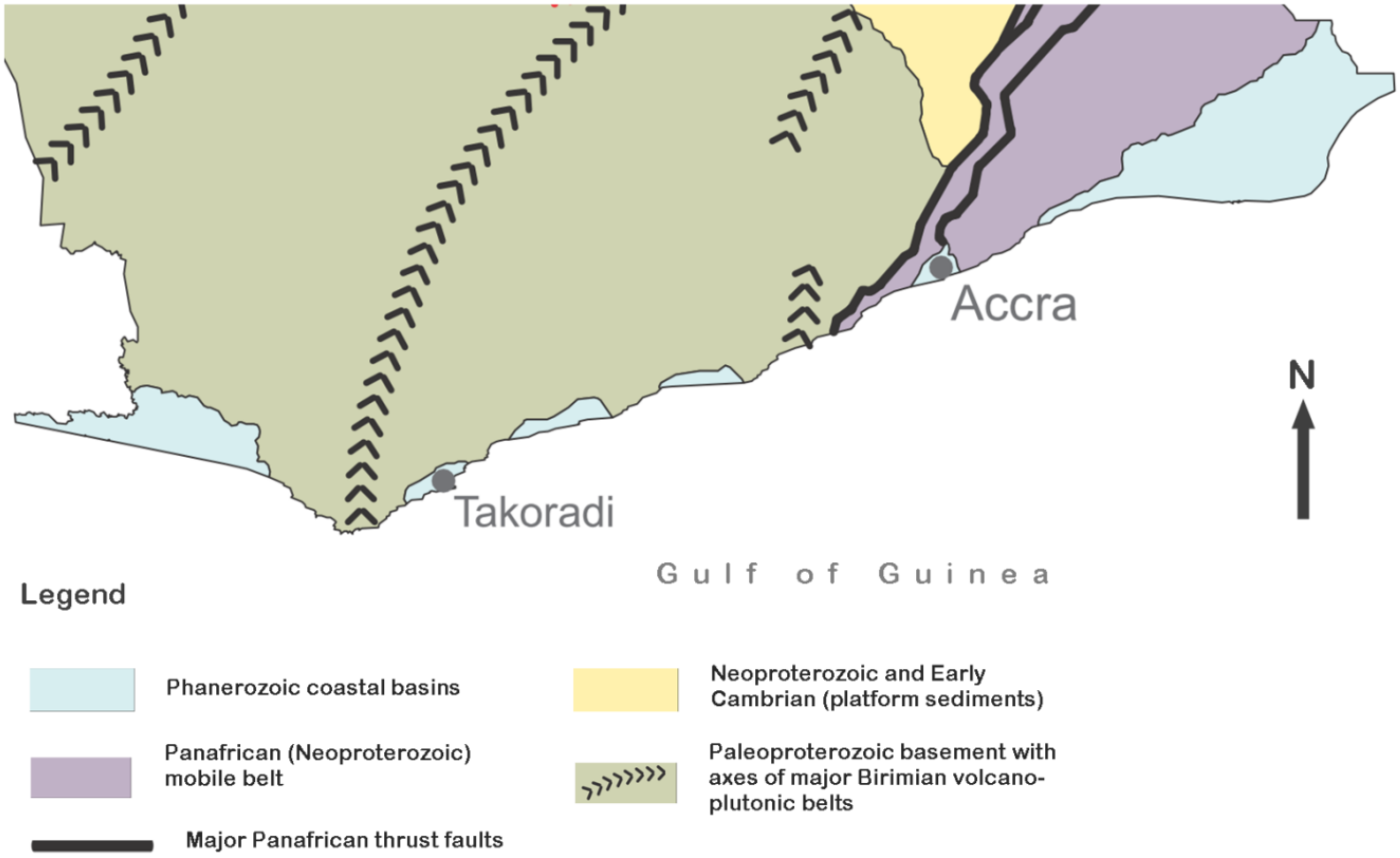

Figure 3.2: Major coastal Geology of Ghana (Adapted from Agyei Duodu et al. (2009))

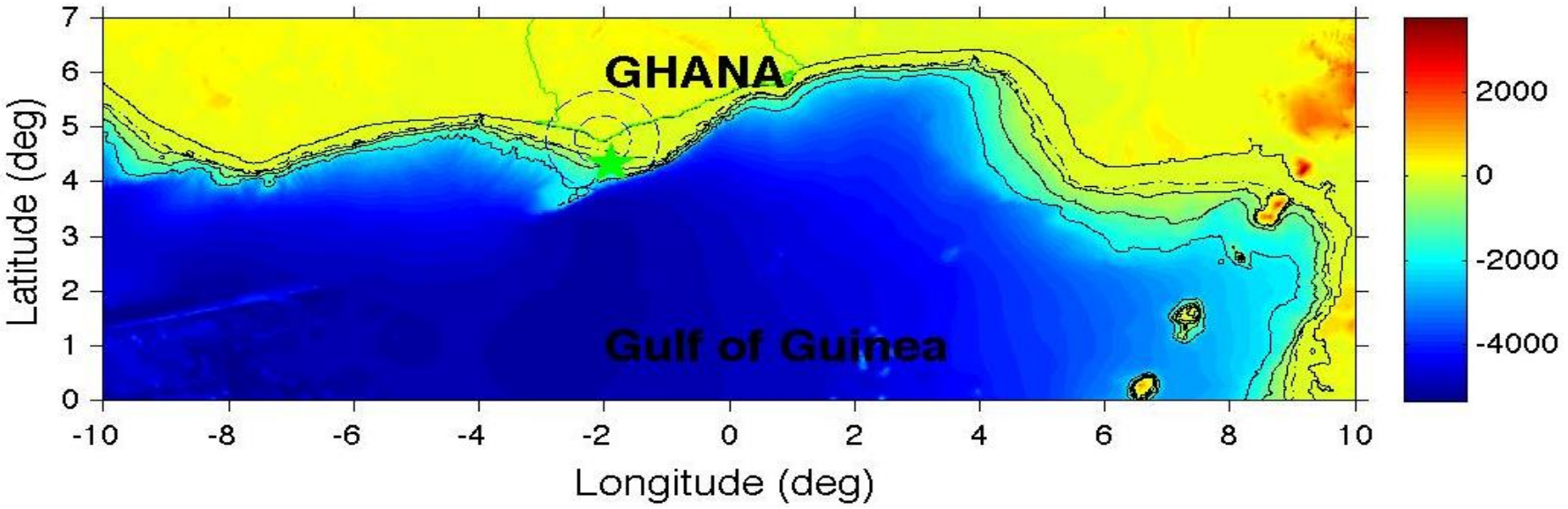

Figure 3.3a: West African Coastal area showing Bathymetry and location of Wave Rider Buoy (green star)

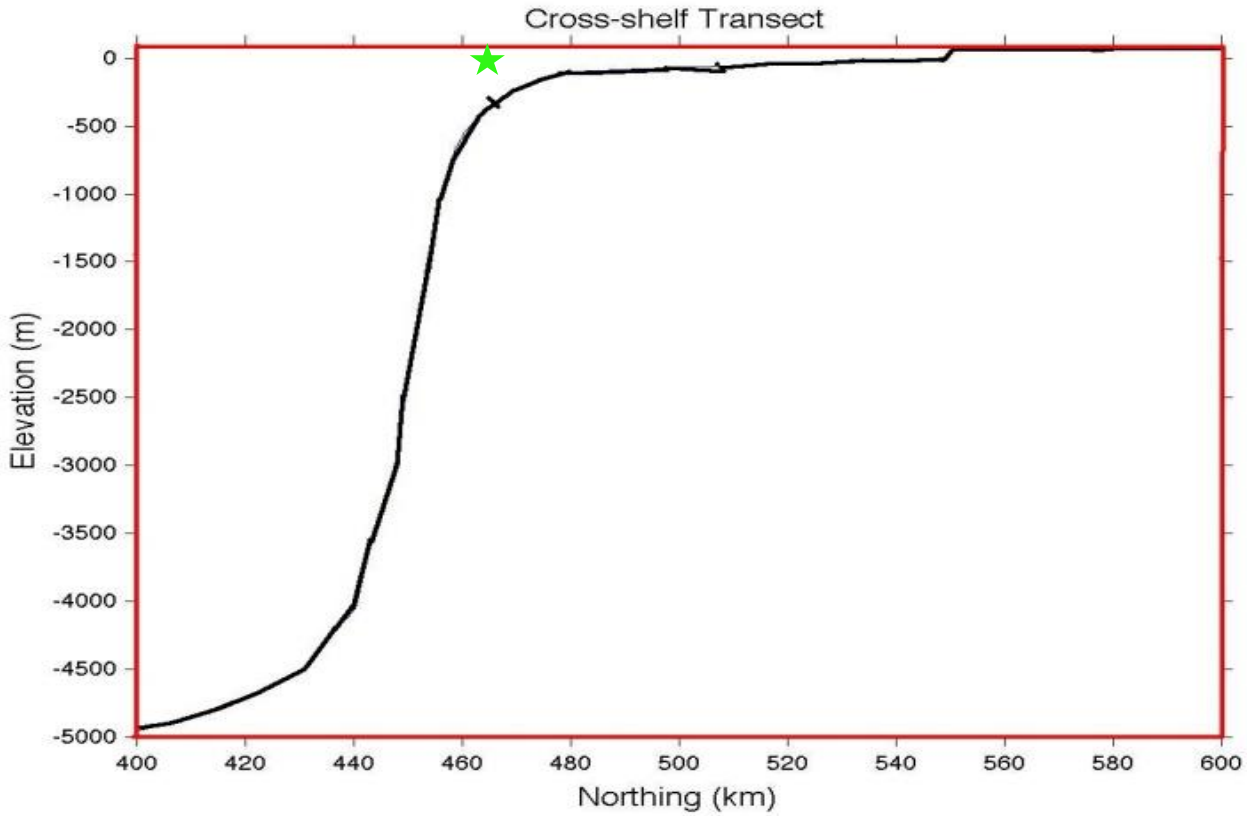

Figure 3.3b: Cross-shelf Bathymetry Transect showing location of Wave Rider Buoy (green star)

3.1.1 Winds Waves and Currents

Surface atmospheric circulation in the study area is largely influenced by north and south trade winds and the position of the ITCZ. Extreme winds are caused by squalls (storms), associated with the leading edge of multi-cell thunderstorms. Winds are predominantly south-western. The average wind speed range between 3.7 - 4.0 m/s with maximum wind speeds ranging between 8.8 - 10.8 m/s. There is also little wind speeds and directions differences over the course of the year (EPA, 2009).

The principal current along the Ghana coastline is the Guinea Current (GCLME, 2006; TGL, 2009), which is an offshoot of the Equatorial Counter Current. The current is less persistent near-shore than farther offshore as it gets attenuated by locally generated currents and winds. The coastal surface currents are predominantly wind-driven and are confined to a layer of 10 to 40 m thickness (TGL, 2009). The wave induced longshore currents are generally in the west to east direction which is an indication of the direction the waves impinge the shoreline. The longshore currents average approximately 1 m/s and vary between 0.5 and 1.5 m/s. The magnitude increases during rough sea conditions (EPA, 2009). Waves reaching the shores of Ghana consist of swells originating from the oceanic area around the Antarctica Continent and seas generated by locally occurring winds (EPA, 2009). The significant height of the waves generally lies between 0.9 m and 1.4 m and rarely attains 2.5 m or more. The significant wave height for 50 percent of the time is about 1.4 m, the period is between 10 to 15 seconds and spring high tide is about 1.26 m (Appeaning *et al.*, 2008) The most common amplitude of waves in the region is 1.0 m but annual significant swells could reach 3.3 m in some instances (Short, 2012; TGL, 2009). Swells attaining heights of approximately five to six meters occur infrequently with a 10 to 20 year periodicity. The peak wave period for the swells

generally falls in the range of seven to fourteen. The swell wave direction is almost always from the south or south-west (EPA, 2009).

3.1.2 The West African Meteorology and Shoreline Topography

Surface wind circulating over the Gulf of Guinea is dominated by the southeast trade winds. The trade winds in the Gulf of Guinea vary seasonally (Brink and Robinson, 2005). The wind speeds along the coast are relatively steady and weak, with monthly means generally less than 5 ms^{-1} in the boreal summer and approximately half that value in the winter (Houghton, 1996). During the summer there is a 10 - 20° rotation counterclockwise in the mean direction (Piton, 1987). In the central and western equatorial Atlantic, where the Inter-Tropical Convergence Zone (ITCZ) reaches the equator in the boreal winter, wind stress changes are more pronounced. Seasonal variations in rainfall are also controlled by the seasonal displacements of the ITCZ (Hastenrath, 1985).

The West African coastline consists of two distinct segments with a zonal and meridional orientation along the northern and eastern boundaries, respectively. The shelf defined by the shelf break at 100-150 m depth is generally narrow, less than 30 km wide except north of 7° N, Southeast of Takoradi, along the Niger River Delta and south of Cape Lopez. The shelf is incised at several locations by submarine canyons such as the Avon, Mahin and Calabar in Nigeria, Trou sans Fonds in Ivory Coast, and the Congo-Zaire Canyon south of Pointe Noire. One of the implications of a narrow continental shelf is that higher energy waves (swells) would reach the shore and influence shoreline stability. The Guinea Gulf and the Bight of Benin are largely open to southwesterly to south-southeasterly long swells induced by fetches in the South Atlantic, while the coast from

Angola to Gabon are affected by southerly to west-southwestherly long swells from the South Atlantic (Brink and Robinson, 2005).

3.3 Data Description

Data sets used include wave and wind data from NOAA global wave model at 4°N, 1°W. The data ranged from January 1997 to January 2006. The data contained significant wave heights with corresponding wave periods, wave directions, wind speeds and wind directions. Wave heights ranged from 0 m (in 2005) – 2.82 m (in 1999); wave periods ranged from 3.11 s (in 2004) – 19.68 s (in 2002); wave directions were within 46.37° and 330.64°. Wind speeds also ranged from 0 ms^{-1} (in 1997) – 11ms^{-1} (in 2002); and wind directions were within 1.1° and 358.94°. Wave data from buoy deployed by the Coastal Processes Project in the University of Ghana were also analysed. The buoy data was from a GPS location at the edge of the continental shelf of Ghana; approximately 04°13′49.11″N; 01°37′30.32″W. Three months wave data from the buoy was analysed covering August, 2010; October and November 2011.

3.4 Wave Data Analysis

Data sets were analysed using scripts developed in MATLAB (R2010a) and Microsoft® Office Excel 2010. Wave data from the Coastal Process Project buoy was also analysed using MATLAB and DATAWELL W@ves21. The World Meteorological Organization Guide to Wave Analysis and Forecasting, (1998) was also used as a guide. Wave analysis and statistics were based on short-term and long-term (Holthuijsen, 2007).

Wave energies E, were calculated using the total energy of a simple linear wave, which is related to the wave height H, as follows:

$$E = \rho_w g H^2/8 \qquad (3.1)$$

Where: ρ_w is the water density (water density = 1000 kgm^{-3}); g is the acceleration due to gravity (9.81 ms^{-2}) and; H is the significant wave height.

Surge height S_h, was calculated using

$$S_h = [\tau/(2g\rho_w)] \times (L/h) \qquad (3.2)$$

Where: wind stress

$$\tau = \rho_a C_D U^2$$

$L =$ distance of water from shoreline over which wind stress is experienced, (this was assumed to be 10^5 m);

$h =$ depth of water, (this was assumed to be 10 m; this follows the assumption that the wind stress from the wind speed will not be enough to lift a total 10 m depth of water);

$\rho_a =$ air density, (1 kgm^{-3});

$C_D =$ drag coefficient, (usually ranging from 0.001 – 0.002)

$U =$ wind speed, (taken from data).

3.5 Sediment Transport Analysis

Sediment transport was calculated based on the Soulsby-Van Rijn's total sediment transport (q_t) equation (Soulsby, 1997). The equation was split to obtain potential bed-

load and suspended transports in the *x* and *y* directions. The Soulsby-Van Rijn's total sediment transport, q_t is written as:

$$q_t = A_s \overline{U} \left[\left(\overline{U}^2 + \frac{0.018}{C_D} U_{rms}^2 \right)^{\frac{1}{2}} - \overline{U}_{cr} \right]^{2.4} (1 - 1.6 \tan \beta) \quad (3.3)$$

Where:

$$q_t = (q_x, q_y)$$

$$A_s = A_{sb} + A_{ss}$$

$$A_{sb} = \frac{0.005h \left({}^{D_{50}}/_{h} \right)^{1.2}}{[(s-1)gD_{50}]^{1.2}}$$

$$A_{ss} = \frac{0.012 D_{50} {D_*}^{-0.6}}{[(s-1)gD_{50}]^{1.2}}$$

$$C_D = \left[\frac{0.40}{\ln\left({}^{h}/_{z_0} - 1 \right)} \right]^2$$

U_{cr} = critical velocity of incipient motion (effective roughness $K_s = 3D_{90}$, $D_{90} = 2D_{50}$)

$$\overline{U}_{cr} = 0.19 (D_{50})^{0.1} \log_{10} \left(\frac{4h}{D_{90}} \right) \qquad ; D_{50} \leq 0.5mm$$

$$\overline{U}_{cr} = 8.5 (D_{50})^{0.6} \log_{10} \left(\frac{4h}{D_{90}} \right) \qquad ; 0.5 \leq D_{50} \leq 2mm$$

$$D_* = \left[\frac{g(s-1)}{\nu^2} \right]^{\frac{1}{3}} D_{50}$$

$\overline{\mathrm{U}}$ = velocity with vertical averaged $(\overline{u}, \overline{v})$

U_{rms} = root mean square orbital velocity, $U_{rms} = \left(u_{orb}, v_{orb,y}\right)_{rms}$

β = slope of bed in streamwise direction, positive if flow runs uphill

h = depth (water depth at which all waves would have broken, this was assume to be 3 m)

D_{50} = diameter corresponding to 50% of the material being finer

D_{90} = diameter corresponding to 90% of the material being finer

z_0 = bed roughness ($\cong 0.006$ m)

g = acceleration due to gravity

ν = kinematics viscosity ($\nu = 2 \cdot 10^{-6}$ m^2s^{-1}); (this was assumed to be 1 instead as the former gave extremely low values).

Soulsby (1997) developed the formulation by finding a suitable form of the equation that could be fitted to the numerical results of Van Rijn's 1993 model (Roelvink and Reniers, 2011). This formulation was used to calculate the potential bed-load and suspended transports in the *x* and *y* directions.

The formulation is as follows:

$$S_{bx} = A_{cal} A_{sb} u \xi \quad (3.4)$$

$$S_{by} = A_{cal} A_{sb} v \xi \quad (3.5)$$

$$S_{bx} = A_{cal} A_{ss} u \xi \quad (3.6)$$

$$S_{by} = A_{cal} A_{ss} v \xi \quad (3.7)$$

Where: A_{cal} is a user-defined calibration factor. A_{cal} was taken as 1.

The term ξ is the square bracketed portion of the total sediment transport equation, q_t which changes to:

$$\xi = \left(\sqrt{u^2 + v^2 + \frac{0.018}{C_D} U_{rms}^2} - \overline{U}_{cr} \right)^{2.4}$$

u and v are orbital velocities in the *x* and *y* directions respectively; all other terms retained their significance.

3.6 Impact Assessment

The geological map of Ghana was digitised in ArcGIS to obtain a coastal geological map. The shoreline was also divided into 8 zones (A, B, C, D, E, F, G and H) with each stretch having a relatively average similar orientation. The coastline orientation is not uniform so each zone was obtained as the coastline angle appreciably changed from the angle of the previous zone moving from West to East.The coastal geological map and the coastline zonation was used with Mangor's coastal classifications (2004), coastal bathymetry map (Figure 3.2) and directional outputs of the wave analysis to assess the impact of the waves on the coast.

CHAPTER FOUR

RESULTS

4.1 Data Distribution and Statistics

Frequency distributions were negatively skewed except for wave heights. Skewness were as follows: 0.557, -0.546, -0.474, -0.077 and -1.176 for wave heights, wave periods, wave directions, wind speeds and wind directions respectively. Periods and wave directions also revealed multimodal and bimodal distributions respectively. Wave heights, periods and wind speeds also revealed a nearly similar yearly pattern.

From Figure 4.1, about 55% of the wave heights were below the mean, 1.39 m. Thus the wave heights below 1.39 m form the majority of waves arriving at the coast of Ghana. The other 45%, though lesser in number were of higher wave heights and therefore contributed more energy. They reach a maximum of about 2.82 m. Two wave heights, 1.26 m and 1.3 m were the most occurring wave heights followed by 1.28 m, 1.27 m, 1.17 m, 1.09 m, 1.16 m, 1.23 m, 1.22 m, 1.19 m, 1.25 m, 1.4 m, 1.31 m and 1.32 m by decreasing frequencies which were also in the 300 range of frequencies. Wave period distribution revealed several groupings with peaks, a multimodal distribution (Figure 4.2). There were approximately 11 groups and a large number of the periods occurred between 9 s and 14 seconds. The periods T, reflected the celerity C (group speed), of various waves arriving at the coast (refer to Figure 4.8 and Table 4.2). The wave celerity is a function of the period ($C = \frac{gT}{2\pi}$), in deep water (Engineers, 2002). Figure 4.2 also gives a reflection of travelling waves as they arrive in sorted groups of identical velocity. The wave periods also observed a relatively similar yearly trend as the wave heights.

Highest periods were however observed in the month of May (Figure 4.14 (B)). Thus, high speed waves occur in May. Most occurring wave periods (about 63%) were between 10 s and 14 s and they occurred with wave heights between 1 m and 2 m (about 80%), (Table 4.4). Wave periods had an annual average decrease rate of -0.079 sy^{-1}. Wind speeds tend to be relatively normally distributed between 0ms^{-1} and 10 ms^{-1} (Figure 4.3). Most wind speeds however occurred between 3ms^{-1} and 7ms^{-1}.

About 88.4% of the waves come from the South-South-East and the South-South-West directions (Figure 4.4) and waves concentrated in this region. Two peaks were also observed; one for the South-South-East direction and the other for the South-South-West direction. The South-South-West direction had the highest peak. The remaining percentage, about 12%, was spread over other directions. Winds come mainly from the South to the West-South-West directions with some few occurrences spread over other directions (Figure 4.5). All data were not normally distributed as KS-test (Kolmogorov-Smirnov test) performed on each data set rejected the hypothesis that data sets were normally distributed.

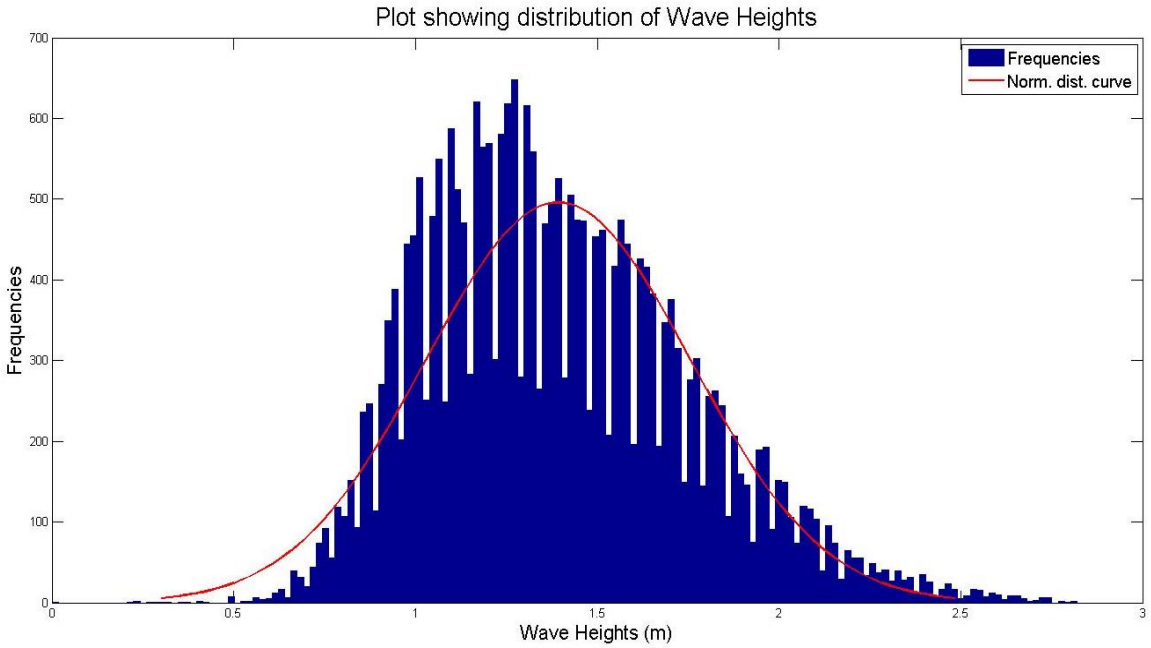

Figure 4.1: Distribution of wave heights.

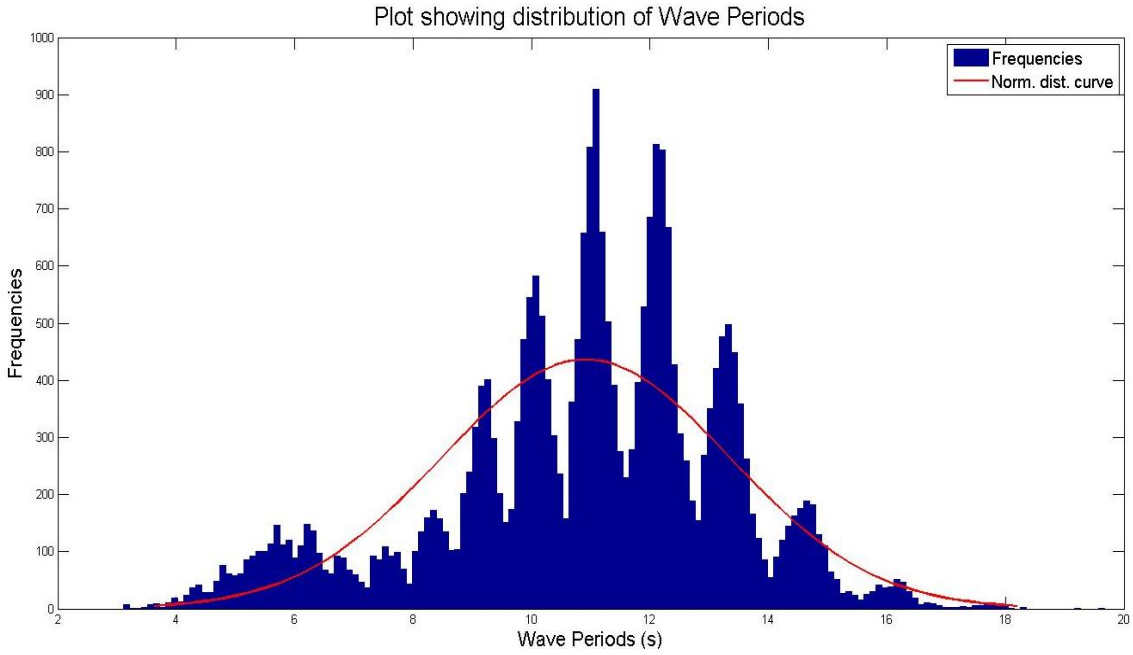

Figure 4.2: Distribution of wave periods

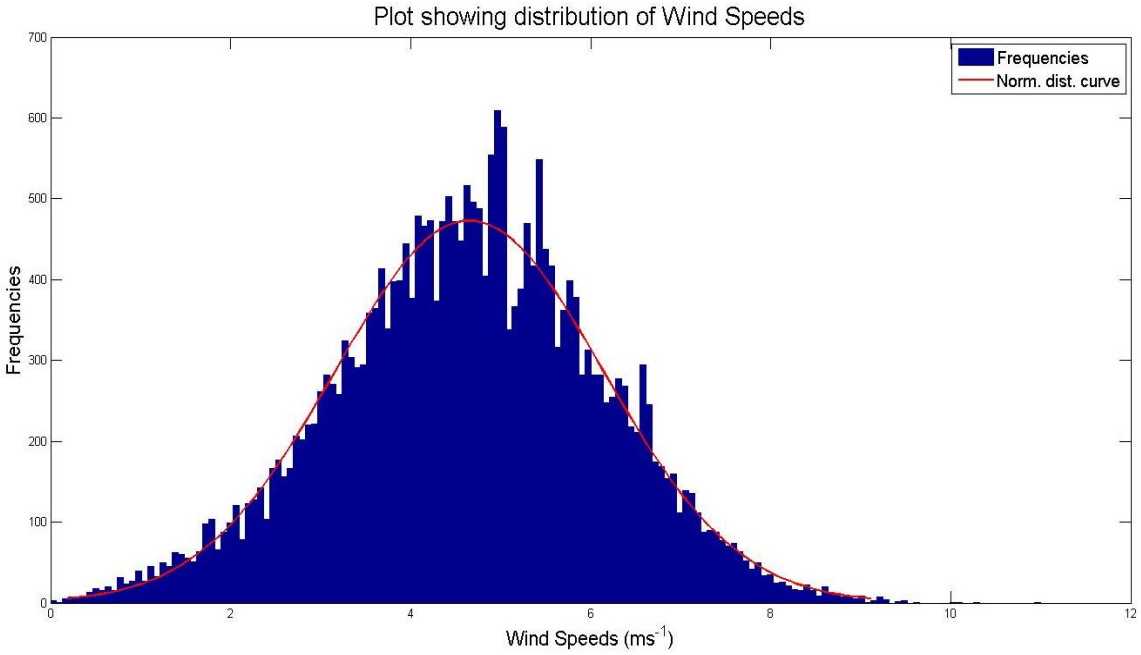

Figure 4.3: Distribution of wind speeds

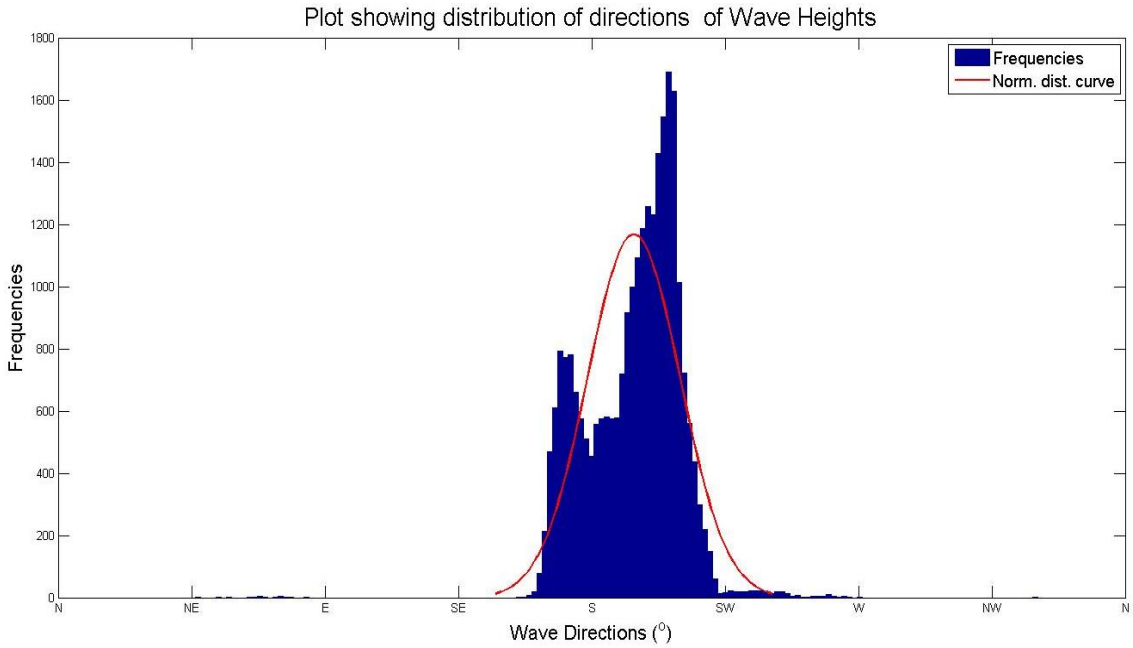

Figure 4.4: Distribution of wave directions

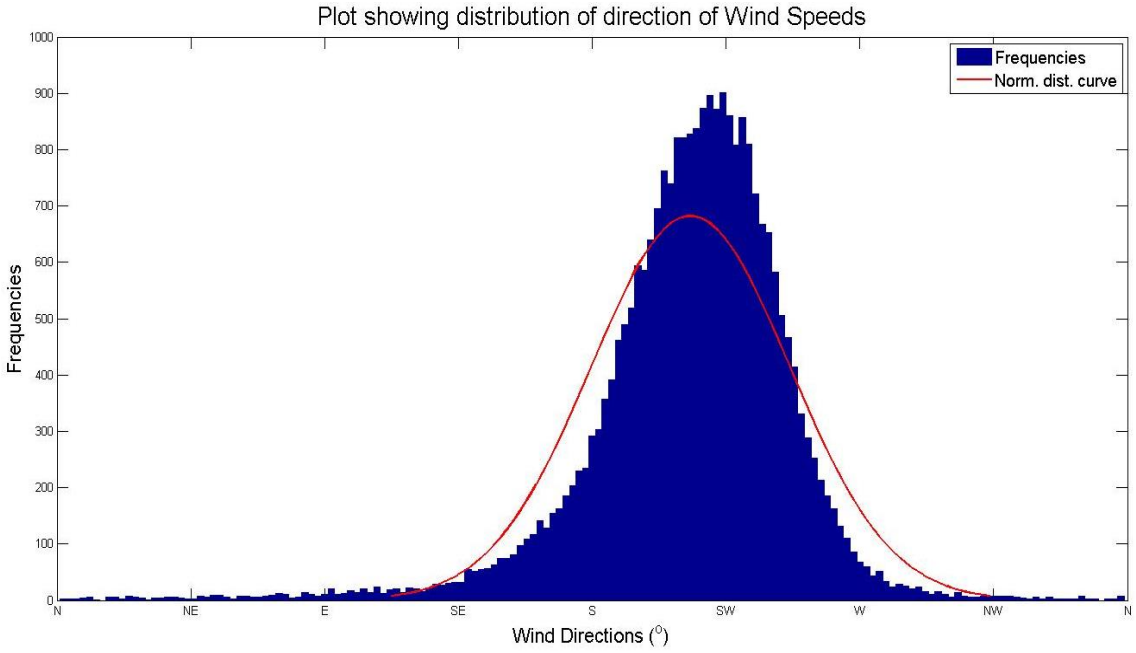

Figure 4.5: Distribution of wind direction

Figure 4.6 shows the wave climate during the years of study with reference to the Douglas sea scale. A 30 day moving average is also shown in light gray. Wave heights ranged from 0 – 2.82 m with a 0.36 standard deviation and variance of 0.13. About 99.5% were between the smooth and moderate sea scale. However, about 0.5% were within rough sea state. Rough sea states were experienced in all years except 1998 and 2001. An average wave height of 1.39 m can be used to describe the Ghanaian sea state as moderate with reference to the Douglas Scale. From Figure 4.6, it could also be observed that wave heights increased gradually from the beginning of the year till it reaches a peak around the middle of the year and then begins to drop gradually to a low at the end of each year. A linear fit gave a slope of 5.7e-006 m (Figure 4.7). This translates to an average of 0.01664 my^{-1}.

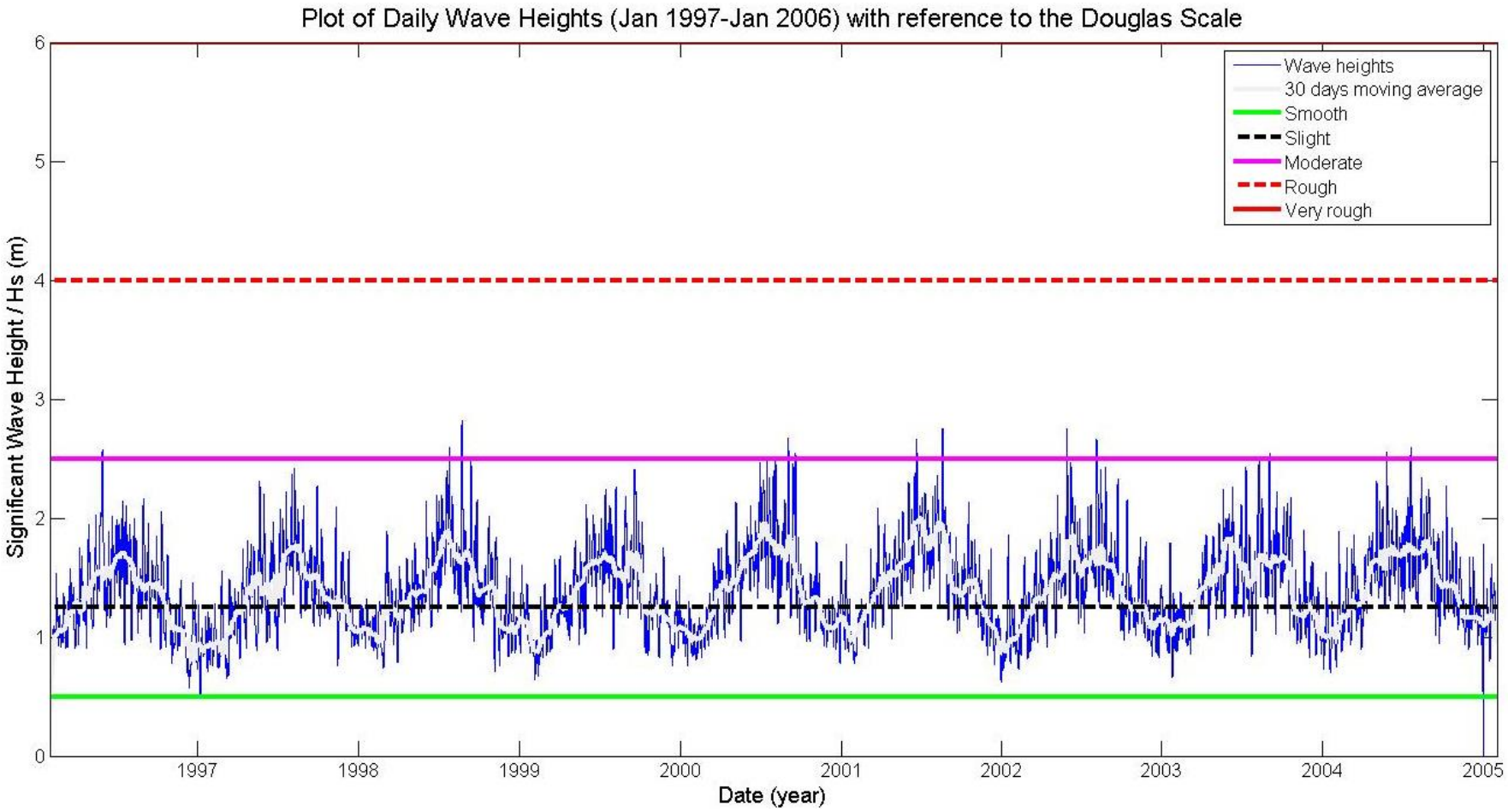

Figure 4.6: Wave heights with reference to the Douglas scale and 30days moving average

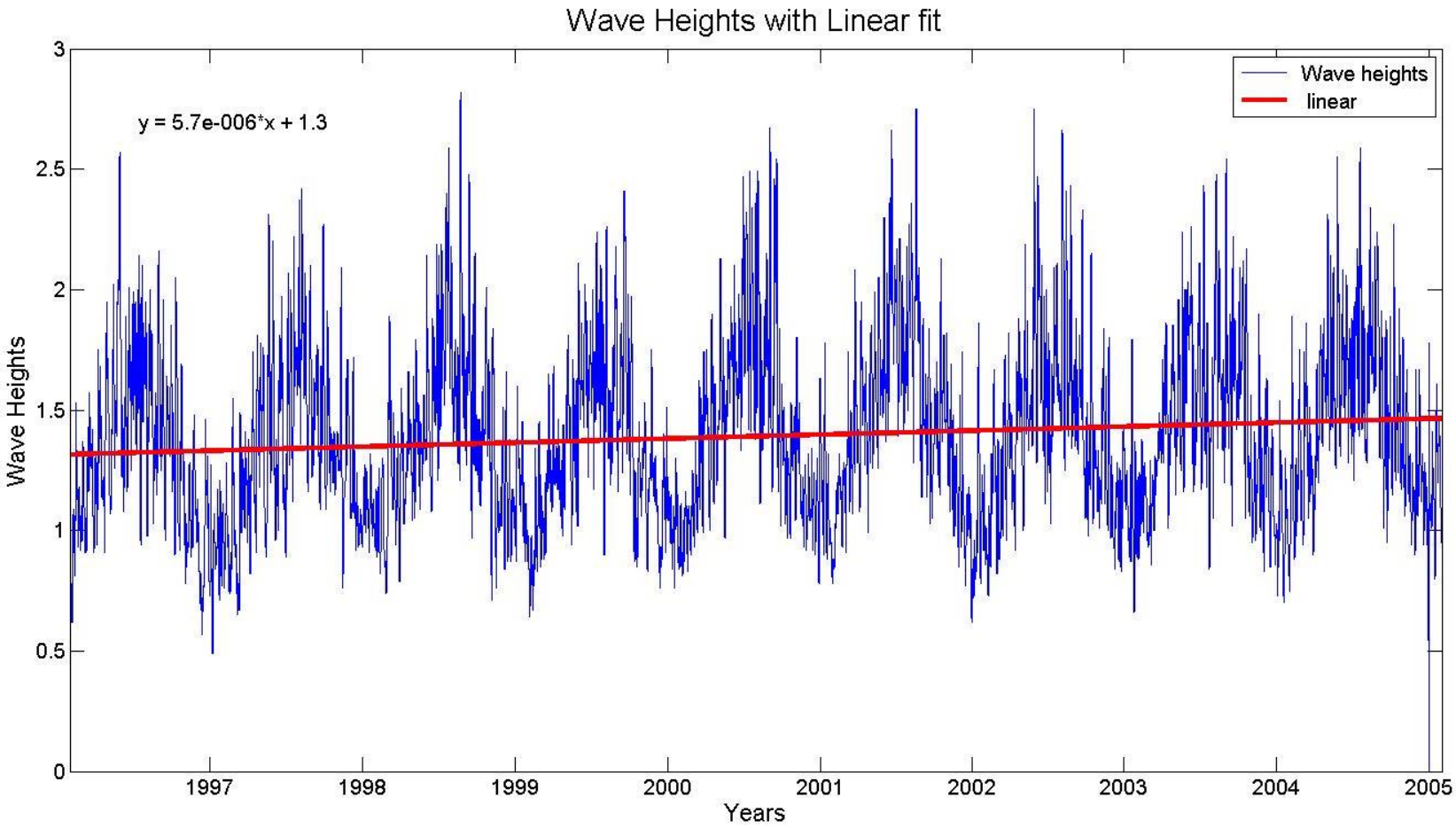

Figure 4.7: Wave heights with linear fit

Figure 4.8 reveals the high variation that exists between next successive wave periods. The wave periods had a variance of 5.90 and standard deviation of 2.43. Wave periods ranged from 3.11 s to 19.68 s. The mean which was 10.91 s was found to be close to the mode, 11.07 s. Majority of the wave periods were between 10 s and 14 s making up about 63%. Linear regression gave a gradient of -2.7e-005 which amounts to -0.07884 sy^{-1} Figure 4.9.

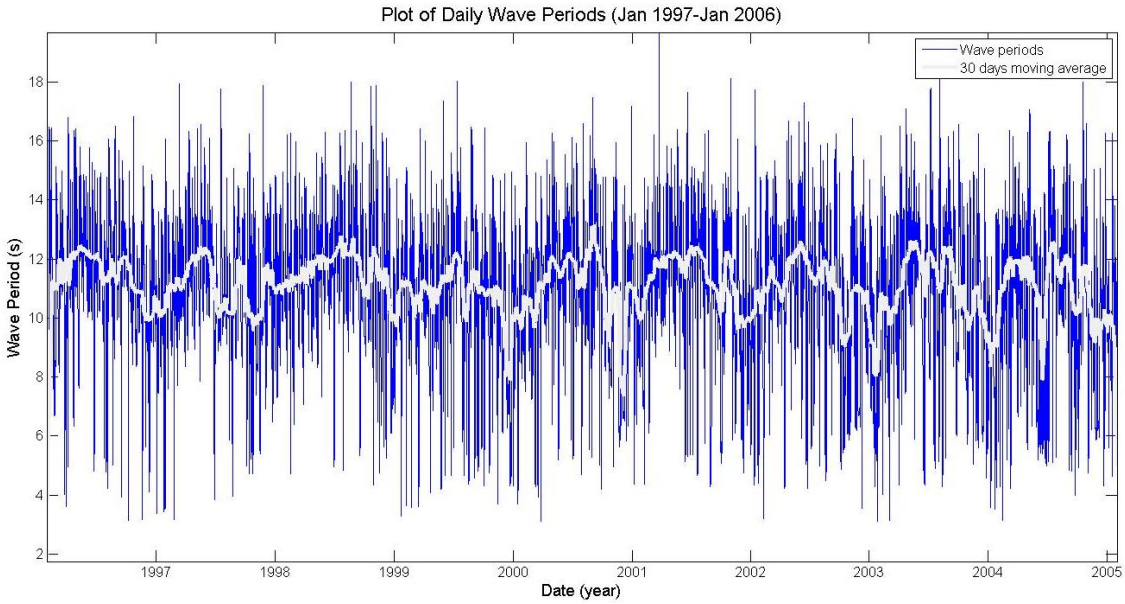

Figure 4.8: Daily wave periods with 30 days moving average (light gray)

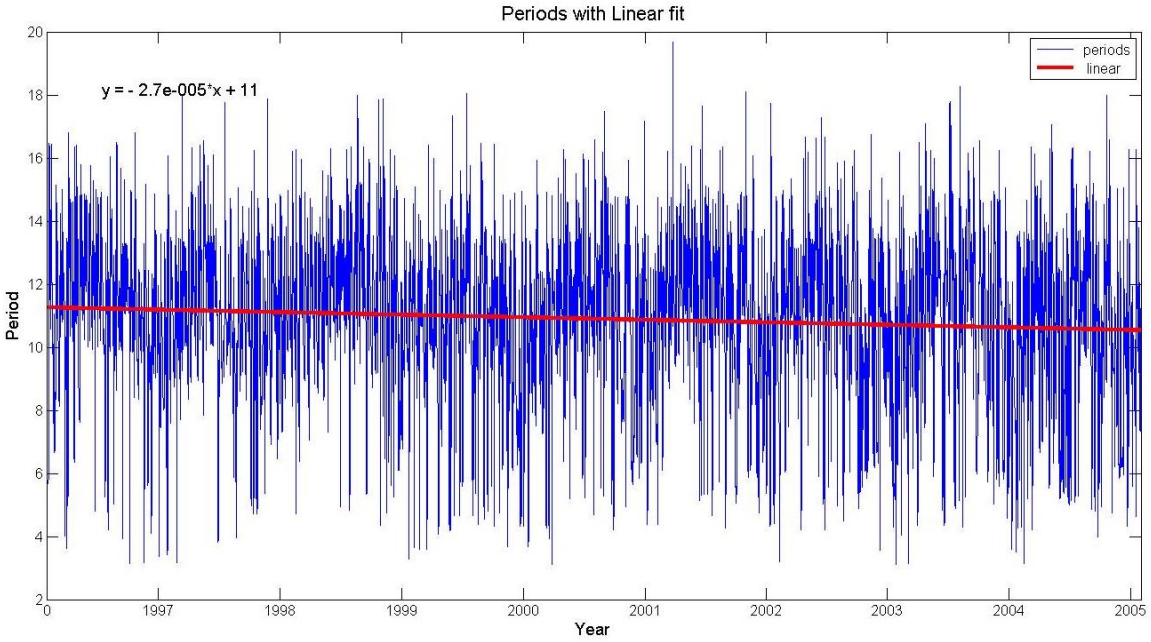

Figure 4.9: Wave periods with linear fit

The wind speeds recorded during the studied years with reference to the Beaufort Wind Force Scale are presented in Figure 4.10. Wind speeds ranged from 0 ms^{-1} to 11 m^{-1} – ranging from calm to fresh breeze on the Beaufort scale. About 99% were between calm air and below moderate breeze while 1% made up fresh breeze. Wind speeds had a mean of 4.65 ms^{-1} and showed high variability with variance of 2.21 and standard deviation of 1.49. Linear regression of wind speeds in Figure 4.11 gave a gradient of 2.5e-005 (0.073 $ms^{-1}y^{-1}$). Figure 4.12 compares monthly average wind speeds from the sea and that on the coast from Jensen (2001). Wind speeds from the sea showed a relatively similar trend to wind speeds from the coast. Sea winds were however higher than their corresponding monthly average winds from the coast by an average of 2 ms^{-1}.

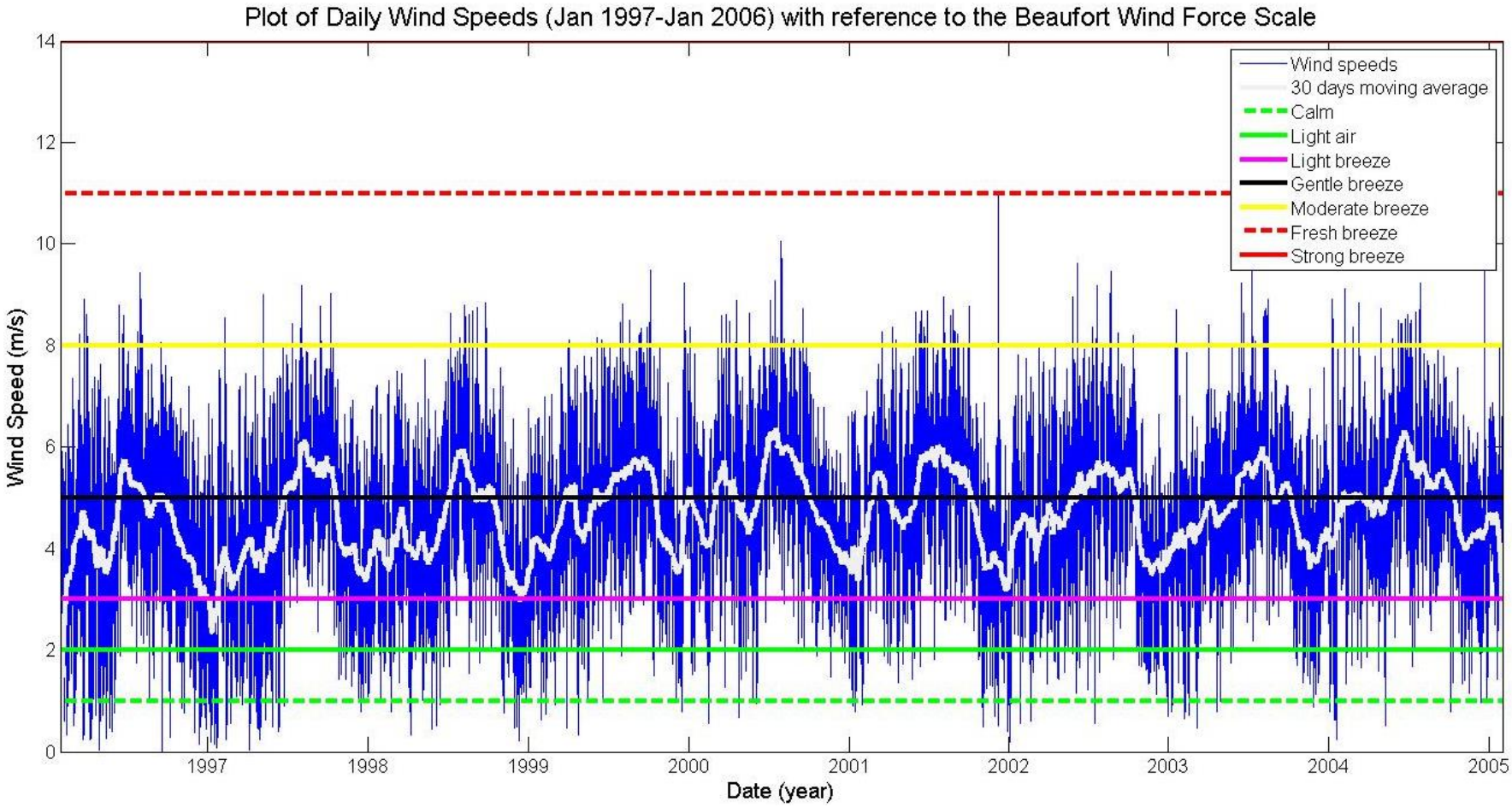

Figure 4.10: Daily wind speeds with 30 days moving average

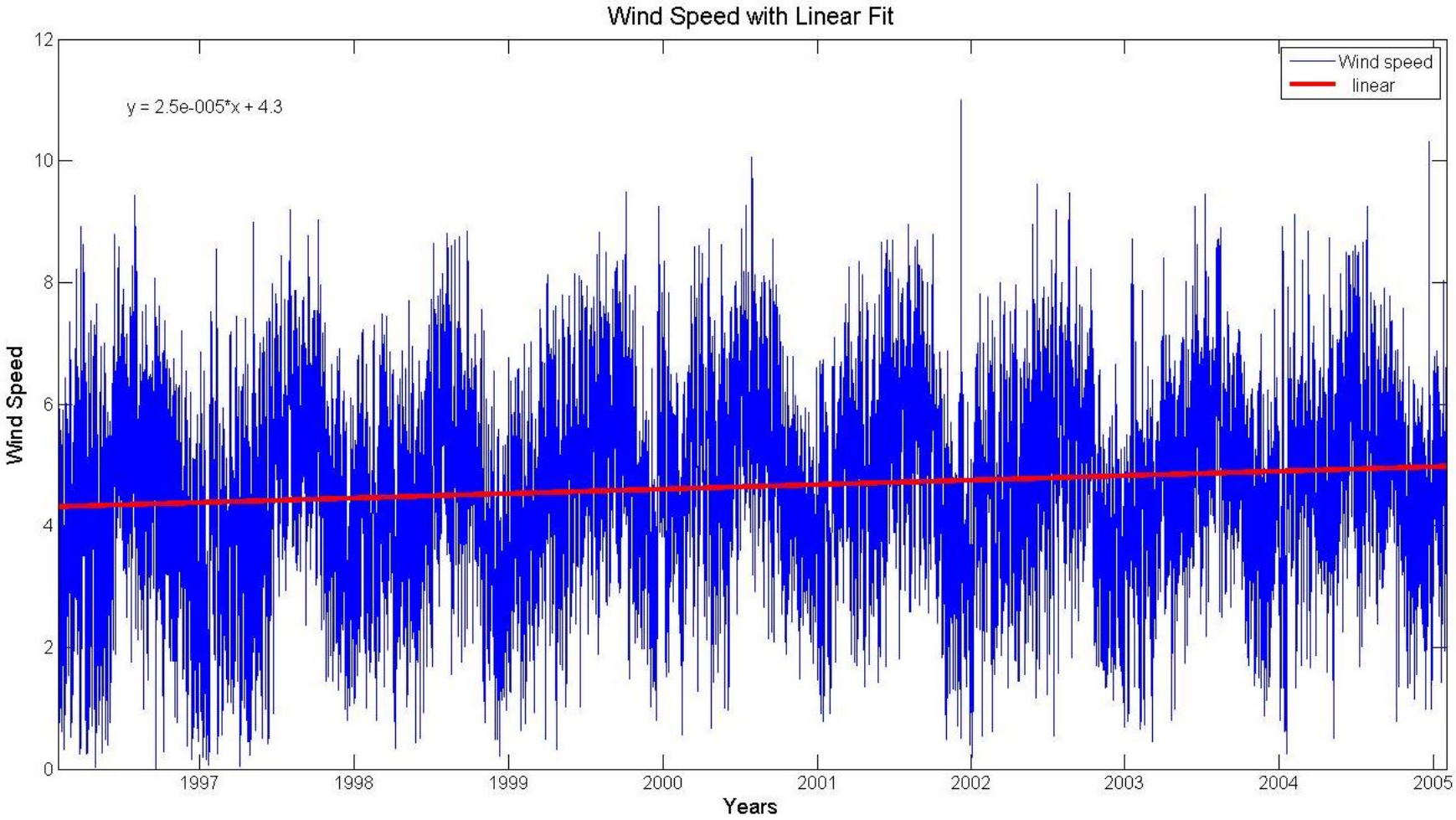

Figure 4.11: Wind speeds with linear fit

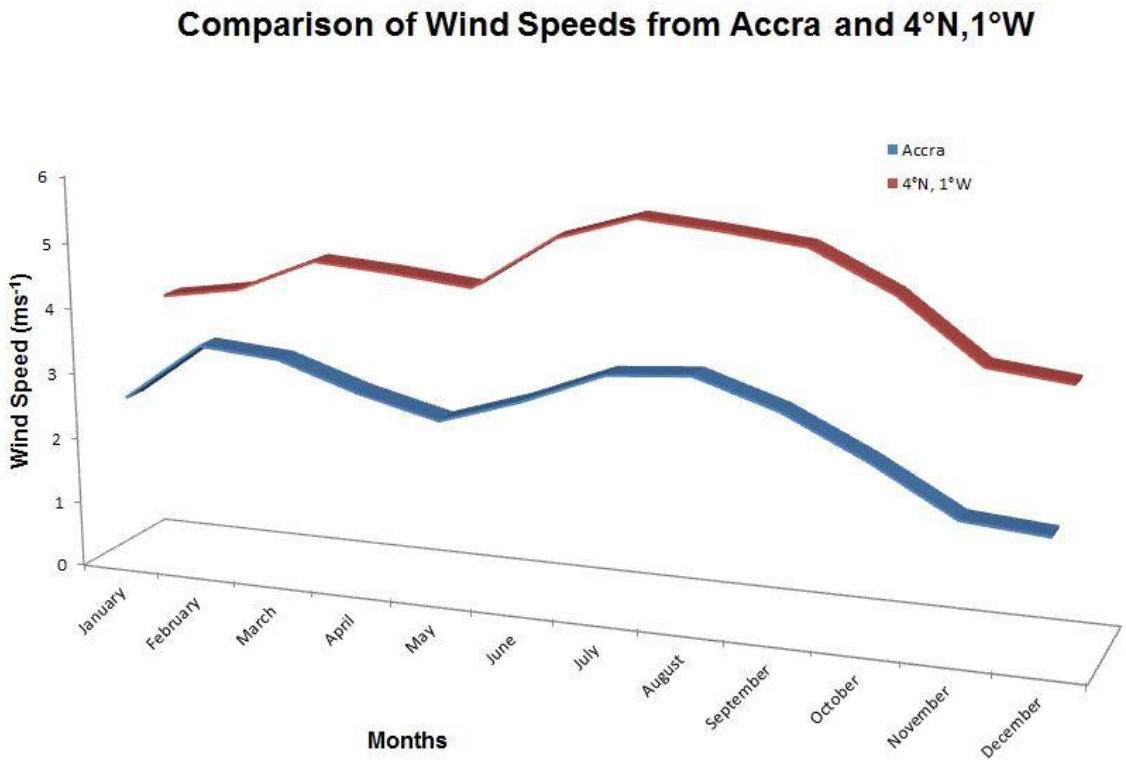

Figure 4.12: Comparison of wind speed from 4°N, 1°W and Accra (a coastal city)

4.2 Exeedence Probabilities

Figure 4.13 gives exeedence probabilities of various parameters from the data. For wave heights (Figure 4.13(A)), 1.35 m had exeedence probability of 50%, 1.12 m had exeedence probability of 75%, 0.88 m had exeedence probability of 95%. Exeedence probability of wave heights exceeding 2 m is 6.5%. Probability of exceeding moderate sea state is 0.46%. Exeedence probability for wave periods (Figure 4.13(B)), decreased slowly at low values, and decreased rapidly at higher wave periods. At 50% exeedence probability wave period was 11.13 s, 9.73 s at 75% and 5.87 s at 95%. For wind speeds (Figure 4.13(C)), wind speed at 50% exeedence probability was 4.68 ms^{-1}. Wind speed at 75% was 3.68 ms^{-1} and 2.1 ms^{-1} at 95%. Probability of exceeding moderate breeze was

1.04%. From Figure 4.13(D) at exeedence probability of 95% wave angle was 168.2°, 182.6° at 75%, and 197.2° at 50%. For wind directions, at exeedence probability of 95% wind angle was 168.2°, at 75% wind angle was 182.6° and 197.2° at 50%.

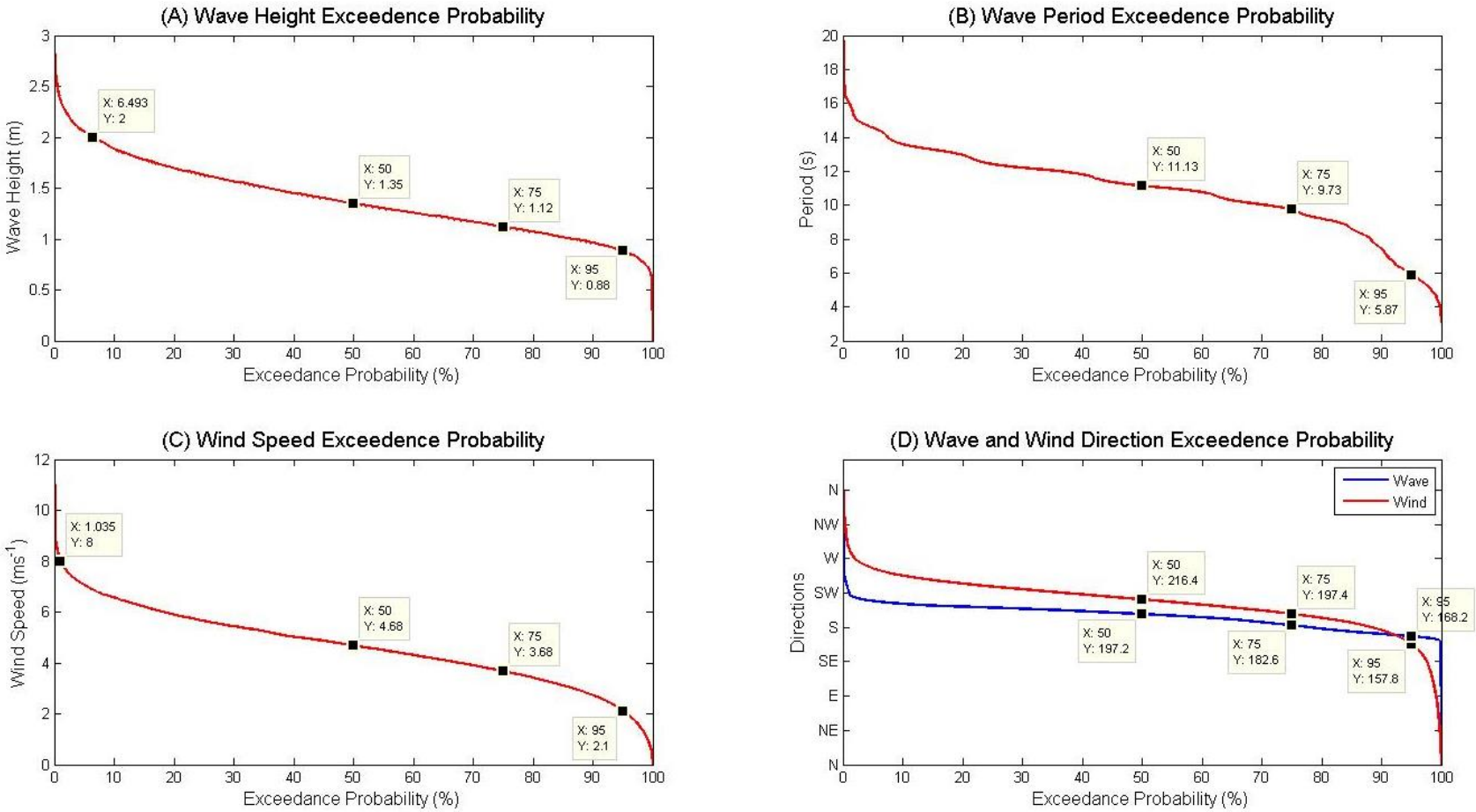

Figure 4.13: Exeedence probabilities

The monthly average plots of wave heights, wave periods and wind speed respectively are shown in Figure 4.14(A). Wave height averages increased slightly from January, 1.00 m to February, 1.05 m and increased almost steadily from February to August, 1.72 m where it recorded the highest and began to decrease steadily to December, 1.10 m. Wave period increased from January, 9.44 s to May where it had the highest of 11.85 s (Figure 4.14(B)). It had a deep (11.15 s) in June and then increased gradually from 11.40 s to 11.52 s in July and August respectively. It began to decrease again from 11.22 s in September till it reached 9.90 s in December. From Figure 4.14(C), the wind speed however had a gentle increase during the first two quarters of the year (Jan-Jun) 3.90 ms^{-1}, 4.10 ms^{-1}, 4.62 ms^{-1}, 4.53 ms^{-1}, 4.41 ms^{-1} January to May respectively and reached its highest at 5.61 ms^{-1} in July. It reduced slightly to 5.37 ms^{-1} in September and decreased further to 3.85 ms^{-1} in November and 3.72 ms^{-1} in December.

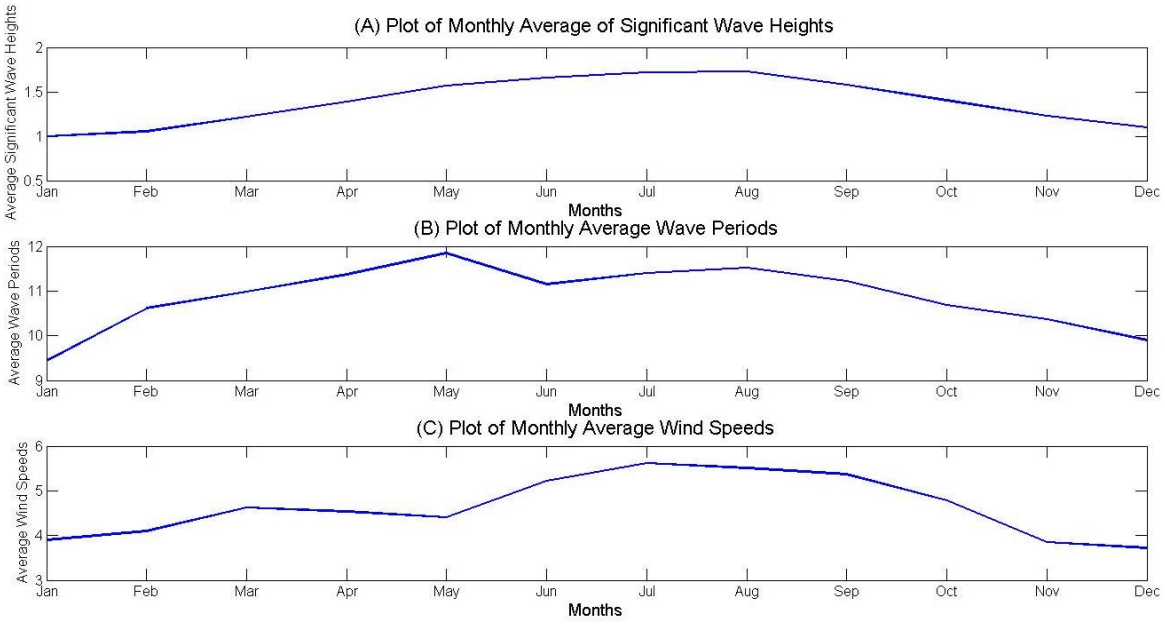

Figure 4.14: Wave height, wave period and wind speed monthly averages

4.3 Directional Wave and Wind Analysis

Most wave heights and periods, about 60%, came from the SSW (South-South-West) direction (Figures 4.15 and Figure 4.16). About 30% came from the South-South direction and remaining 10% spread in other directions, namely; SW (South-West), SSE (South-South-East), NE (North-East), ENE (East-North-East), E (East) and W (West). The colours (legend) depict magnitudes of parameters thus wave heights or periods. Size and length also depict percentage of occurrence.

Wind directions were diverse with speeds however occurring mainly within SSE (South-South-East) and W (West) as shown in Figure 4.16. Majority, about 33%, of the wind came from the SW (South-West) direction with the rest spread through the range (SSE - W). Tables 4.1 to 4.5 give an elaborate description of Figures 4.15 to 4.17. Prevalent wind directions however changed from SW to SSW from May to July and then in November with December having almost equal proportions in the SW and SSW directions. The changes in wind directions may be as a result of changes in the seasons. Tables 4.6 to 4.8 also give monthly wind and wave direction changes over the seasons with corresponding coincidences.

Monthly wave direction analysis showed that waves maintained their proportional directions throughout the year with about 60% occurring in the SSW direction and about 30% occurring in the S direction (Tables 4.6, 4.7 and 4.8). Prevalent wind direction however changed through the year. Between January – April, about 30% of the wind originated from SW direction, about 25% in the WSW direction with 45% spread over other directions. From, May – August wind directions concentrated in three directions, SSW, SW and WSW, by the end of August and mid-September. The spread then began again by October and reaches all directions by December. Prevalent wind direction also

changed from SW to SSW from May to July, and then in November, with December having almost equal percentage each of 30%, coming from SSW and SW directions. Wave and wind direction coincidences increased gradually from 15.7% to 31.5 from January to July and then began to decrease 16.6% in September, increased slightly to 26.1% in November and decreased to 19.8% in December.

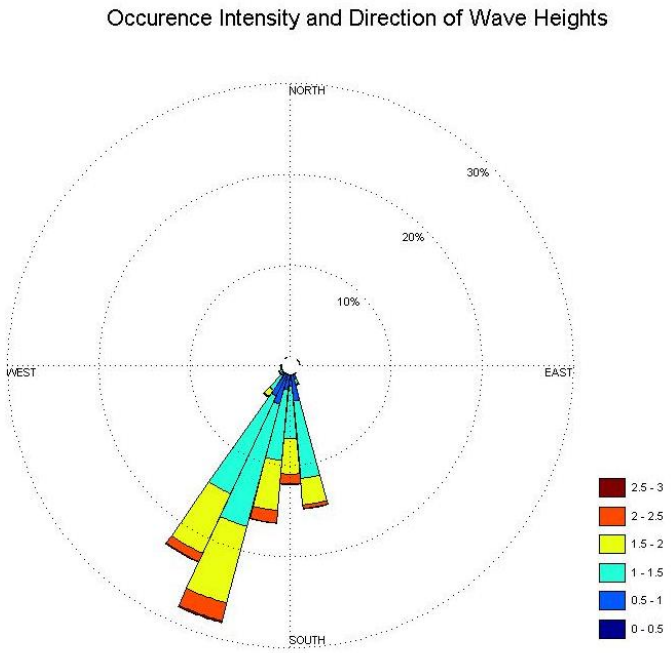

Figure 4.15: Rose plot of wave height showing percentage of occurrence and direction

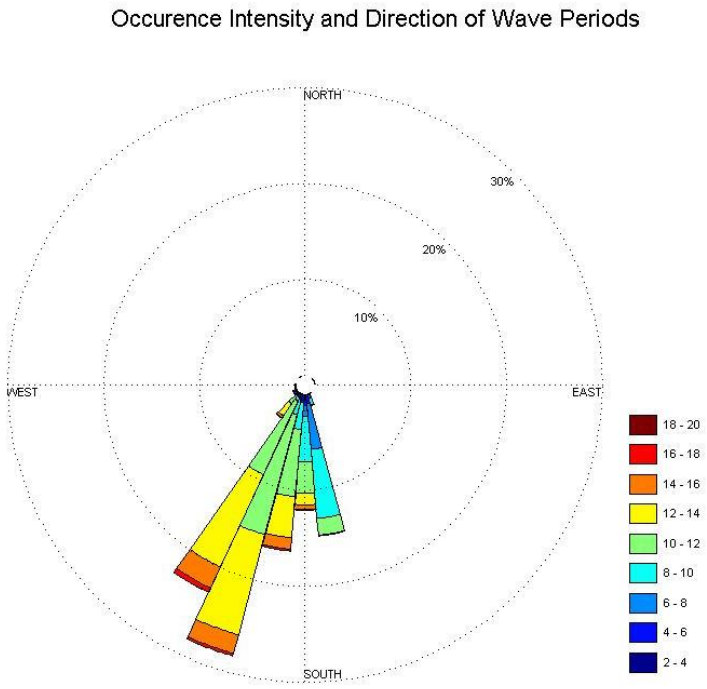

Figure 4.16: Rose plot of wave period showing percentage of occurrence and direction

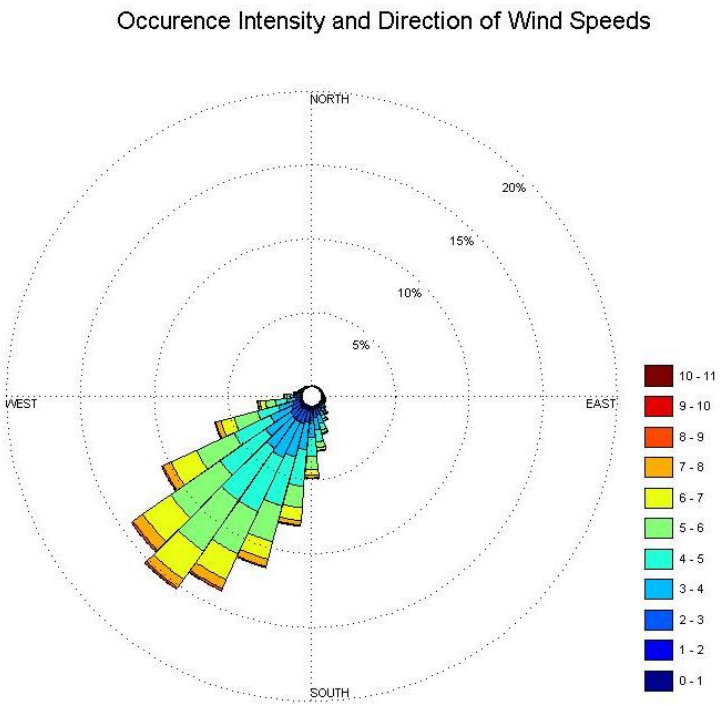

Figure 4.17: Rose plot showing direction and percentage occurrence of wind speeds

Table 4.1: Directional percentage occurrence of wave heights (m)

Wave Heights	Directions																TOTAL
	N	NNE	NE	ENE	E	ESE	SE	SSE	S	SSW	SW	WSW	W	WNW	NW	NNW	
0 - 0.5	0	0	0	0	0	0	0	0.03	0.01	0	0	0.01	0.03	0	0	0	0.08
0.5 - 1	0	0	0	0	0	0	0	1.56	4.20	7.22	0.62	0.03	0	0	0	0	13.63
1 - 1.5	0	0	0.01	0.05	0.01	0	0	3.24	15.44	29.04	2.91	0.40	0.03	0	0	0	51.13
1.5 - 2	0	0	0	0.01	0	0	0	0.85	8.89	17.77	1.33	0.06	0.03	0	0	0	28.94
2 - 2.5	0	0	0	0	0	0	0	0.12	1.99	3.45	0.19	0	0	0	0	0	5.76
2.5 - 3	0	0	0	0	0	0	0	0.03	0.13	0.29	0.02	0	0	0	0	0	0.46
TOTAL	0	0	0.01	0.06	0.01	0	0	5.82	30.66	57.78	5.07	0.50	0.08	0	0	0	**100**

-Increasing colour intensity = Increasing percentage of occurrence

Table 4.2: Directional percentage occurrence of wave periods (s)

Wave Periods	Directions																TOTAL
	N	NNE	NE	ENE	E	ESE	SE	SSE	S	SSW	SW	WSW	W	WNW	NW	NNW	
2 - 4	0	0	0.004	0	0	0	0	0	0	0.01	0.08	0.08	0.03	0	0	0	0.22
4 - 6	0	0	0.004	0.06	0.01	0	0	0.30	2.47	1.15	0.84	0.42	0.05	0	0	0	5.30
6 - 8	0	0	0	0	0	0	0	1.84	4.43	0.05	0	0	0	0	0	0	6.32
8 - 10	0	0	0	0	0	0	0	3.07	11.54	3.08	0.02	0	0	0	0	0	17.71
10 - 12	0	0	0	0	0	0	0	0.56	7.92	24.63	1.50	0	0	0	0	0	34.61
12 - 14	0	0	0	0	0	0	0	0.05	3.13	22.98	2.21	0	0	0	0	0	28.36
14 - 16	0	0	0	0	0	0	0	0.01	1.05	4.99	0.37	0	0	0	0	0	6.42
16 - 18	0	0	0	0	0	0	0	0	0.11	0.87	0.05	0	0	0	0	0	1.03
18 - 20	0	0	0	0	0	0	0	0	0	0.03	0	0	0	0	0	0	0.03
TOTAL	0	0	0.01	0.06	0.01	0	0	5.82	30.66	57.78	5.07	0.50	0.08	0	0	0	100

Table 4.3: Directional percentage occurrence of wind speeds (ms^{-1})

Wind speed	Directions																TOTAL
	N	NNE	NE	ENE	E	ESE	SE	SSE	S	SSW	SW	WSW	W	WNW	NW	NNW	
0 - 1	0.03	0.03	0.02	0.01	0.05	0.06	0.08	0.10	0.08	0.09	0.08	0.08	0.05	0.05	0.04	0.03	0.85
1 - 2	0.03	0.02	0.05	0.08	0.07	0.15	0.17	0.45	0.51	0.60	0.58	0.38	0.19	0.15	0.07	0.05	3.53
2 - 3	0.01	0.03	0.03	0.05	0.11	0.16	0.39	0.84	1.57	2.04	1.98	1.11	0.50	0.13	0.09	0.04	9.06
3 - 4	0.02	0.02	0.06	0.05	0.12	0.16	0.49	1.18	2.81	5.50	5.10	2.64	0.65	0.10	0.04	0.02	18.96
4 - 5	0.01	0.02	0.03	0.04	0.05	0.11	0.26	0.96	3.25	8.11	8.99	4.25	0.77	0.10	0.01	0	26.97
5 - 6	0	0	0.01	0.02	0.03	0.04	0.11	0.45	1.91	5.90	9.00	4.33	0.67	0.07	0.02	0.01	22.57
6 - 7	0	0.02	0	0	0.02	0.01	0.03	0.14	1.00	3.23	5.12	2.69	0.36	0.03	0	0	12.65
7 - 8	0	0.01	0.01	0.01	0	0	0.01	0.02	0.40	1.20	1.68	0.91	0.14	0.01	0	0	4.40
8 - 9	0	0	0.01	0.02	0	0	0	0.02	0.07	0.24	0.30	0.18	0.04	0.02	0	0	0.89
9 - 10	0	0	0	0	0	0	0	0.01	0.02	0.02	0.03	0.01	0	0	0	0	0.10
10 - 11	0	0	0	0	0	0	0	0	0.01	0	0	0	0	0	0	0	0.01
TOTAL	0.11	0.14	0.21	0.29	0.45	0.69	1.52	4.16	11.63	26.93	32.85	16.56	3.37	0.67	0.26	0.14	**100**

Table 4.4: Wave height (m) occurrence percentage probability with corresponding periods (s)

Wave Heights	Wave Periods									TOTAL
	2 - 4	4 - 6	6 - 8	8 - 10	10 - 12	12 - 14	14 - 16	16 - 18	18 - 20	
0 - 0.5	0.02	0.02	0.03	0	0	0	0	0	0	0.08
0.5 - 1	0.05	0.89	1.65	4.32	5.06	1.48	0.16	0.03	0	13.63
1 - 1.5	0.14	3.00	3.84	10.53	19.15	12.05	2.04	0.37	0.01	51.13
1.5 - 2	0	1.35	0.67	2.81	8.61	12.12	2.86	0.51	0.02	28.94
2 - 2.5	0	0.05	0.13	0.05	1.71	2.51	1.19	0.12	0	5.76
2.5 - 3	0	0	0	0	0.08	0.20	0.17	0.01	0	0.46
TOTAL	0.22	5.30	6.32	17.71	34.61	28.36	6.42	1.03	0.03	**100**

Table 4.5: Wave height (m) occurrence percentage probability with corresponding wind speed (ms^{-1})

Wave Heights	Wind Speeds											TOTAL
	0 - 1	1 - 2	2 - 3	3 - 4	4 - 5	5 - 6	6 - 7	7 - 8	8 - 9	9 - 10	10 - 11	
0 - 0.5	0.01	0.03	0.02	0.02	0.01	0	0	0	0	0	0	0.08
0.5 - 1	0.37	1.26	2.55	3.99	3.36	1.72	0.35	0.03	0	0	0	13.63
1 - 1.5	0.37	1.74	5.11	10.76	14.95	11.33	5.37	1.28	0.21	0.02	0.004	51.13
1.5 - 2	0.10	0.47	1.21	3.61	7.25	7.82	5.50	2.42	0.53	0.04	0.004	28.94
2 - 2.5	0.01	0.04	0.17	0.54	1.26	1.57	1.35	0.62	0.14	0.04	0.004	5.76
2.5 - 3	0	0	0	0.05	0.14	0.12	0.09	0.05	0	0	0	0.46
TOTAL	0.85	3.53	9.06	18.96	26.97	22.57	12.65	4.40	0.89	0.10	0.01	**100**

Table 4.6: Monthly direction probability of wave and wind with percentage coincidence

Dir	January			February			March			April		
	Wv Dir Prob/ %	Wd Dir Prob/ %	Coincid. / %	Wv Dir Prob/ %	Wd Dir Prob/ %	Coincid. / %	Wv Dir Prob/ %	Wd Dir Prob/ %	Coincid. / %	Wv Dir Prob/ %	Wd Dir Prob/ %	Coincid. / %
N	0	0.31	0	0	0.25	0	0	0.18	0	0	0.32	0
NNE	0	0.93	0	0	0.30	0	0	0.04	0	0	0.28	0
NE	0.09	1.16	0.04	0	0.34	0	0	0.04	0	0	0.37	0
ENE	0.71	1.56	0.40	0	0.94	0	0	0.04	0	0	0.14	0
E	0.09	1.56	0	0	1.13	0	0	0.13	0	0	0.51	0
ESE	0	1.07	0	0	1.38	0	0	0.36	0	0	0.60	0
SE	0	1.11	0	0	1.77	0	0	1.57	0	0	1.44	0
SSE	9.74	2.67	0.18	4.72	3.35	0	3.81	3.14	0.63	4.81	4.58	0.05
S	29.49	6.14	1.78	31.59	8.07	3.64	32.62	7.80	2.87	21.81	11.25	3.75
SSW	53.29	18.02	10.68	57.53	21.11	11.32	57.08	18.86	10.53	65.23	25.28	18.19
SW	4.94	30.83	1.73	5.17	32.97	2.17	4.35	35.04	1.84	7.55	30.97	3.29
WSW	1.25	24.38	0.80	0.69	22.34	0.39	2.02	25.58	1.30	0.60	18.70	0.23
W	0.40	7.52	0.04	0.30	4.23	0.05	0.09	5.38	0	0	3.98	0
WNW	0	1.60	0	0	1.23	0	0	0.99	0	0	1.06	0
NW	0	0.67	0	0	0.44	0	0	0.54	0	0	0.32	0
NNW	0	0.49	0	0	0.15	0	0.04	0.31	0.04	0	0.19	0
TOTAL	100	100	15.66	100	100	17.57	100	100	17.20	100	100	25.51

Wv Dir – Wave direction ; Wd Dir – Wind direction ; Prob – Probability ; Coincid – Conincidence
-Increasing colour intensity = Increasing percentage
-Red – occurrence; Green – coincidence

Table 4.7: Monthly direction probability of wave and wind with percentage coincidence

Dir	May			Jun			July			August		
	Wv Dir Prob/ %	Wd Dir Prob/ %	Coincid. / %	Wv Dir Prob/ %	Wd Dir Prob/ %	Coincid. / %	Wv Dir Prob/ %	Wd Dir Prob/ %	Coincid. / %	Wv Dir Prob/ %	Wd Dir Prob/ %	Coincid. / %
N	0	0	0	0	0	0	0	0	0	0	0	0
NNE	0	0	0	0	0.05	0	0	0	0	0	0	0
NE	0	0.18	0	0	0	0	0	0	0	0	0	0
ENE	0	0.13	0	0	0.14	0	0	0	0	0	0	0
E	0	0.45	0	0	0.14	0	0	0	0	0	0.04	0
ESE	0	1.03	0	0	0.37	0	0	0	0	0	0.04	0
SE	0	2.51	0	0	1.62	0	0	0	0	0	0	0
SSE	1.39	9.72	0.13	0.97	5.83	0.23	5.02	1.25	0	3.94	0.18	0
S	26.93	20.34	5.82	30.09	21.57	6.81	29.08	13.53	4.88	31.72	4.66	1.66
SSW	67.38	27.51	18.86	61.16	34.81	21.81	58.51	40.32	23.12	61.83	29.17	15.55
SW	3.94	22.63	0.94	7.73	24.26	3.01	7.39	33.60	3.49	2.37	45.43	0.90
WSW	0.31	10.93	0.09	0.05	8.70	0.05	0	9.72	0	0.13	18.10	0.13
W	0.04	3.00	0.04	0	2.18	0	0	1.43	0	0	2.37	0
WNW	0	1.03	0	0	0.32	0	0	0.04	0	0	0	0
NW	0	0.40	0	0	0	0	0	0.09	0	0	0	0
NNW	0	0.13	0	0	0	0	0	0	0	0	0	0
TOTAL	100	100	25.90	100	100	31.90	100	100	31.50	100	100	18.23

Table 4.8: Monthly direction probability of wave and wind with percentage coincidence

Dir	September			October			November			December		
	Wv Dir Prob/ %	Wd Dir Prob/ %	Coincid. / %	Wv Dir Prob/ %	Wd Dir Prob/ %	Coincid. / %	Wv Dir Prob/ %	Wd Dir Prob/ %	Coincid. / %	Wv Dir Prob/ %	Wd Dir Prob/ %	Coincid. / %
N	0	0	0	0	0	0	0	0	0	0	0.22	0
NNE	0	0	0	0	0	0	0	0	0	0	0.09	0
NE	0	0	0	0	0	0	0	0	0	0	0.45	0
ENE	0	0	0	0	0	0	0	0.14	0	0	0.45	0
E	0	0	0	0	0	0	0	0.23	0	0	1.25	0
ESE	0	0	0	0	0.31	0	0	1.62	0	0	1.57	0
SE	0	0	0	0	0.76	0	0	3.24	0	0	4.26	0
SSE	3.32	0.09	0	7.30	1.39	0.27	12.82	8.98	1.20	11.83	8.69	1.25
S	35.63	4.17	0.98	34.68	7.97	3.14	31.53	19.72	7.96	32.80	14.34	5.73
SSW	54.78	25.28	13.53	55.38	29.66	13.17	53.15	29.63	16.25	48.12	23.30	10.66
SW	6.27	52.11	2.06	2.46	38.04	1.30	2.5	24.77	0.69	6.32	23.84	1.48
WSW	0	16.25	0	0.13	19.71	0.04	0	9.91	0	0.81	14.47	0.63
W	0	2.11	0	0.04	1.93	0.04	0	1.53	0	0.13	4.66	0
WNW	0	0	0	0	0.18	0	0	0.23	0	0	1.34	0
NW	0	0	0	0	0	0	0	0	0	0	0.67	0
NNW	0	0	0	0	0.04	0	0	0	0	0	0.40	0
TOTAL	100	100	16.57	100	100	17.97	100	100	26.11	100	100	19.76

From Figure 4.18 (A), the highest occurring wave heights were within the range of about 1.5 – 2 m and occurred relatively in the SSW direction (approximately 180 - 210° clockwise). Amidst these, wave heights of about 1.5 made up about 30% of the occurrence whilst those above 1.5 m but not greater than 2 m had an occurrence of about 20%. Figure 4.18 (B) spider plot gives the occurrence of various periods with respect to wave heights in such directions. The 30% occurrence of waves occurred with periods of about 11 s whilst those of the 20% occurred with periods of about 12 s. Other southerly waves with increasing wave heights occurred with increasing periods. Solitary waves with very low wave heights coming from NNW – NW had the highest surge and wind speed. Surge and wind speed tend to increase with increasing wave heights. Also see Tables 4.1, 4.4 and 4.5.

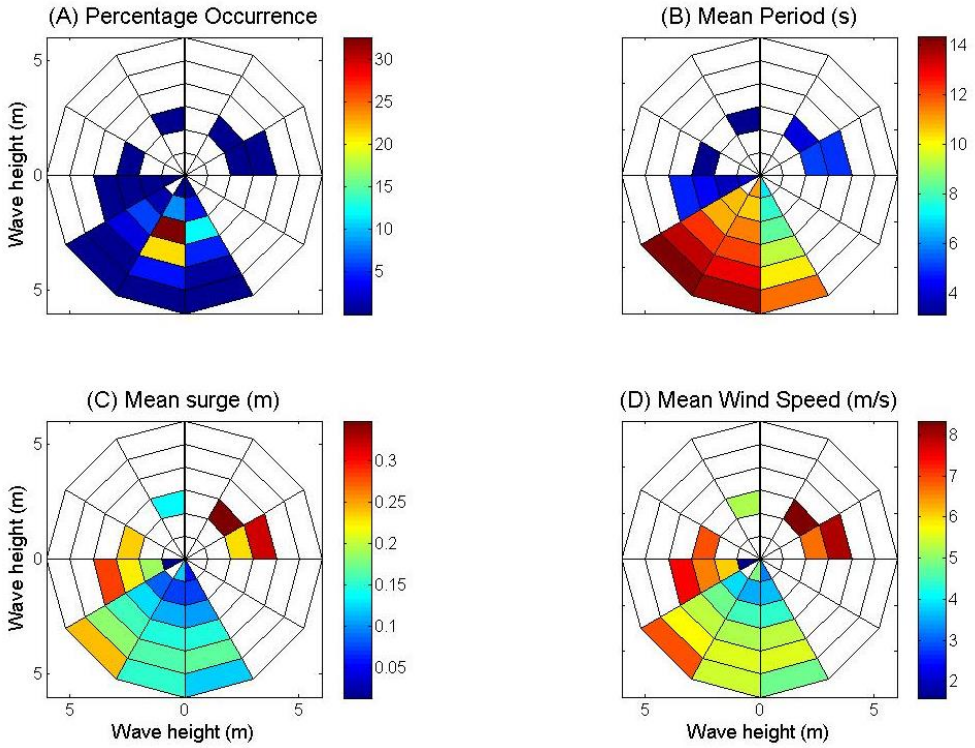

Figure 4.18: Direction and percentage occurrence of wave height and occurrence of other parameters with respect to wave heights

4.4 Correlations of Wave and Wind parameters

Figure 4.19 (A) gives correlation between wave heights and periods. Correlation was low for low wave heights up to about 2 m with corresponding periods. Correlation then increased at about 2.2 m wave height and decreased slightly at about 4.2 m with their respective periods. Correlation between wave heights and wind speeds, Figure 4.19 (B) also followed similar trend. The correlation increased for wave heights beyond 4.3 m with their corresponding wind speeds. Correlation for wave heights and surge, Figure 4.19 (C) were fairly constant for all values. However they are low. Wave and wind direction correlation were the lowest. In general correlations increased at higher values of parameters. Table 4.9 also gives correlations with their corresponding P values and in Table 4.10. Expected correlations (correlations between wave and wind parameters) were generally low

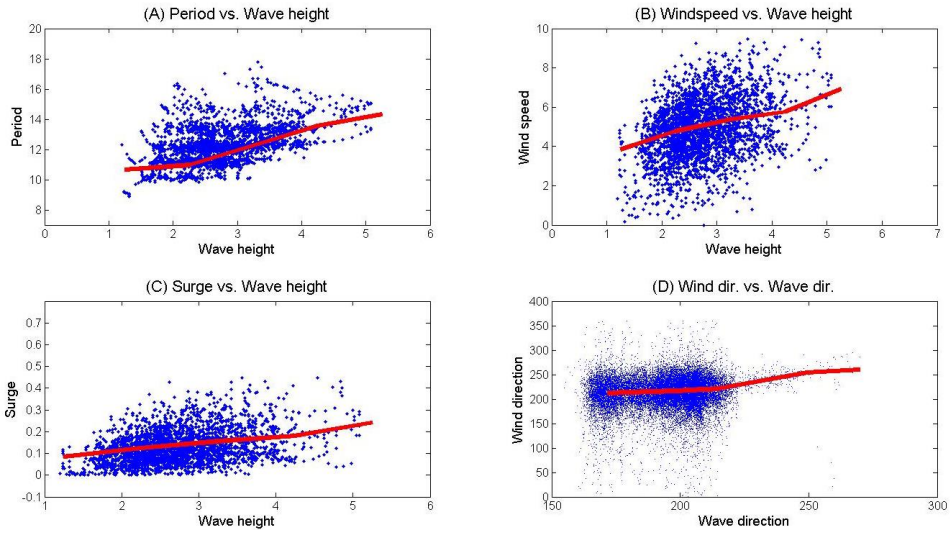

Figure 4.19: Correlation of wave height with other parameters and correlation of wind direction and wave direction (D)

Table 4.9: Correlations of parameters

Correlations (corresponding P Values)					
	Period	Wave speed	Surge	Wave direction	Wind direction
Wave height	0.363 (0.000)	0.391 (0.000)	0.390 (0.000)	0.068 (0.000)	-0.017 (0.007)
Period		-0.007 (0.275)	-0.021 (0.001)	0.435 (0.000)	0.015 (0.016)
Wave speed			0.975 (0.000)	0.065 (0.000)	0.184 (0.000)
Surge				0.073 (0.000)	0.167 (0.000)
Wave direction					0.122 (0.000)

- Shaded cells -relations of main importance

4.5 Wave Energy

Figure 4.20 shows wave energies that had influenced the coast from January 1997 to January 2006. 1999 had one of the highest wave energy impacts of about 10000 kgs^{-2}. Figure 4.20 shows the average amount of energy per wave for each month experienced during the years of study. A similar trend was observed as the wave heights for each month (as wave energy is related to wave height). January recorded the lowest of 1251.26 kgs^{-2} and increased gradually through the months of February, March through (1389.85 kgs^{-2}, 1874.00 kgs^{-2}, 2423.69 kgs^{-2}, 3096.78 kgs^{-2}, 3452.37 kgs^{-2}, 3709.03 kgs^{-2} respectively) to August, where it recorded the highest wave energy of 3760.26 kgs^{-2} . The average wave energy then begun to reduce again to 1514.07 kgs^{-2} in December where the third lowest was recorded. The highest total energy was recorded in 2002, followed by 2005, 2001, 2004, 2003, 1999, 2000, 1998 and 1997 with total energies, 8408628.03 kgs^{-2}, 8238692.66 kgs^{-2}, 7933743.28 kgs^{-2}, 7927134.07 kgs^{-2}, 7707331.90 kgs^{-2}, 7552253.58 kgs^{-2}, 7073377.67 kgs^{-2}, 6821355.28 kgs^{-2}, 6456178.06 kgs^{-2} respectively (Figure 4.22(A)). Figure 4.22(B) also shows the mean energy for each year.

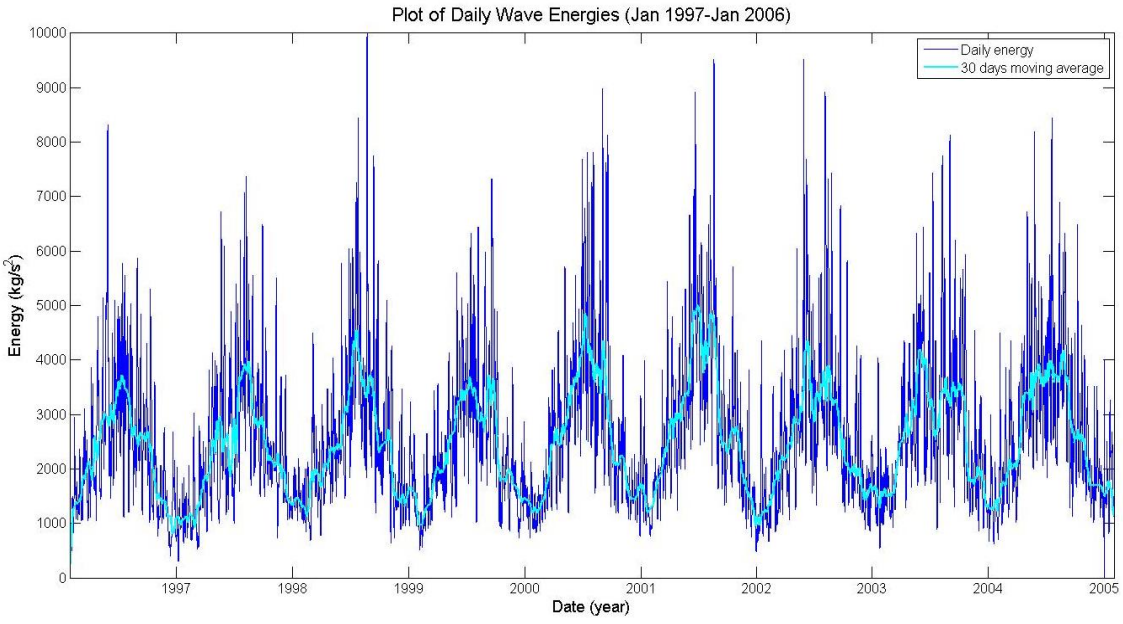

Figure 4.20: Daily plot of wave energy with 30 days moving average

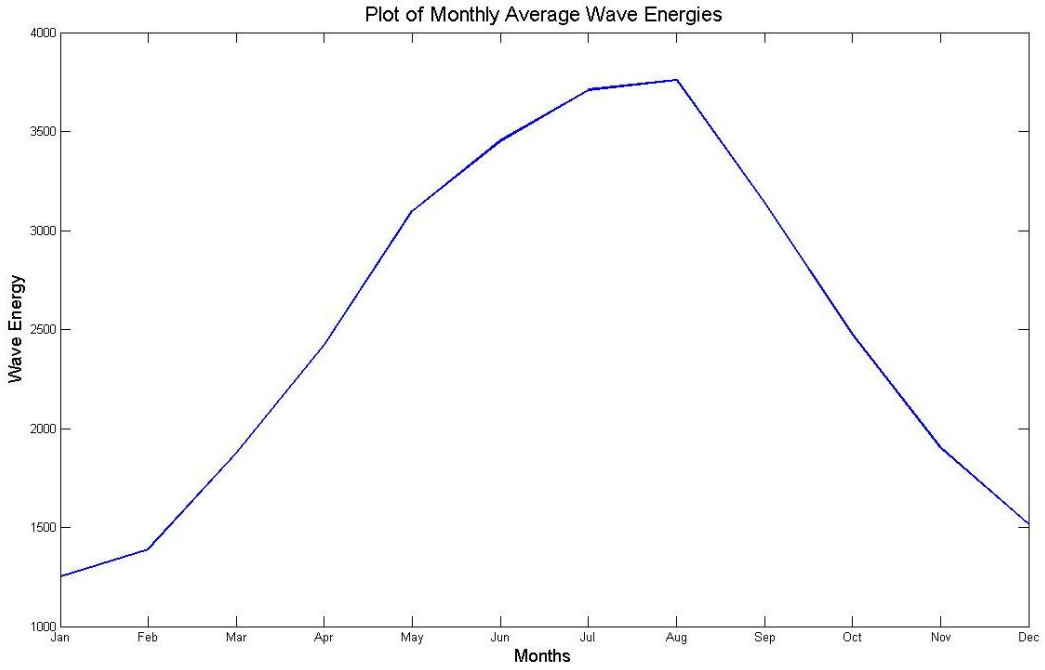

Figure 4.21: Monthly average energy

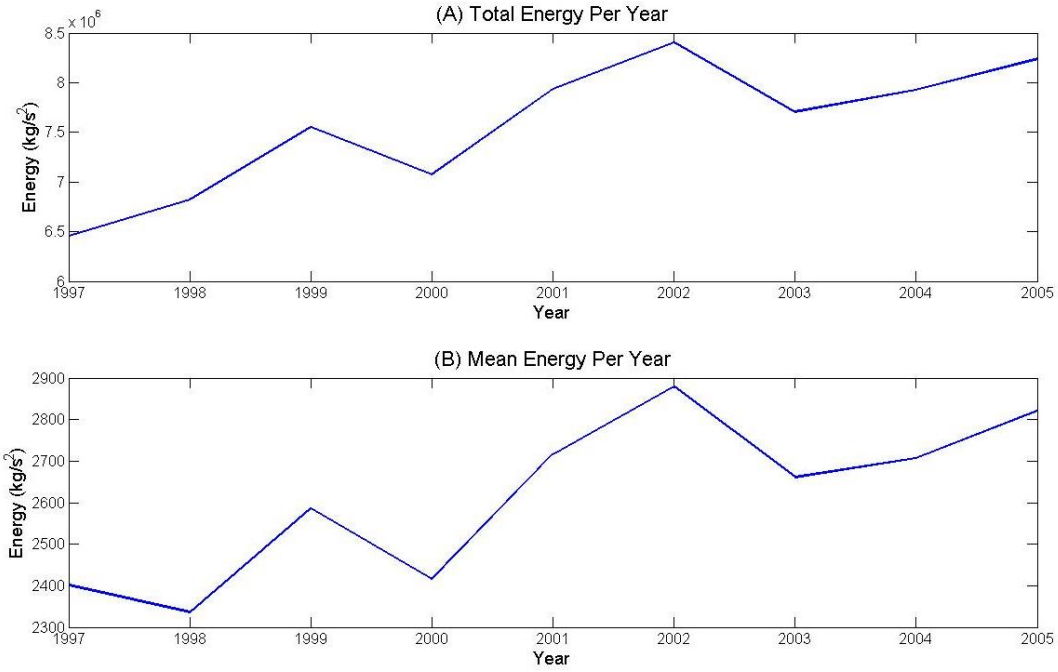

Figure 4.22: Total wave energy (A), Mean wave energy (B)

4.6 Sediment Transport Rates

Sediment transports generally reflected wave energy patterns. Suspended transports were higher than bottom transports. Crosshore transports were also higher than longshore transports. Lower wave heights tend to result in a relatively equal suspended, longshore and crosshore sediment transports.

Figure 4.23 shows potential sediment transport rates for each year based on the Soulsby-Van Rijn sediment transport equation. The year 2002 had the highest transport followed by 2005 then 2004 and that of 1998 being the least with 4.79E+08 m^3yr^{-1}, 4.71E+08 m^3yr^{-1}, 4.45E+08 m^3yr^{-1}, and 3.47E+08 m^3yr^{-1}as total transport rates respectively. Figure 4.24 also shows monthly potential sediment transport rates. The month of August had the highest total potential sediment transport of 6.71E+07 m^3 per month followed by July with potential sediment transport of 6.57E+07 m^3 per month while January had the least potential sediment transport rate of 1.29E+07 m^3 per month. Monthly total potential sediment transport was 3.74E+07 m^3 per month whiles annual total potential sediment transport was 4.07E+08 m^3 per year (Figures 4.23 and 4.24). Also see Appendix B for wave climate used in computation of sediment transport and Appendix C and D for tabulated potential sediment volume transports.

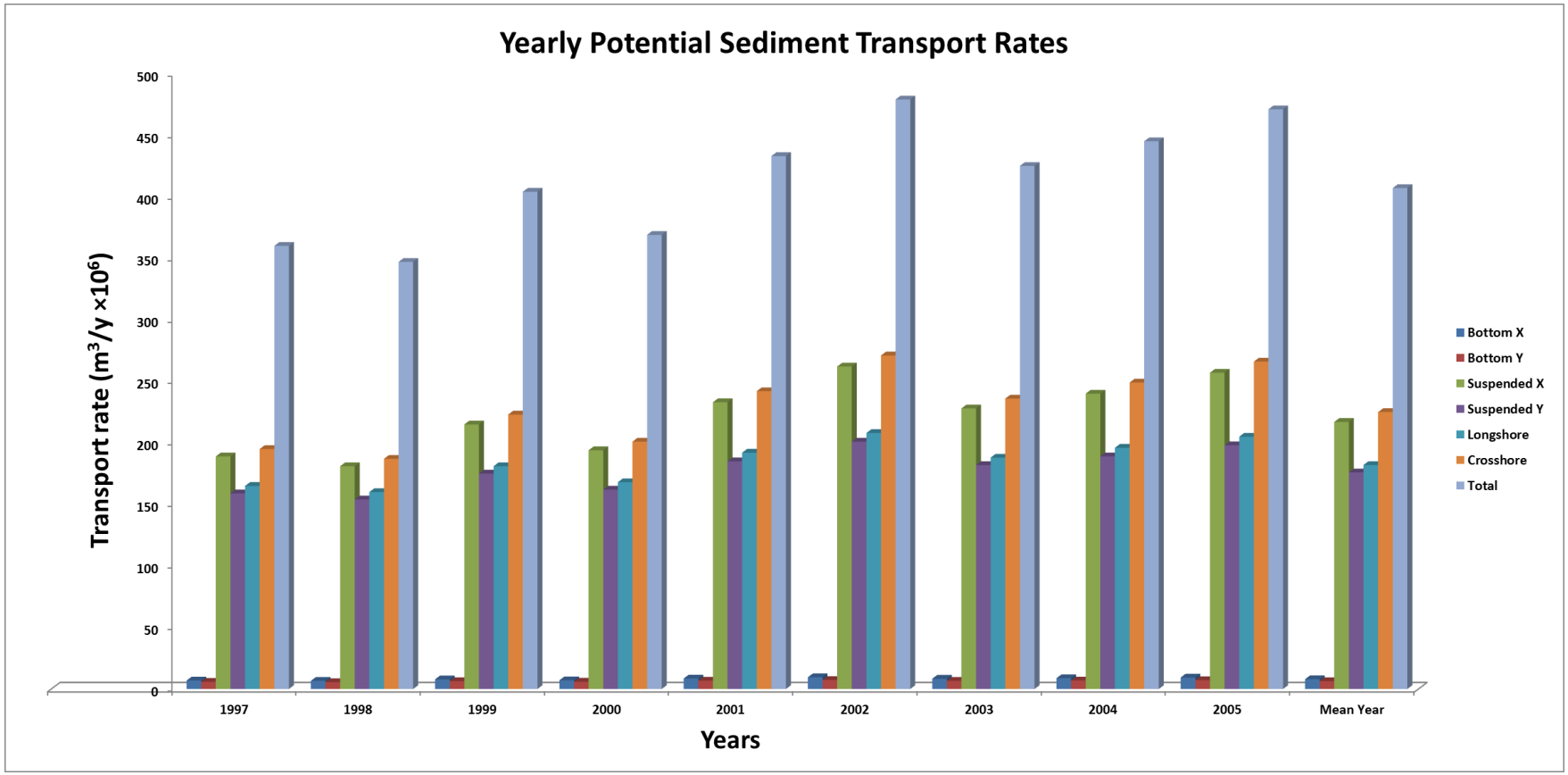

Figure 4.23: Yearly Potential Sediment Volume Transport

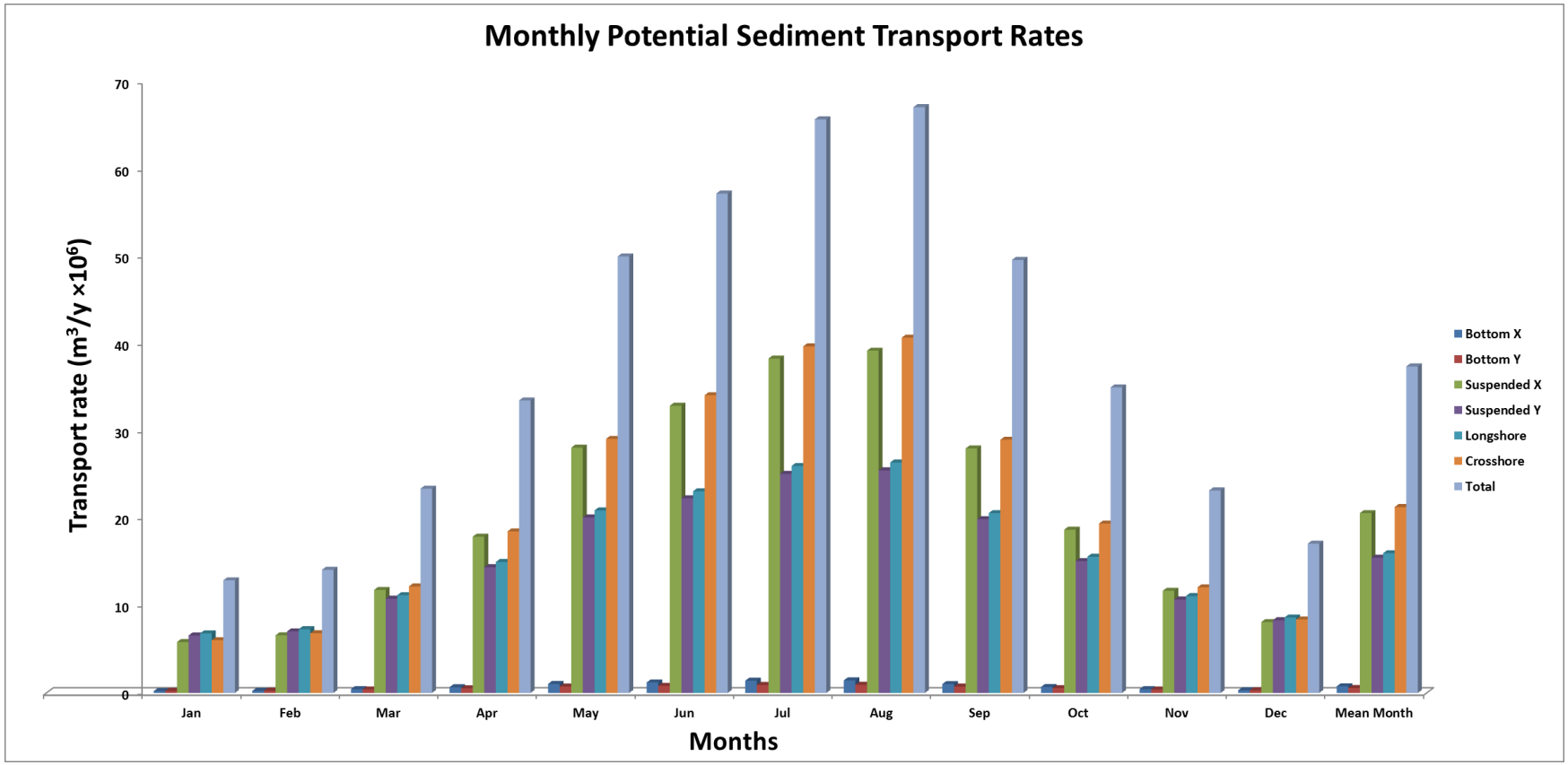

Figure 4.24: Monthly potential sediment volume transport

4.7 Wave Buoy Data Analysis

89.3% of the waves occurred between SSE and SSW directions. 92.2% of the wave heights were between 1.00 m and 2.00 m. Very few, 6.8% were also below 0.50m. The highest wave height of 1.98 m was obtained in the month of November. Minimum wave height was 0.00m, November also recorded the highest period of 28.57s followed by August which recorded 25.00s Mean wave direction was found to be in the south direction (refer to Figures 4.25 and 4.26 and Tables 4.11 and 4.12). Figures 4.27 and 4.28 also show some results of short-term analysis performed. They show wave intensities, groups and directions as they pass the buoy.

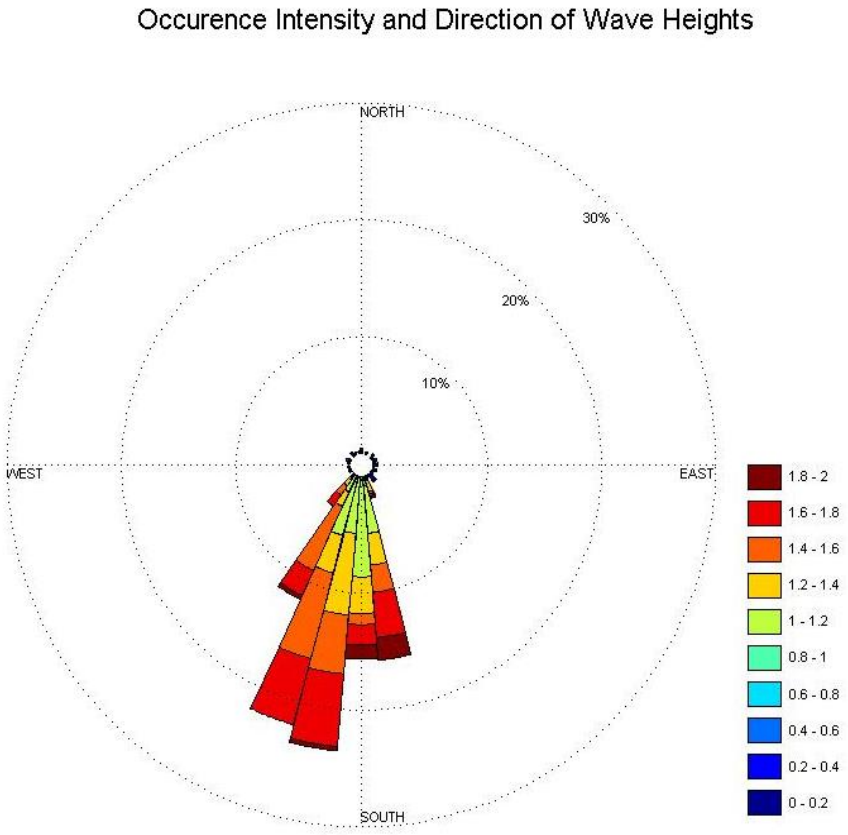

Figure 4.25: Directional occurrence intensity of wave heights from buoy

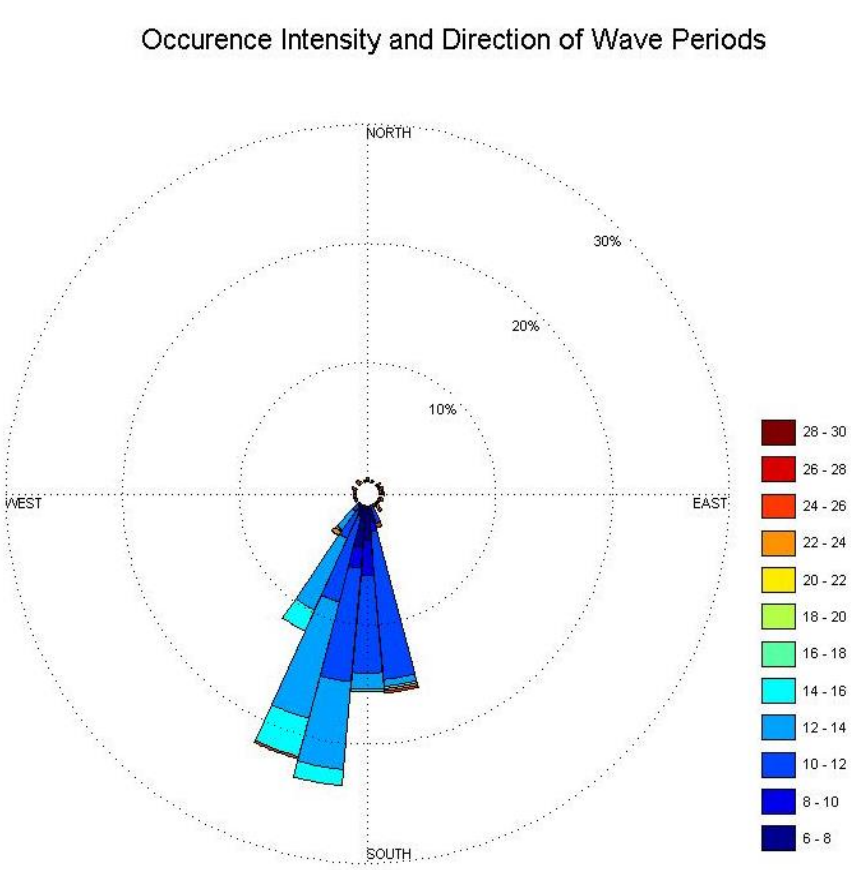

Figure 4.26: Directional occurrence intensity of wave periods from buoy

Table 4.10 Summary of NOAA wave data

Statistics	Significant Wave Height (Hs /m)	Wave Period (Tp /s)	Wave Direction (°)	Wind Speed (ms^{-1})	Wind Direction (°)
Maximum	2.82	19.68	330.64 (NNW)	11.00	358.94 (N)
Minimum	0.00	3.11	46.37 (NE)	0.00	1.10 (N)
Mean	1.39	10.91	194.21 (SSW)	4.65	213.04 (SSW)
Mode	1.26, 1.3	11.07	206.51 (SSW)	4.96	224.99 (SW)

Table 4.11: Data statistics from Buoy

		Wave Height	**Wave Period**	**Wave Direction**
Aug-10	Mean	1.46	13.72	197.88 (SSW)
	Mode	1.50	13.33	198.28 (SSW)
	Max	1.96	25.00	352.97 (N)
	Min	0.00	10.00	53.44 (NE)
Oct-11	Mean	1.28	10.47	195.13 (SSW)
	Mode	1.17	10.53	194.06 (SSW)
	Max	1.84	15.38	219.38 (SW)
	Min	0.97	6.67	170.16 (S)
Nov-11	Mean	1.23	12.04	177.57 (S)
	Mode	0.00	10.53	171.56 (S)
	Max	1.98	28.57	355.78 (N)
	Min	0.00	6.25	2.81 (N)
Mean		**1.32**	**12.21**	**188.77 (S)**

Table 4.12: Comparison of NOAA and Buoy data

		August	October	November	**Mean**
Mean Wave Height (m)	NOAA	1.73	1.40	1.23	**1.39**
	BUOY	1.46	1.28	1.23	**1.32**
Mean Wave Period (s)	NOAA	11.52	10.68	10.36	**10.91**
	BUOY	13.72	10.47	12.04	**12.21**
Mean Wave Direction (^{0})	NOAA	194.62	192.39	190.28	**194.21 (SSW)**
	BUOY	197.88	195.13	177.57	**188.77 (S)**

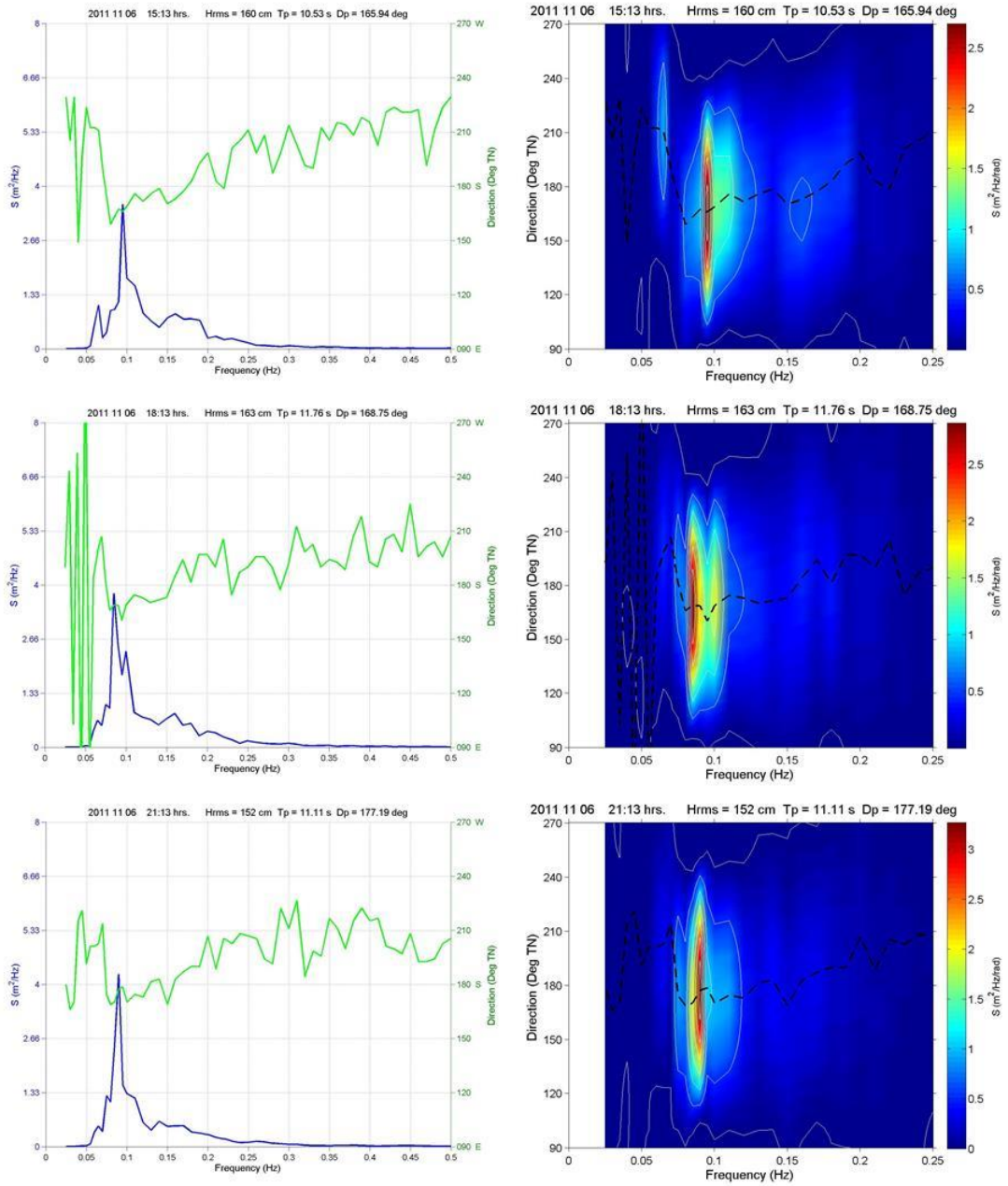

Figure 4.27: Some outputs of Short-Term Analysis of Buoy Data (2011-11-06 15:13-21:13)

See Appendix E for other Short Term Analysis

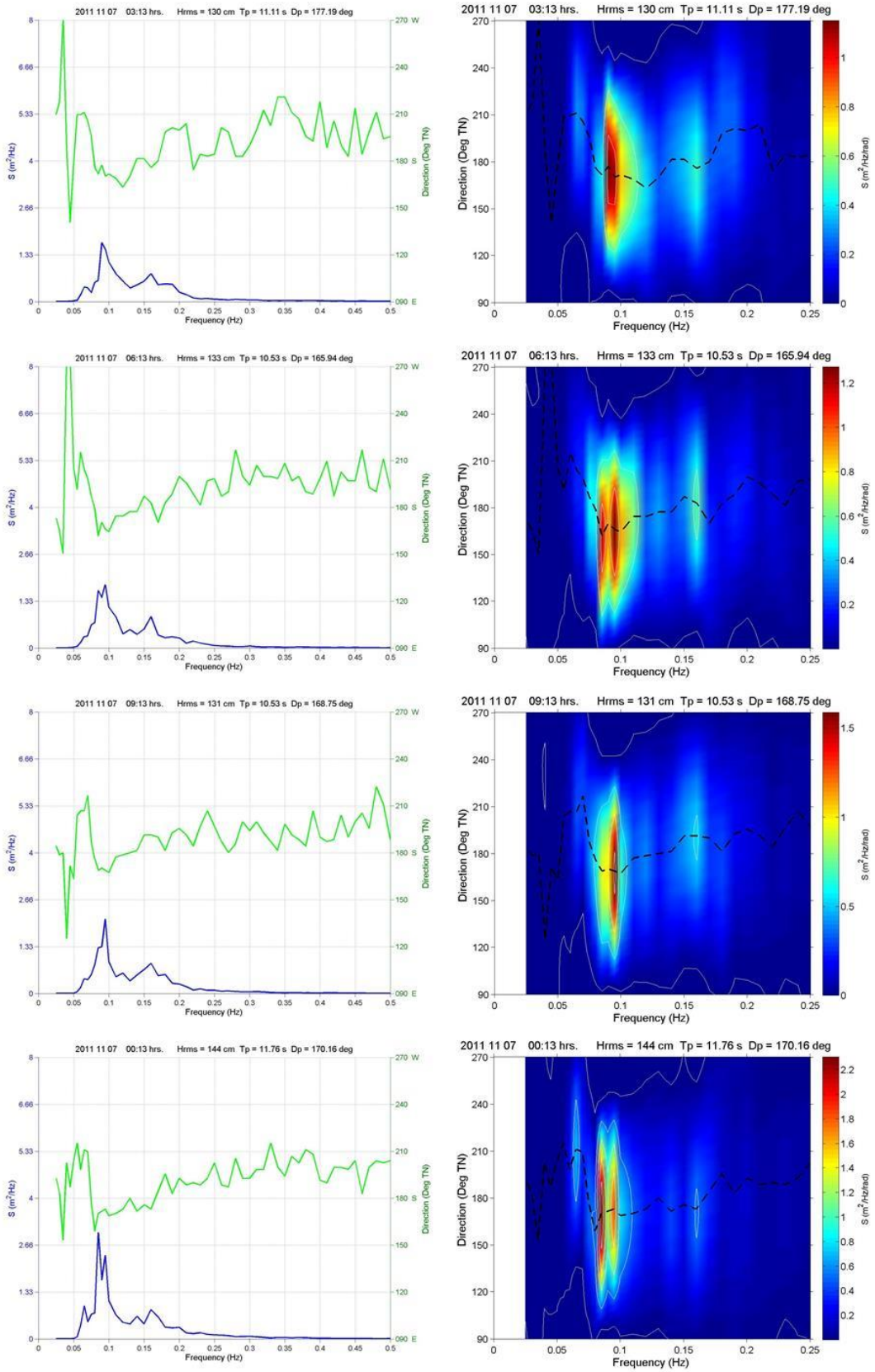

Figure 4.28: Some ouputs of Short-Term Analysis of Buoy Data (2011-11-07 03:13-00:13)

4.8 Impact Assessment

In Figure 4.29, at zone “A”, prevailing waves made 15° with the coast; at “B” 12°; “C” 56°; “D” 45°; “E” 27°; “F” 53°; “G” 26° and; 80° at “H”. According to the classification of coast by the angle of prevailing waves, “A”, “B”, “D”, “E” and “G”, were of Type 3 classification – Moderate Oblique; whiles “C”, “F” and “H” were of Type 4 – Very Oblique.

Figures 4.30, 4.31 and 4.32 are the coastal geological settings divided into three sections, Eastern, Central and Western respectively. Below are the interpretations of codes to the legends in the coastal basins (refer to Figure 3.2):

Sek - Sandstone (5 formations) and interbedded shale (2 formations), undifferentiated; Cul - Limestone, marl, mudstone with intercalated sandy beds (includes minor Cenozoic clastic sediments in the Tano basin area); Sek - Sandstone (5 formations) and interbedded shale (2 formations), undifferentiated; Ackb - Mudstone, finely laminated ('Korle Bu Fm‘); Bs - Sediment/volcaniclastic sediment, undifferentiated, locally mica schist; Bsv - volcaniclastics sediment dominant; Bsw - Wacke sediment dominant; Ackl - Sandstone, interbedded with shale ('Korle Lagoon Fm‘); Acks - Sandstone, thickly bedded, medium grained ('Kaneshie Fm‘); Amcs - Conglomerate, micaceous sandstone, arkose, mudstone; Tect - Arenaceous and argillaceous sediment, locally gravel (‘Continental terminal‘ sensu lato); Qa - Alluvial sand, silt, clay (Keta basin only); Tcq - Detrital sediment, mainly sandstone and conglomerate, undifferentiated. The entire geological sedimentary materials above are susceptible to erosion under wave action. Refer to Appendix F for definition of all geological legend codes

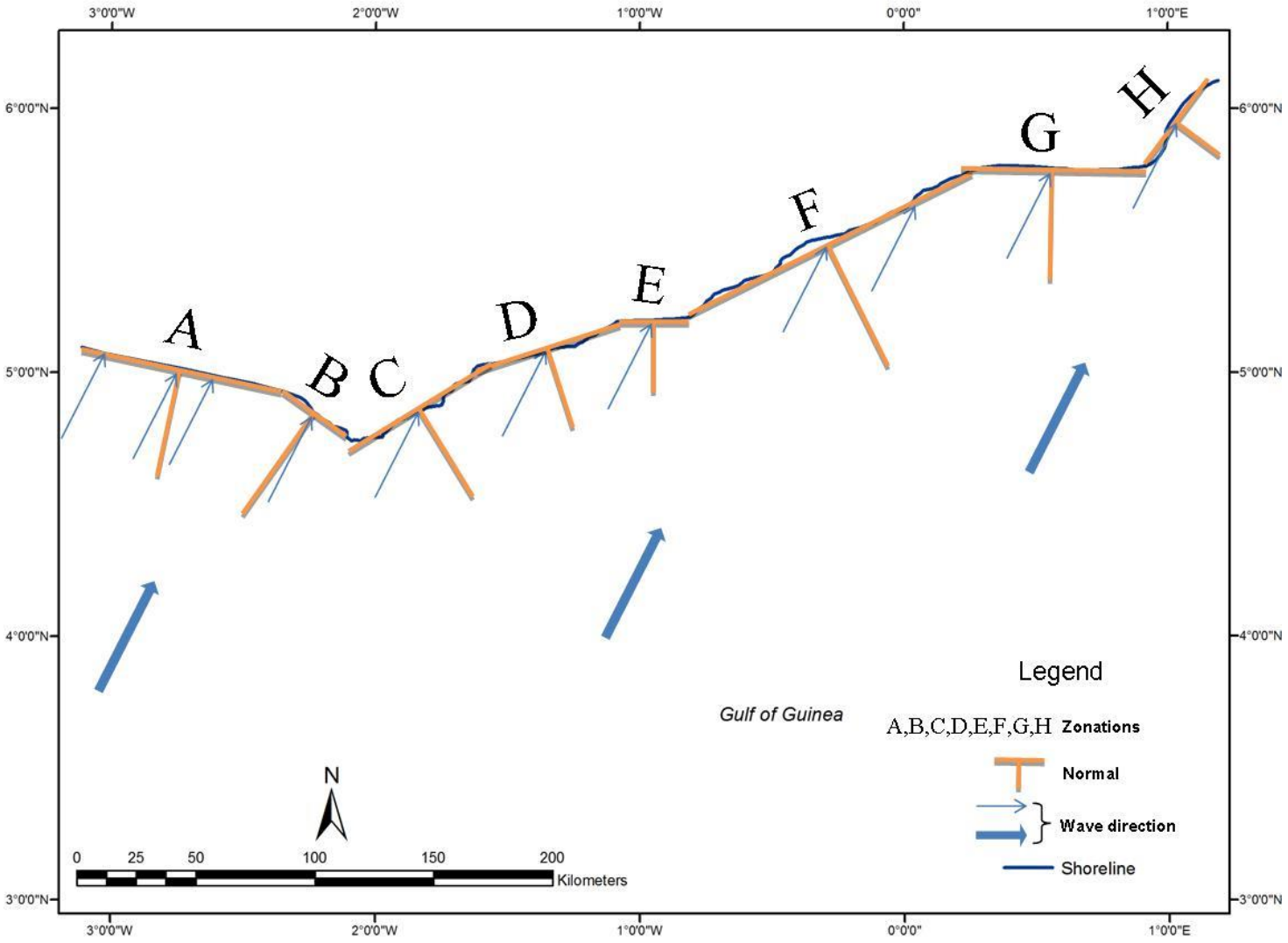

Figure 4.29: Shoreline of Ghana with orientation zonations

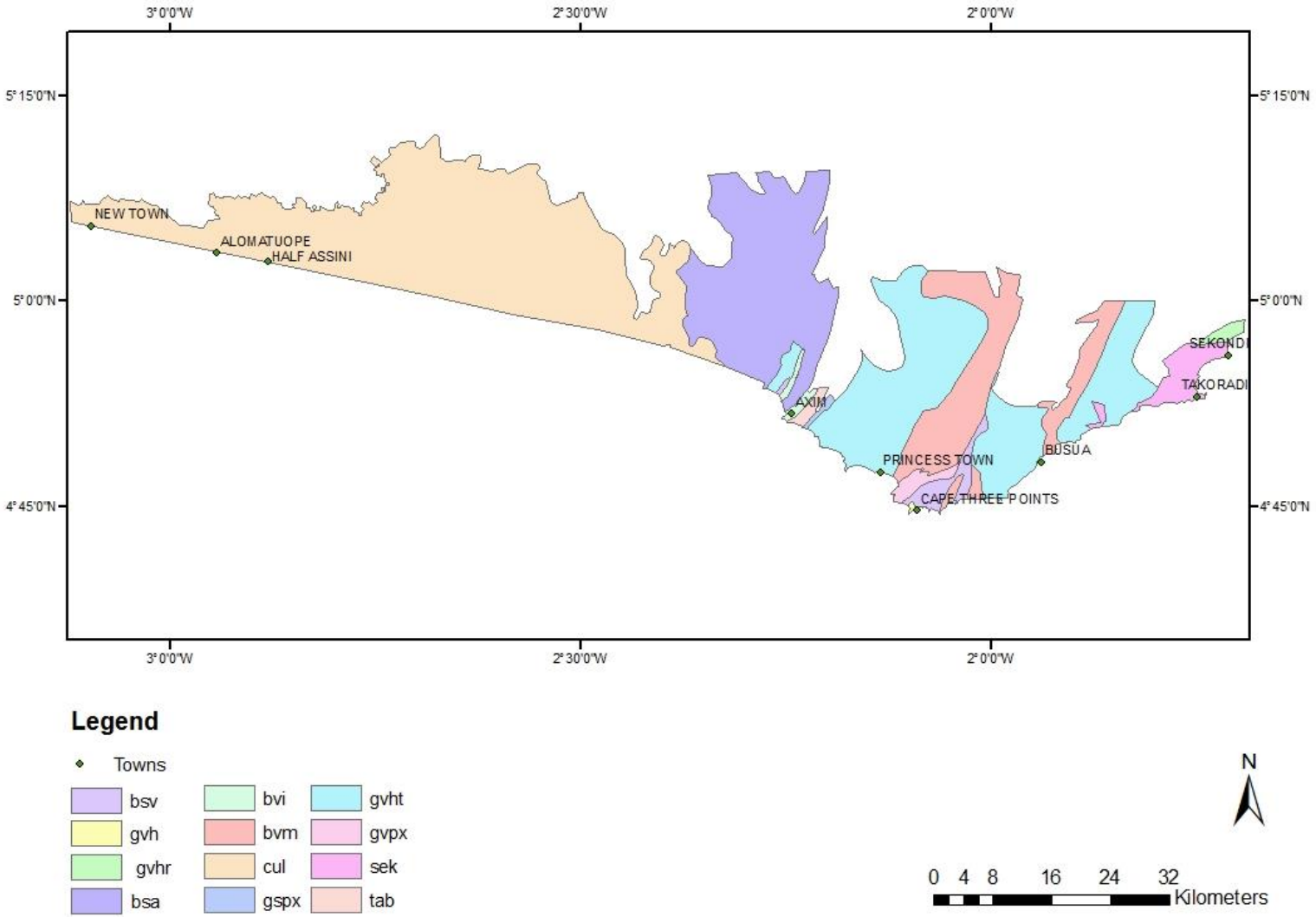

Figure 4.30: Coastal geology (Western Section)

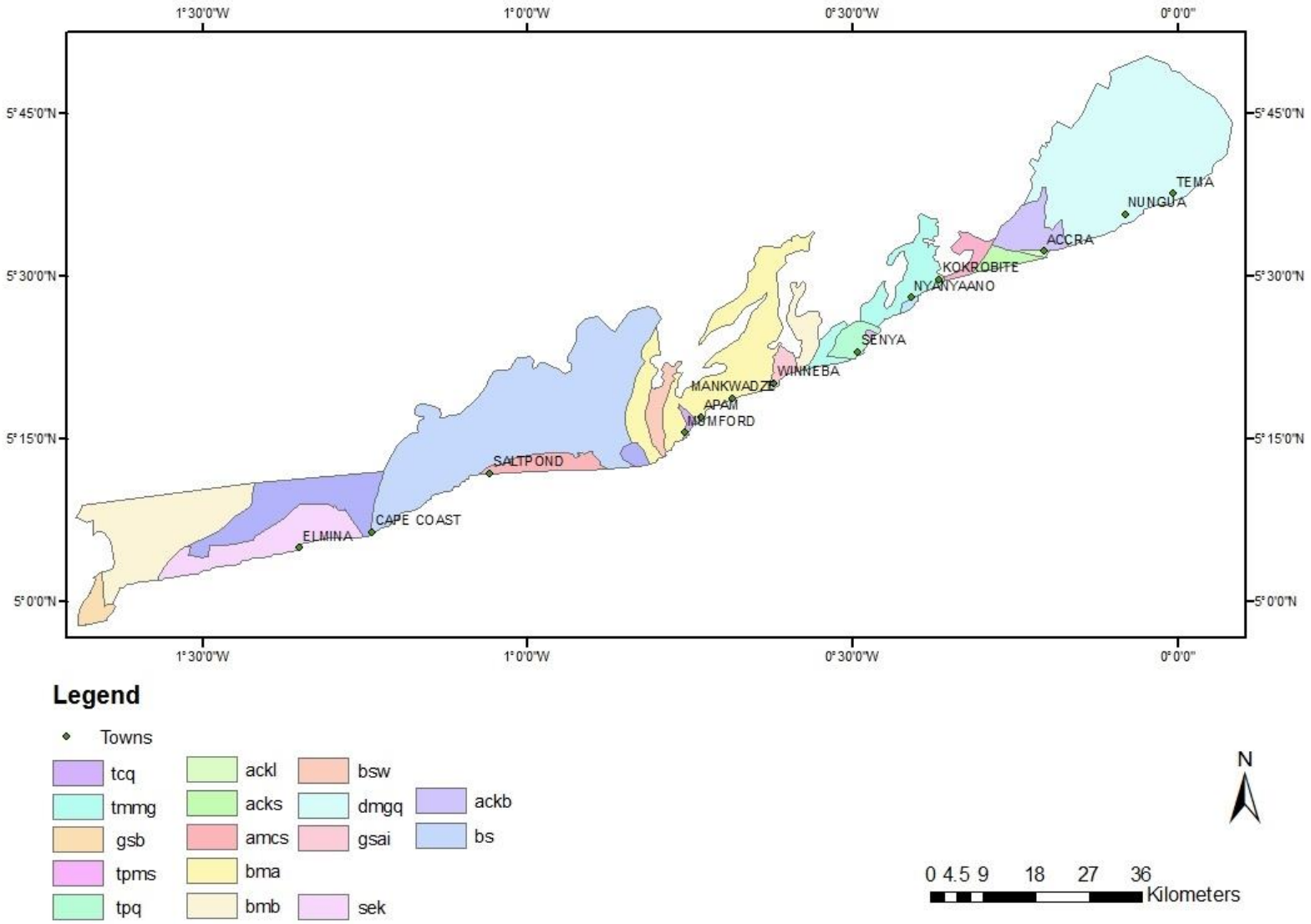

Figure 4.31: Coastal geology (Central Section)

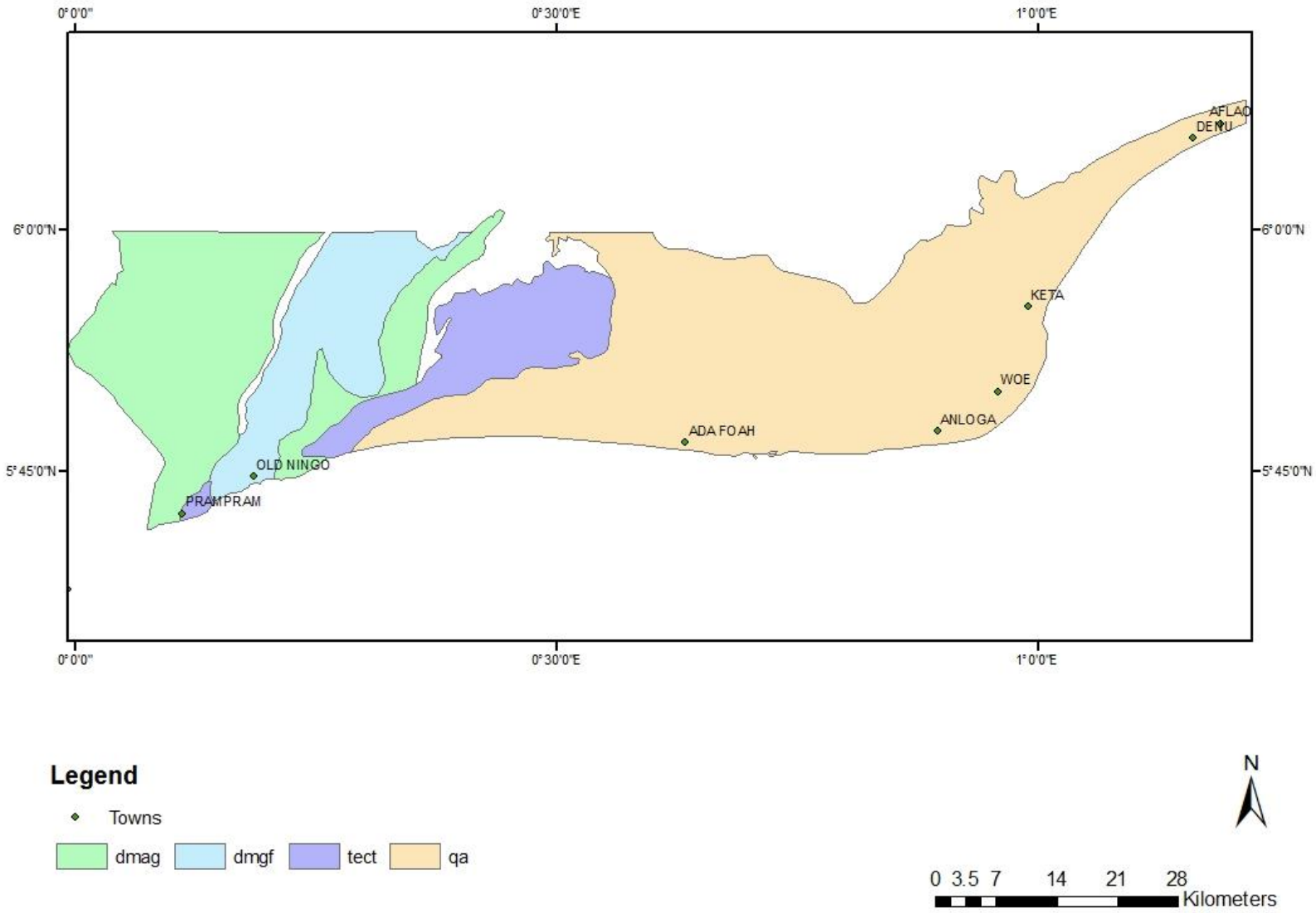

Figure 4.32: Coastal geology (Eastern Section)

CHAPTER FIVE

DISCUSSION

5.1 Wave Heights

The wave heights did not follow a normal distribution. A KS-test on the wave heights gave a result of 1, thus wave heights did not followed a standard normal distribution. Wave heights have been theoretically and empirically tested to follow a Rayleigh distribution (Bouws *et al*., 1998), which is a positively skewed distribution. Wave heights arriving at the coast are mainly made of relatively low wave heights (1.39 m and below). The yearly trend observed in wave heights could be explained by taking a close look at the 30-days moving average in Figure 4.6. The trend observed could be related to the gradual change in seasons at the point of generation, especially wind speed, through the year. Thus the waves (wind generated waves) are influenced by the wind. A correlation of 0.391 between wave heights and wind speeds is not very strong though a p-value of zero showed that this was significant. The low correlation could also mean that a larger number of wave heights recorded did not originate from the point of recording but were made up of swells which have been confirmed by various studies (Brink and Robinson, 2005; Saenger, 2002; Schwartz, 2005). Annual monthly wave heights (Figure 4.14(A)), confirmed Draper's work in Sekondi where the highest waves tend to occur in August followed by July (Draper, 1966). Monthly wave height pattern also means sediment transport will follow this pattern with highest transport rates occurring in the month of August (Table 4.12). Wave heights had an exeedance probability of 0.48% of exceeding moderate sea state. A linear fit showed a gradual increase in wave height with an annual rate of 0.017 my^{-1}. This annual increase could be attributed to climate change (McInnes

and Engineers, 2003). Further analysis however showed that wave heights were not increasing but rather the frequency of occurrence of higher waves (those from the mean and above) was increasing. This again could be attributed to increase in storminess due to climate change (Fowler and Hennessy, 1995). This signifies that wave energy impacts on the coast are likely to increase in the coming years leading to increased coastal erosion.

There were some disparities between the NOAA data and recorded data from the Buoy. Difference between monthly wave heights was as high as 0.3m for August. Whiles November had the same mean value. The absence of in situ wind data made it impossible to determine seas from swells. Also a three month data may not be sufficient to make thorough comparison.

5.2 Wave Periods

A result of wave periods ranging between 0.1s and 30s shows that the waves arriving at the ranged between ultragravity (0.1 s) and gravity (30 s) waves (Kinsman, 2002). The period record signifies that more surging breakers may be occurring in the month of May thus, waves may overtop coastal dunes pushing them inland and may cause flooding in low lying areas once the dunes are breached at high tide. In places where the slope is relatively low, plunging breakers may occur (Mangor, 2008) causing severe erosion. A decreasing trend of period also means future waves will arrive along the coast at a lower speed and probably with shorter wave lengths. Thus erosion will be reduced. But this cannot occur if climate change parameters such as greenhouse gases keep increasing.

5.3 Wind Speeds

Most wind speeds were between 2 and 8 ms^{-1} (Table 4.3). Low wind speeds may be as a result of daily transitions from sea breeze to land breeze. The few high wind speeds may also be attributed to by storms. Variability in wind speed may be accounted for by the daily atmospheric energy (mainly in the form of heat) flux changes. During the day, due to pressure differences between land and the sea as a result of the land getting quickly heated up, air flows from sea to land (sea breeze). A reverse occurs at night (land breeze) as the land loses its heat more quickly becoming cold (Ahrens, 2007; Schwartz, 2005; Sharan and Raman, 2007). Ocean waves are mainly wind generated – it was therefore expected that the winds will have substantial influence on the wave. However correlation between wind speed and wave heights was 0.391, indicating a higher composition of swells. The presence of swells are also known to restrict wind-water interactions thereby inhibiting the formation of seas (Violante-Carvalho *et al*., 2004).

From its exeedence probability, wind speeds had a probability of 1% of exceeding the moderate breeze and virtually 0% of exceeding the fresh breeze limit. Annual monthly wind speeds (Figure 4.14 (C)) also followed a similar trend recorded in Jensen (2001), Figure 4.12 shows. Though a similar trend is observed, wind speeds from land tend to be lower, and this is expected as sea breeze tends to slow down as they encounter obstacles on land. Thus they have much less impact on land. Also sea breeze, onshore winds are always stronger as compared to land breeze due to an almost efficient water-atmosphere interaction. Wind speeds had an average annual increase rate of 0.073 $ms^{-1}y^{-1}$. Again this annual increase in wind speed could be attributed to global warming as a result of climate change. Global warming results in increased weather and climatic conditions such as increased storm frequencies, increased surge conditions (causing flooding along low

lying coastal areas), along the coast due to increased wind speeds and storms with an eventual increase in wave heights (Appeaning *et al*., 2011; McInnes and Engineers, 2003; Thorne *et al*., 2007).

5.4 Wave and Wind Directions and their Impact on the Coast of Ghana

A prevalent SSW direction of waves of 1-2m meant there is a resultant eastward drift current along the coast. This direction is kept throughout the year since wave direction barely changes. Coincidences of wave and wind directions being less than 50% (highest equals about 32%), reflected in the correlation between wave and wind directions, which was 0.065 (refer to Table 4.9). Changes in wind directions during the year may not be significant as change in angle is less than 45°. Angle between prevalent wave directions is also less than 45° which may also not be significant.

Sediment transport along the beach is not only by water. Apart from the wind generating waves that dislodge sediment or create currents that influence sediment transport, the wind plays an important direct role as well in sediment transport. Onshore winds play significant role in the formation and maintenance of foredunes (Nordstrom *et al*., 1996). Sediment transportation is however affected by moisture in the air. The moisture tends to reduce the rate of transport. This effect is however reduced as wind speed increases (Nordstrom *et al*., 1996). The wind also with a good fetch may create local nearshore waves that influence sediment transport or interact with incoming waves, reinforcing them or reducing their effects. Wind tends to blow to the North through to East-North-East, onshore direction with North-North-East and North-East being the most prevalent onshore directions. Sediments are therefore expected to be transported in this direction. A frequent and mean speed of 4.96 ms^{-1} and 4.65 ms^{-1} respectively are quite significant to

lift sediments as large as 3 mm in diameter (Bagnold, 1941). The wave and wind directions also predict direction of substances in case of spills at sea.

Sediment transport involves several factors such as, sediment particle size and arrangement, existence of sufficient current, bottom features, shoreline orientation and so on. The coast of Ghana is not uniform and therefore sediment transport is expected to vary from one point to the other.

5.5 Wave Energy and Potential Sediment Transport

From the wave height distribution, wave heights equal and below the mean formed 61% whiles those above the mean formed 39%. However, wave energies equal and below the mean formed 34% whiles those above the mean formed 66%. This shows that though majority of the waves have wave heights lower than the mean, the few higher ones contribute greater energy. This also shows the Ghanaian coast is dominated by high energy waves. Wave energies also followed the same trend as wave heights. Monthly energy trends may be described as a bell shaped where energies began from a low at the start of the year till it reached a peak in August then began to decrease to a low in December. Maximum sediment transport is therefore expected to be high in the middle of the year with low transports occurring at both ends of the year. An average energy of 2432.4 kgs^{-2} per wave is significant to cause a strong transport of sediments along the unprotected sandy beaches of Ghana.

This trend is also reflected in the potential sediment transport for each month where mean wave heights were paired with their most probable periods and potential sediment transport rate calculated for (Figure 4.24). These transport rates may help in decision making of what kind of shore management system to put in place with regards to erosion,

either soft or hard. Beach nourishment may be a good choice where there is high crosshore sediment transport on gentle sloping beaches with no submarine canyons or trenches where sediments will not be recoverable. Monthly and yearly crosshore potential sediment transports were: 2.13E+07 m^3 per month and 2.25E+08 m^3 per year respectively. Longshore transports were 1.60E+07 m^3 per month and 1.82E+08 m^3 per year for monthly and yearly transports respectively. The yearly longshore transport confirms Hayes *et al*., 2008, who estimated that Ghana's longshore transport exceeds 764554.9 m^3 per year. It should be however noted that wave details are often recorded well offshore or taken from global wave models well offshore where the hindcast wave parameters are considered free from nearshore bathymetry that is coarsely represented or assume deep water in these models due to their scale (Callaghan and Wainwright, 2013). These values will vary in real terms thus may be higher or lower depending on nearshore morphological features.

5.6 Wave-Wind Correlations

Correlations got stronger at higher values for all progressive correlation analysis. It was also noticed that low changes in surge resulted in high changes in wave height. Increasing correlation at higher values supports research by Dattatri *et al*., (1977) where high speed winds showed good correlations with wave heights. Low wave and wind correlation may also mean that most of the waves are not generated from the point of data collection (4N, 1W) but rather made up of swells coming from long distances as swells do not have good correlations with the local wind, confirming literature by Ardhuin *et al*., (2009)

This implies that winds will only have significant impact of generating seas when they get strong enough to break the inhibition caused by the swells. Surges are able to generate

high waves with a little stress meaning waves cause significant impact during storm surges.

5.7 Impact of Waves on the Coast

Impact of waves on the coast was assessed using direction of wave impact, coastal geology and shore bathymetry. According to the classification of the Ghanaian shoreline by the angle of incident waves, two categories were obtained: Types 3 and 4 which are moderately oblique and very oblique respectively. Both types have potentially large net transport of sediment. This adds up to other confirmations like Wiafe, (2010), that the coast is dominated by erosion. The wave directions also indicate a net eastwards littoral drift. From the bathymetry (refer to Figure 3.3), the shelf on the eastern section of the coast is narrow and drops rapidly as compared to shelf on the western section. The shelf on the eastern section reaches a maximum of 12km at some point whiles the western portion has a wide, about 80km at some points, and relatively gentle sloping shelf as compared to the eastern section. This implies that waves with full energy reach the coast on the eastern section as these waves would have experienced little shoaling for them to lose some energy. On the contrary waves on the western section would have dissipated a considerable amount of their energy before reaching the shore. Hence it is expected that erosion will be more on the eastern section as compared to the western section.

The Coastal Basins are believed to have been formed as a result of Gondwana break up and the opening of the Atlantic Ocean (Agyei Duodu et al., 2009). These basins were then filled with eroded sedimentary material from nearby rocks and fluvial activity with time. Thus these basins are made of relatively movable clastic material and concurrently

these basins tend to be the main sandy beaches along the coast. This implies that along the coast, these basins are vulnerable to coastal erosion and possible flooding

CHAPTER SIX

CONCLUSION AND RECOMMENDATION

6.1 Conclusion

The objectives of this studies were: to examine the offshore wave characteristics of Ghana from in situ and modelled data; to ascertain the effect of wind on the propagation of waves; to identify the energy regime of waves along the coast of Ghana and; to determine how waves impact the coast through sediment transport. All these objectives were achieved as yearly and seasonal wave patterns along the coast of Ghana was obtained; the effect of wind on the propagation of waves was also determined; the direction of waves and their impact in the littoral zone was determined; the energy regime of waves along the coast was also determined; and the influence of waves on sediment transport was determined.

Yearly seasonal mean wave pattern along the coast was developed where it starts on a low in January (1.00m) increases gradually and peaks up in August (1.72m) and decreases again to December (1.10m). The general sea state was also determined to be Moderate with a mean wave height of 1.39m. Predominant wave direction was found to be in the SSW direction thus producing a net eastwards littoral drift. Winds were not found to have any significant impact on the approaching waves as they consisted of mainly swells. Analysis however showed they had a relative impact at higher values. Highest mean wind speed of 5.61ms^{-1} occurred in July and lowest of 3.72ms^{-1} in December. Wind speeds barely crossed fresh breeze and were barely calm as most, over 90%, were within 2 and 8 ms^{-1}. Hence an average wind speed of 4.65 ms^{-1} could describe

the winds along the coast of Ghana as gentle breeze. Winds change direction during the year but the angle of change is not significant.

The main objective of ascertaining how the waves impact the coast was also achieved through the estimation of the energy and direction of waves and modeling of sediment volume transport. The shoreline configuration was also used to determine how these waves are influenced and how they in turn impact the shore.

Wave energies were found to be moderately high and their monthly energy trends followed that of the waves. The year 2002 was found to have the highest wave activity and hence the highest impact of sediment transport. The Soulsby-Van Rijn sediment transport equation enabled potential sediment volume transports modeling for both suspended and bed transports along the coast. Crosshore transports were generally higher than longshore transports. After the classification of the coast based on incident waves it was concluded that the entire coast will have a large net transport. The nearshore bathymetry was also found to influence incoming waves where the large relatively sloping western shelf is perceived to have significant dissipating effect on in coming waves through bottom friction. The eastern coast on the otherhand with little shelf receives waves with their full energy. The coastal geology of the coast revealed major basins that are filled with eroded sediment from close by rocks hence they are vulnerable to wave action.

6.2 Recommendations

The coastal zone being a dynamic and ever evolving place needs constant monitoring especially during this era of increasing sea level rise and climate change. Vigorous

policies are also needed to protect the shore especially from anthropogenic activities that tend to exacerbate beach erosion.

Large in situ wave measurements are needed to develop a reliable wave climate for the region as the minimal in situ data used in this study made it quite impossible to make definite conclusions.

A thorough study of the continental shelf waves is needed to better understand their dynamics and impact on the shore. Coastal sediment dynamics are highly dependent on the wave dynamics in the surf zone.

Field experiments are required to calibrate and certify the potential sediment volume transport in this study.

An interdisciplinary approach of study is needed for a total understanding of the complex processes that go on in the coastal environment.

SST studies should incorporate the effect of waves and winds as these have significant impacts on such phenomenon.

More studies could be done to ascertain the stability of the waves along the coast and their energy harnessed for the production of electricity.

REFERENCES

Addo, A. K. (2003). *To Determine the Rate of Coastal Erosion in a GIS environment.* MPhil, Kwame Nkrumah University of Science and Technology, Kumasi.

Agyei Duodu, J., Loh, G., Boamah, K., Baba, M., Hirdes, W., Toloczyki, M., and Davis, D. (2009). Geological Map of Ghana 1: 1,000,000. *Geological Survey of Ghana, Map, 1*(1).

Ahrens, C. D. (2007). *Meteorology Today: An Introduction to Weather, Climate, and the Environment*: Thomson/Brooks/Cole.

Akrasi, S. A. (2011). Sediment Discharges from Ghanaian Rivers into the Sea. *West African Journal of Applied Ecology*.

Allaby, M. (2002). *Encyclopedia of Weather and Climate*: Facts On File.

Al-Tahir, R., and Ali, A. (2004). Assessing land cover changes in the coastal zone using aerial photography. *Surveying and Land Information Science, 64*, 107-112.

Alves, J.-H. G. M. (2006). Numerical modeling of ocean swell contributions to the global wind-wave climate. *Ocean Modelling, 11*(1–2), 98-122. doi: 10.1016/j.ocemod.2004.11.007

Anadón, R., Danovaro, R., Dippner, J. W., Drinkwater, K. F., Hawkins, S. J., O'Sullivan, G., . . . Reid, P. C. (2007). Impacts of Climate Change on the European Marine and Coastal Environment. In N. Connolly (Ed.), *Marine Board*.

Appeaning Addo, K. (2010). Changing morphology of Ghana's Accra coast. *Journal of Coastal Conservation, 15*(4), 433-443. doi: 10.1007/s11852-010-0134-z

Appeaning Addo, K., Walkden, M., and Mills, J. P. (2008). Detection, measurement and prediction of shoreline recession in Accra, Ghana. *ISPRS Journal of Photogrammetry and Remote Sensing, 63*(5), 543-558. doi: 10.1016/j.isprsjprs.2008.04.001

Appeaning, A. K., Larbi, L., Amisigo, B., and Ofori-Danson, P. K. (2011). Impacts of Coastal Inundation Due to Climate Change in a CLUSTER of Urban Coastal Communities in Ghana, West Africa. *Remote Sensing, 3*(9), 2029-2050. doi: 10.3390/rs3092029

Ardhuin, F., Chapron, B., and Collard, F. (2009). Observation of swell dissipation across oceans. *Geophysical Research Letters, 36*(6).

Armah, A. K. (2005). The Coastal Zone Of Ghana : Vulnerability and Adaptation Assessment to Climate Change. Maputo.

Armah, A. K., and Amlalo, D. S. (1998). Coastal Zone Profile of Ghana. *Gulf of Guinea Large Marine Ecosystem Project*. Accra: Ministry of Environment, Science and Technology.

Ashton, Q. A. (2011). *Issues in Global Environment: Freshwater and Marine Environments: 2011 Edition*: ScholarlyEditions.

Backstrom, J., Jackson, D., and Cooper, J. (2008). Storm-Driven Shoreface Morphodynamics on a Low-Wave Energy Delta: The Role of Nearshore Topography and Shoreline Orientation. *Journal of Coastal Research*(24), 1379-1387.

Bagnold, R. A. (1941). *The Physics of Blown Sand and Desert Dunes*: Chapman and Hall.

Bailard, J. (1981). An energetics total load sediment transport model for a plane sloping beach. *Journal of Geophysical Research, 86*(C11), 10938-10954.

Bailard, J., and Inman, D. (1981). An energetics bedload model for a plane sloping beach: local transport. *Journal of Geophysical Research, 86*(C11), 10938-10954.

Bapentire, A. D. (2011). *Impacts of Keta Sea Defence Project (KSDP) on the Down-drift Coast.* Master of Science in Physical Oceanography and Applications, University of Abomey-Calavi, Cotonou.

Bayram, A., Larson, M., Miller, H. C., and Kraus, N. C. (2001). Cross-shore distribution of longshore sediment transport: comparison between predictive formulas and field measurements. *Coastal Engineering, 44*(2), 79-99. doi: 10.1016/s0378-3839(01)00023-0

Bea, R., Xu, T., Stear, J., and Ramos, R. (1999). Wave forces on decks of offshore platforms. *Journal of Waterway, Port, Coastal, and Ocean Engineering, 125*(3), 136-144.

Bijker, E. (1967). Some considerations about scales for coastal models with movable bed *Tech. Rep* (Vol. 50). Netherlands: Delft Hydraulics Laboratory.

Bird, E. (2011). *Coastal Geomorphology: An Introduction*: John Wiley and Sons, Incorporated.

Bird, E. C. F. (1985). *Coastline Changes*. Wiley and Sons, New York.

Boateng, I. (2006). *Shoreline Management Planning: Can It Benefit Ghana? A Case Study of UK SMPs and Their Potential Relevance in Ghana*. Paper presented at the Promoting Land Administration and Good Governance 5th FIG Regional Conference, Accra, Ghana.

Boateng, I. (2009). *Development of Integrated Shoreline Management Planning: A Case Study of Keta, Ghana.* Paper presented at the FIG Working Week 2009, Surveyors Key Role in Accelerated Development Eilat, Israel.

Boateng, I., Bray, M., and Hooke, J. (2012). Estimating the fluvial sediment input to the coastal sediment budget: A case study of Ghana. *Geomorphology, 138*(1), 100-110. doi: 10.1016/j.geomorph.2011.08.028

Bouws, E., Draper, L., Shearman, E. D. R., Laing, A. K., Feit, D., Mass, W., Battjes, J. A. (1998). *Guide to Wave analysis and forecasting. WMO-No. 702. World Meteorological Organization second edition*. doi: citeulike-article-id:2248812

Brander, R. W. (1999). Sediment Transport in Low-Energy Rip Current Systems. *Journal of Coastal Research, 15*(3), 839-849. doi: 10.2307/4298997

Brink, K. H., and Robinson, A. R. (2005). *Global Coastal Ocean: The Regional Studies and Syntheses*: Harvard University Press.

Bullock, G. N., Crawford, A. R., Hewson, P. J., Walkden, M. J. A., and Bird, P. A. D. (2001). The influence of air and scale on wave impact pressures. *Coastal Engineering, 42*(4), 291-312. doi: http://dx.doi.org/10.1016/S0378-3839(00)00065-X

Callaghan, D. P., and Wainwright, D. (2013). The impact of various methods of wave transfers from deep water to nearshore when determining extreme beach erosion. *Coastal Engineering, 74*(0), 50-58. doi:

Camenen, B. t., and Larroudé, P. (2003). Comparison of sediment transport formulae for the coastal environment. *Coastal Engineering, 48*(2), 111-132. doi: 10.1016/s0378-3839(03)00002-4

Casale, R., and Margottini, C. (2004). *Natural Disasters and Sustainable Development*: Springer.

Casas-Prat, M., and Sierra, J. (2012). Trend analysis of wave direction and associated impacts on the Catalan coast. *Climatic Change, 115*(3-4), 667-691.

Charlier, and Meyer, D. (1998). Chapter I: Bed material suspension and transport in steady uniform currents *Coastal Erosion* (Vol. 70, pp. 49-84): Springer Berlin / Heidelberg.

Charlier, R. H., and De Meyer, C. P. (1998). *Coastal Erosion: Response and Management*: Springer.

CoastalProcesses. (n.d.). Coastal Processes Retrieved 28-06, 2012, from http://www.nature.nps.gov/views/kcs/coastalg/html/ET_Processes.htm

Crooks, S., and Turner, R. K. (1999). Integrated coastal management: sustaining estuarine natural resources. *Advances in Ecological Research, 29*, 241-289.

Crowley, T. J. (2000). Causes of climate change over the past 1000 years. *Science, 289*(5477), 270-277.

Cubasch, U., Meehl, G., Boer, G., Stouffer, R., Dix, M., Noda, A., . . . Yap, K. (2001). Projections of future climate change. *, in: JT Houghton, Y. Ding, DJ Griggs, M. Noguer, PJ Van der Linden, X. Dai, K. Maskell, and CA Johnson (eds.): Climate Change 2001: The Scientific Basis: Contribution of Working Group I to the Third Assessment Report of the Intergovernmental Panel*, 526-582.

da Silva, P. A., Temperville, A., and Seabra Santos, F. (2006). Sand transport under combined current and wave conditions: A semi-unsteady, practical model. *Coastal Engineering, 53*(11), 897-913. doi: 10.1016/j.coastaleng.2006.06.010

Dattatri, J., Shankar, N. J., and Raman, H. (1977). Wind velocity distribution over wind-generated water waves. *Coastal Engineering, 1*(0), 243-260. doi: http://dx.doi.org/10.1016/0378-3839(77)90017-5

Davidson-Arnott, R. G. D., MacQuarrie, K., and Aagaard, T. (2005). The effect of wind gusts, moisture content and fetch length on sand transport on a beach. *Geomorphology, 68*(1–2), 115-129. doi: 10.1016/j.geomorph.2004.04.008

Dean, R. G., and Dalrymple, R. A. (2001). *Tides and Storm Surges Coastal Processes with Engineering Applications*: Cambridge University Press.

Dean, R. G., and Dalrymple, R. A. (2004). *Coastal Processes With Engineering Applications*: Cambridge University Press.

Dibajnia, M., and Watanabe, A. (1992). *Sheet flow under nonlinear waves and currents.* Paper presented at the Proceedings of 23rd International Conference on Coastal Engineering, Venice, Italy.

Draper, L. (1966). Waves at Sekondi, Ghana. *Coastal Engineering*. Retrieved from http://journals.tdl.org/ICCE/article/view/2399/2074

Drennan, W., Kahma, K., Terray, E., Donelan, M., and Kitaigorodskii, S. (1992). Observations of the enhancement of kinetic energy dissipation beneath breaking wind waves *Breaking waves* (pp. 95-101): Springer.

Dube, S., Rao, A., Sinha, P., Murty, T., and Bahulayan, N. (1997). Storm surge in the Bay of Bengal and Arabian Sea: the problem and its prediction.

Edge, B. L. (2011). Proceedings of the International Conference on Coastal Engineering Retrieved from http://journals.tdl.org/ICCE/article/view/1960/1453

Edwards, J. (2005). *Plate tectonics and continental drift*. London: Evans.

Einstein, H. A. (1950). *The bed-load function for sediment transportation in open channel flows*: US Department of Agriculture.

Einstein, H. A. (1950). The bed-load function for sediment transportation in open channel flows *Technical Bulletin* (Vol. 1026): U.S. Department of Agriculture.

Elfrink, B., and Baldock, T. (2002). Hydrodynamics and sediment transport in the swash zone: a review and perspectives. *Coastal Engineering, 45*(3–4), 149-167. doi: http://dx.doi.org/10.1016/S0378-3839(02)00032-7

Engineers, U. S. A. C. o. (2002). *Coastal Engineering Manual*. Washington, D.C.: US Army Corps of Engineers.

EPA. (2009). Environmental and Socio-Economic Baseline *Jubilee Field Draft EIA Chapter 4* (2009 ed.).

Finkl, C. W., and Bruun, P. (1998). Potentials for manipulating wave action via port and coastal engineering *Journal of Coastal Research, 26*(Special issue), 1-10.

Forces, N. R. C. C. o. N. S. I. o. C. C. f. U. S. N. (2011). *National Security Implications of Climate Change for U.S. Naval Forces*: National Academies Press.

Fowler, A., and Hennessy, K. (1995). Potential impacts of global warming on the frequency and magnitude of heavy precipitation. *Natural Hazards, 11*(3), 283-303.

Fredsoee, J., and Deigaard, R. (1992). *Mechanics of coastal sediment transport*: World Scientific Publishing Company Incorporated.

Garrison, T. S. (2009). *Oceanography: An Invitation to Marine Science*: Brooks/Cole, Cengage Learning.

GCLME. (2006). Transboundary Diagnostic Analysis. Accra, Ghana.

Grabemann, I., and Weisse, R. (2008). Climate change impact on extreme wave conditions in the North Sea: an ensemble study. *Ocean Dynamics, 58*(3-4), 199-212.

Hastenrath, S. (1985). *Climate and circulation of the tropics*: D. Reidel Pub. Co.

Hayes, M. O., Michel, J., and Holmes, J. M. (2008). *A Coast for All Seasons: A Naturalist's Guide to the Coast of South Carolina*: Pandion Books.

Héquette, A., and Tremblay, P. (2009). Effects of Low Water Temperature on Longshore Sediment Transport on a Subarctic Beach, Hudson Bay, Canada. *Journal of Coastal Research, 25*(1), 171-180. doi: 10.2307/40065109

Holthuijsen, L. H. (2007). *Waves in Oceanic And Coastal Waters*: Cambridge University Press.

Houghton, J. T., and Change, I. P. o. C. (1996). *Climate Change 1995: The Science of Climate Change: Contribution of Working Group I to the Second Assessment Report of the Intergovernmental Panel on Climate Change*: Cambridge University Press.

http://dx.doi.org/10.1016/j.coastaleng.2012.12.001

IPCC. (1990). Response Strategies Working Group, 1990.

IPCC. (2001). Third Assessment Report - Climate Change 2001. In I. P. o. C. Change (Ed.). Cambridge.

IPCC. (2007). Fourth Assessment Report: Contribution of Working Group II to the Fourth Assessment Report of the Intergovernmental Panel on Climate Change. Cambridge, UK.

Janssen, P. A. E. M. (2008). Progress in ocean wave forecasting. *Journal of Computational Physics, 227*(7), 3572-3594. doi: http://dx.doi.org/10.1016/j.jcp.2007.04.029

Jensen, S. Ø. (2001). Ghanaian weather data for simulation purposes Solar Energy Centre Denmark Danish Technological Institute, Vol. SEC-R-5.

Kalinske, A. (1947). Movement of sediment as bed load in rivers. *Transactions, American Geophysical Union, 28*, 615-620.

Kamphuis, J. W. (2000). *Introduction to Coastal Engineering and Management*: World Scientific.

Kantha, L. H., and Anne Clayson, C. (2004). On the effect of surface gravity waves on mixing in the oceanic mixed layer. *Ocean Modelling, 6*(2), 101-124.

Kelly, D. (2003). *Storm Surges*. Dalhousie University, Halifax NS Canada

Khandekar, M. L. (1989). *Operational analysis and prediction of ocean wind waves* (Vol. 33): American Geophysical Union.

Kinsman, B. (2002). *Wind Waves: Their Generation and Propagation on the Ocean Surface*: Dover Publications.

Kocurek, G., Havholm, K. G., Deynoux, M., and Blakey, R. C. (1991). Amalgamated accumulations resulting from climatic and eustatic changes, Akchar Erg, Mauritania. *Sedimentology*(38), 751-772.

Krishnamurti, T. N., Xue, J., Bedi, H., Ingles, K., and Oosterhof, D. (1991). Physical initialization for numerical weather prediction over the tropics. *Tellus B, 43*(4), 53-81.

Larson, M., Erikson, L., and Hanson, H. (2004). An analytical model to predict dune erosion due to wave impact. *Coastal Engineering, 51*(8–9), 675-696. doi: http://dx.doi.org/10.1016/j.coastaleng.2004.07.003

Lindorm. (2007). Engineering Side Effects Retrieved 28/06, 2012, from http://lindorm.com/beaches/humans.php

Ly, C. K. (1980). The role of the Akosombo Dam on the Volta river in causing coastal erosion in central and eastern Ghana (West Africa). *Marine Geology, 37*(3–4), 323-332. doi: 10.1016/0025-3227(80)90108-5

Lynch, K., Delgado-Fernandez, I., Jackson, D. W. T., Cooper, J. A. G., Baas, A. C. W., and Beyers, J. H. M. (2013). Alongshore variation of aeolian sediment transport

on a beach, under offshore winds. *Aeolian Research, 8*(0), 11-18. doi: http://dx.doi.org/10.1016/j.aeolia.2012.10.004

Mandal, S., and Prabaharan, N. (2010). Ocean Wave Prediction Using Numerical and Neural Network Models. *The Open Ocean Engineering Journal, 3*, 12-17.

Mangor, K. (2004). *Shoreline Management Guidelines*: DHI Water and Environment.

Mangor, K. (2008). *Waves*: DHI Water and Environment.

Mason, T., and Coates, T. T. (2001). Sediment Transport Processes on Mixed Beaches: A Review for Shoreline Management. *Journal of Coastal Research, 17*(3), 645-657. doi: 10.2307/4300216

Massel, S. R. (1996). Ocean Surface Waves: Their Physics and Prediction.

Masselink, G., Evans, D., Hughes, M. G., and Russell, P. (2005). Suspended sediment transport in the swash zone of a dissipative beach. *Marine Geology, 216*(3), 169-189. doi: http://dx.doi.org/10.1016/j.margeo.2005.02.017

May, V., and Hansom, J. D. (2003). *Coastal Geomorphology of Great Britain* (Vol. 28): Joint Nature Conservation Committee Peterborough.

McInnes, R., and Engineers, I. o. C. (2003). *International Conference on Coastal Management 2003: Proceedings of the International Conference on Coastal Management, Organised by the Institution of Civil Engineers and Held in Brighton, UK, on 15-17 October 2003*: Thomas Telford.

Mensah, J. V. (1997). Causes and effects of coastal sand mining in Ghana. *Singapore Journal of Tropical Geography, 18*(1), 69-88.

MetOffice. (n.d.). The Beaufort Scale. *National Meteorological Library and Archive, Fact sheet 6*(version 01). www.metoffice.gov.uk/learning/library/publications/factsheets

Meyer-Peter, E., and Müller, R. (1948). Formulas for bed-load transport. In: Report on the 2nd Meeting International Association Hydraulic Structure Research (pp. 39-64). Stockholm, Sweden.

Moon, I.-J. (2005). Impact of a coupled ocean wave–tide–circulation system on coastal modeling. *Ocean Modelling, 8*(3), 203-236.

Müller, P., and Briscoe, M. (1998). Diapycnal Mixing and Internal Waves. *Dynamics of Oceanic Internal Gravity Waves*.

Mustapha, S. (2011, 28 Jan 2011). Ghana's coast dwellers flee encroaching seas Retrieved 28-05-2013, 2013, from http://www.trust.org/item/?map=ghanas-coast-dwellers-flee-encroaching-seas

Needham, H., and Keim, B. D. (2009). *Storm Surge : Physical Processes and an Impact Scale.* Louisiana State University.

Needham, H., and Keim, B. D. (2011). Storm surge: physical processes and an impact scale (pp. 385-407): InTech.

Nielsen, P. (1992). *Coastal bottom boundary layers and sediment transport* (Vol. 4): World Scientific Publishing Company.

Nordstrom, K. F., Bauer, B. O., Davidson-Arnott, R. G. D., Gares, P. A., Carter, R. W. G., Jackson, D. W. T., and Sherman, D. J. (1996). Offshore Aeolian Transport Across a Beach: Carrick Finn Strand, Ireland. *Journal of Coastal Research, 12*(3), 664-672.

Ostdiek, V. J., and Bord, D. J. (2007). *Inquiry Into Physics*: Thomson Brooks/Cole.

Oteng-ababio, M., Owusu, K., and Appeaning Addo, K. (2011). The vulnerable state of the Ghana coast : The case of Faana-Bortianor. *JAMBA: Journal of Disaster Risk Studies, 3*(2), 429-442.

Pérez, A. A., Gatti, R. C., and Fernández, B. H. (2011). *Building Resilience to Climate Change: Ecosystem-Based Adaptation and Lessons from the Field*: Island Press.

Piton, B. (1987). Les anomalies océanographiques et climatiques de 1983 et 1984 dans le Golfe de Guinée. *Veille Climatique Satellitaire*(16), 18-31.

Rascle, N., Ardhuin, F., Queffeulou, P., and Croizé-Fillon, D. (2008). A global wave parameter database for geophysical applications. Part 1: Wave-current–turbulence interaction parameters for the open ocean based on traditional parameterizations. *Ocean Modelling, 25*(3), 154-171.

Raubenheimer, B. (2004). Shaping the Beach, One Wave at a Time. *Oceanus*.

RESPONSE. (2006). Coastal Processes and Climate Change Predictions in the Coastal Study Areas *LIFE Environment Project*: Isle of Wight Centre for the Coastal Environment.

Ribberink, J. (1998). Bed-load transport for steady flows and unsteady oscillatory flows. *Coastal Engineering, 34*, 52-82.

Ribberink, J., and Al Salem, A. (1994). Sediment transport in oscillatory boundary layers in cases of rippled beds and sheet flow. *Journal of Geophysical Research, 99*(C6), 707-727.

Roelvink, J. A., and Reniers, A. J. H. M. (2011). *A Guide to Modelling Coastal Morphology*: World Scientific Publishing Company Incorporated.

Rossouw, M., and Theron, A. (2009). Maritime Transport and the Climate Change Challenge *Aspects of Potential Climate Change Impacts on Ports and Maritime Operations around the Southern African Coast*: CSIR, South Africa; UNCTAD.

Ruessink, B. G., Houwman, K. T., and Hoekstra, P. (1998). The systematic contribution of transporting mechanisms to the cross-shore sediment transport in water depths of 3 to 9 m. *Marine Geology, 152*(4), 295-324. doi: http://dx.doi.org/10.1016/S0025-3227(98)00133-9

Saenger, P. (2002). *Mangrove Ecology, Silviculture, and Conservation*: Kluwer Academic Publishers.

Schellnhuber, H. J., and Cramer, W. P. (2006). *Avoiding Dangerous Climate Change: Key Vulnerabilities of the Climate System and Critical Thresholds; Part II. General Perspectives on Dangerous Impacts; Part III. Key Vulnerabilities for Ecosystems and Biodiversity; Part IV. Socio-Economic Effects; Part V. Regional Perspectives; Part VI. Emission Pathways; Part VII. Technological Options*: Cambridge University Press.

Schwartz, M. L. (2005). Encyclopedia of Coastal Science (pp. 1211-1211): Springer.

Sharan, M., and Raman, S. (2007). *Atmospheric and Oceanic Mesoscale Processes*: Birkhäuser.

Short, A. D. (1985). Rip current type, spacing and persistence, Narrabeen beach, Australia. *Marine Geology, 65*, 47-71.

Short, A. D. (2012). Coastal Processes and Beaches. *Nature Education Knowledge* Retrieved 28-05-2013, 2013, from http://www.nature.com/scitable/knowledge/library/coastal-processes-and-beaches-26276621

Singapore. *World Scientific*.

Small, C., and Cohen, J. E. (2004). Continental Physiography, Climate, and the Global Distribution of Human Population. *Current Anthropology, 45*, 269-279.

Smith E., W. P., Zhang J. (2003). *Evaluation of the Cerc Formula Using Large-Scale Model Data*. Paper presented at the Proceedings Coastal Sediments, ASCE.

Smith, E. R., Wang, P., Ebersole, B. A., and Zhang, J. (2009). Dependence of total longshore sediment transport rates on incident wave parameters and breaker type. *Journal of Coastal Research*, 675-683.

Soulsby, R. (1997). *Dynamics of Marine Sands: A Manual for Practical Applications*: Telford.

Soulsby, R. L., and Clarke, S. (2005). Bed Shear-stresses Under Combined Waves and Currents on Smooth and Rough Beds *Defra project FD1905 (EstProc)* (Vol. R 1.0): HR Wallingford.

Stewart, R. H. (2008). *Introduction to Physical Oceanography*: University Press of Florida.

Stutz, M. L., and Pilkey, O. H. (1999). Discussion of: Wang, P.; N.C. Kraus, and R.A. Davis. 1998. Total Longshore Sediment Transport Rate in the Surf Zone: Field

Measurements and Empirical Predictions. *Journal of Coastal Research, 14*(1), 269-282.

Tang, Y. M., Grimshaw, R., Sanderson, B., and Holland, G. (1996). A numerical study of storm surges and tide, with application to the north Queensland coast. *J. Phys. Oceanogr, 26*, 2700-2711.

TGL. (2009). DRAFT Non Technical Executive Summary of Environmental Impact Statement *Ghana Jubilee Field Phase 1 Development*: Tullow Ghana Limited. http://www.tullowoil.com/ghana/files/pdf/Jubilee_Field_EIA_Chapter_4_27Nov09_Part1.pdf

Thorne, C., Thorne, C. R., Evans, E. P., and Penning-Rowsell, E. C. (2007). *Future Flooding and Coastal Erosion Risks*: Thomas Telford.

Titus, J., G. , Cahoon, D., R. , Williams, J., Gutierrez, B., T. , Anderson, E., K. , Thieler, R., E. , and Gesch, D., B. . (2009). Coastal Sensitivity to Sea-Level Rise: A Focus on the Mid-Atlantic Region *U.S. Climate Change Science Program* (Vol. Synthesis and Assessment Product 4.1): USGS.

Tolman, H. L. (2008). *Practical Wind Wave Modeling.* Paper presented at the WSPC - Proceedings.

Tolman, H. L., Balasubramaniyan, B., Burroughs, L. D., Chalikov, D. V., Chao, Y. Y., Chen, H. S., and Gerald, V. M. (2002). Development and Implementation of Wind-Generated Ocean Surface Wave Modelsat NCEP*. *Weather and Forecasting, 17*(2), 311-333. doi: 10.1175/1520-0434(2002)017<0311:daiowg>2.0.co;2

UNEP. (1985). Coastal erosion in West and Central Africa *Regional Seas Reports and Studies* (pp. 237). New York: UNEP/ UNESCO/ UN.

UNEP. (2007). Draft National Status Report for Ghana: National State of Coast Reports (Vol. 24). Abidjan.

UNEP. (2008). UNEP climate change strategy. UNEP Knowledge Repository

Van Rijn, L. C. (1984). Sediment transport, Part II: Suspended load transport. *Journal of Hydraulic Engineering, 110*(11), 1613-1641.

Violante-Carvalho, N., Ocampo-Torres, F. J., and Robinson, I. S. (2004). Buoy observations of the influence of swell on wind waves in the open ocean. *Applied Ocean Research, 26*(1–2), 49-60. doi: 10.1016/j.apor.2003.11.002

Wang, P., Kraus, N. C., and Davis, R. A., Jr. (1998). Total Longshore Sediment Transport Rate in the Surf Zone: Field Measurements and Empirical Predictions. *Journal of Coastal Research, 14*(1), 269-282. doi: 10.2307/4298775

Wang, X. L., and Swail, V. R. (2006). Climate change signal and uncertainty in projections of ocean wave heights. *Climate Dynamics, 26*(2-3), 109-126.

Wang, X. L., Zwiers, F. W., and Swail, V. R. (2004). North Atlantic ocean wave climate change scenarios for the twenty-first century. *Journal of Climate, 17*(12), 2368-2383.

Ward, K. D., Watts, S., Tough, R. J. A., Engineering, I. o., Technology, and Engineers, I. o. E. (2006). *Sea Clutter: Scattering, the K-Distribution and Radar Performance*: Institution of Engineering and Technology.

Wellens-Mensah, J., Armah, A. K., Amlalo, D. S., and Tetteh, K. (2002). Ghana National Report Phase 1: Integrated Problem Analysis. GEF MSP Sub-Saharan Africa Project (GF/6010-0016): Development and Protection of the Coastal and Marine Environment in Sub-Saharan Africa. Accra, Ghana.

Wiafe, G. (2010). Coastal and Continental Shelf Processes in Ghana (D. o. M. a. F. Sciences, Trans.): UNIVERSITY OF GHANA.

Winter, R. C. d., Sterl, A., Vries, J. d., Weber, S. L., and Ruessink, G. (2012). The effect of climate change on extreme waves in front of the Dutch coast. *Ocean Dynamics*. doi: 10.1007/s10236-012-0551-7

Xu, J. P., Noble, M., and Eittreim, S. L. (2002). Suspended sediment transport on the continental shelf near Davenport, California. *Marine Geology, 181*(1–3), 171-193. doi: http://dx.doi.org/10.1016/S0025-3227(01)00266-3

Young, I., Zieger, S., and Babanin, A. (2011). Global trends in wind speed and wave height. *Science, 332*(6028), 451-455.

Zhang, K., Douglas, B. C., and Leatherman, S. P. (2004). Global warming and coastal erosion. *Climatic Change, 64*(1-2), 41-58.

Zhang, K., Douglas, B. C., and Leatherman, S. P. (1997). U.S. East Coast Storm Surges Provide Unique Climate Record. *EOS Transactions, 78*(37), 396-397.

Zhang, K., Douglas, B. C., and Leatherman, S. P. (2000). Twentieth Century Storm Activity along the U.S. East Coast. *Climate, 13*, 1748-1761.

Zhang, K., Douglas, B. C., and Leatherman, S. P. (2004). Global warming and coastal erosion. *Climatic Change, 64*(1-2), 41-58.

APPENDIX

Appendix A: Matlab Scripts

Sediment Potential Volume Transport

```
function [S] = SoulsbyVanRijn(H,T)

%--------------------------------------------------------------------------

% This script was written by Sowah Wahab Laryea (University of Ghana),

% Trinity Mensah-Senoo(University of Ghana)

% ALL RIGHTS RESERVED

%--------------------------------------------------------------------------

% h - depth at breaking point

% r - ??? constant

% v - ??? constant

% g - gravity

% rho - water density, pure water=1000 surface sea water=1027kg per metre cube

% D - sediment diametre

% rho_sed - ???

% final unit of final output - metre cube per second

% T0=T(T~=0);
```

```
% H0=H(T~=0);


H=1.18;T=8; % this is for testing function - this should be replaced by

% input data - :,by 2 matrix

h=3;r=0.06; v=1;g=9.81;rho=1000;

D50=0.002; D90=0.003; rho_sed=2000;

w=2*pi./T(1:end)';

k=w/sqrt(g*h);

%Calculating current shear stress tc

% 1. Find Chezy C (or friction factor Cf)then tc

C=18*log(12*h/r);

tc=rho*g*v^2/C^2;

%Calculating wave shear stress tw

% 1. Find orbital vel (u0)

u0=pi*H./T./sinh(k'*h);

% 2. Find orbital excursion (radius) A0

A0=u0'./w ;% A0=u*T/(2*pi)

% 3. Find friction factor (fw) then tw
```

```
fw=1.39*(A0/r).^(-0.52); %fw=1.39(A0/z0)

tw=(1/2)*rho*fw*u0.^2; %uw=u0

% Calculating bedload transport (Sb)

% 1. find the critical velocity and coeff of friction

if D50<=0.0005

   Ucr=0.19*D50^0.1*log(4*h/D90);

else

   if D50>0.0005 || D50>=0.002

   Ucr=8.5*D50^0.6*log(4*h/D90);

   end

end

Cf=g/C^2;  % Cf=(ks/(ln(h/zo)-1))^2

% 2. Find the general multipliction factor

u=u0;

EEs=(sqrt(u.^2+v.^2+(0.018*u0.^2./Cf)-Ucr)).^2.4;

% 3. Find grain diameter D*

rho_rel=(rho_sed-rho)./rho;

Acal=1;
```

```
Dstar=(g*rho_rel./v.^2).^(1/3)*D50;

Ass=0.012*D50*(Dstar.^-0.6./(rho_rel*g*D50).^1.2);

Asb=0.05*h*(D50./h).^1.2./(rho_rel*g*D50).^1.2;

S.Sbx=Acal*Asb*u.*EEs;

S.Sby=Acal*Asb*v.*EEs;

S.Ssx=Acal*Ass*u.*EEs;

S.Ssy=Acal*Ass*v.*EEs;
```

Appendix B: Table A.1: Wave Climate with corresponding sediment transport.

Wave Height	Wave Period	Bottom X	Bottom Y	Suspended X	Suspended Y
0.25	3.670000	0.000107	0.000549	0.002932	0.015000
0.25	11.540000	0.000289	0.001298	0.007896	0.035463
0.25	3.490000	0.000093	0.000482	0.002534	0.013156
0.25	3.883333	0.000123	0.000621	0.003368	0.016971
0.75	8.923723	0.028409	0.042961	0.776132	1.173679
0.75	10.965482	0.029278	0.043901	0.799864	1.199373
0.75	10.682639	0.029185	0.043801	0.797330	1.196640
0.75	11.004474	0.029290	0.043914	0.800198	1.199734
0.75	11.421075	0.029414	0.044047	0.803571	1.203367
0.75	11.068889	0.029310	0.043936	0.800744	1.200321
0.75	6.854000	0.026708	0.041094	0.729654	1.122682
1.25	3.670000	0.111960	0.114539	3.058718	3.129181
1.25	3.940000	0.119486	0.119967	3.264326	3.277489
1.25	3.838571	0.116783	0.118030	3.190478	3.224546
1.25	11.308521	0.175288	0.157547	4.788825	4.304146
1.25	11.195383	0.175095	0.157424	4.783574	4.300793
1.25	11.233964	0.175162	0.157466	4.785382	4.301947
1.25	10.895824	0.174559	0.157081	4.768906	4.291419
1.25	11.198738	0.175101	0.157428	4.783732	4.300894
1.25	9.589825	0.171633	0.155205	4.688973	4.240185
1.25	7.726250	0.164833	0.150810	4.503202	4.120111
1.25	5.630769	0.149005	0.140367	4.070779	3.834811
1.25	3.490000	0.106317	0.110398	2.904563	3.016065
1.25	3.490000	0.106317	0.110398	2.904563	3.016065
1.75	3.760000	0.365889	0.265588	9.996021	7.255828
1.75	11.576667	0.558979	0.358603	15.271191	9.796974
1.75	11.064983	0.556280	0.357376	15.197473	9.763457
1.75	11.032167	0.556095	0.357292	15.192407	9.761151
1.75	11.224376	0.557159	0.357776	15.221477	9.774376
1.75	11.164781	0.556835	0.357629	15.212618	9.770346
1.75	10.453902	0.552548	0.355677	15.095520	9.717022
1.75	11.914444	0.560579	0.359330	15.314924	9.816836
1.75	5.787500	0.480048	0.321948	13.114828	8.795561
2.25	11.886667	1.324245	0.660251	36.178111	18.037933
2.25	10.814751	1.310990	0.655570	35.815993	17.910043
2.25	11.202877	1.316212	0.657416	35.958675	17.960479
2.25	11.499724	1.319869	0.658707	36.058565	17.995754

Table A.1: Continues

Wave Height	Wave Period	Bottom X	Bottom Y	Suspended X	Suspended Y
2.25	12.013978	1.325596	0.660727	36.215030	18.050950
2.75	12.538889	2.639881	1.075355	72.121063	29.378491
2.75	10.267500	2.584207	1.059275	70.600042	28.939181
2.75	11.738955	2.623778	1.070714	71.681123	29.251708
2.75	10.880000	2.602550	1.064584	71.101181	29.084227

Appendix C: Table A.2: Yearly potential sediment transport rates.

Year	Parameter		Transport rate (m^3 per year)						
	Wave Height	Wave Period	Bottom X	Bottom Y	Suspended X	Suspended Y	Longshore	Crosshore	Total
1997	1.33	11.07	6.90E+06	5.82E+06	1.89E+08	1.59E+08	1.65E+08	1.95E+08	3.60E+08
1998	1.31	12.12	6.62E+06	5.65E+06	1.81E+08	1.54E+08	1.60E+08	1.87E+08	3.47E+08
1999	1.39	11.07	7.89E+06	6.39E+06	2.15E+08	1.75E+08	1.81E+08	2.23E+08	4.04E+08
2000	1.34	11.07	7.10E+06	5.94E+06	1.94E+08	1.62E+08	1.68E+08	2.01E+08	3.69E+08
2001	1.42	11.07	8.53E+06	6.76E+06	2.33E+08	1.85E+08	1.92E+08	2.42E+08	4.33E+08
2002	1.46	12.12	9.58E+06	7.34E+06	2.62E+08	2.01E+08	2.08E+08	2.71E+08	4.79E+08
2003	1.41	12.12	8.34E+06	6.66E+06	2.28E+08	1.82E+08	1.88E+08	2.36E+08	4.25E+08
2004	1.43	12.12	8.79E+06	6.91E+06	2.40E+08	1.89E+08	1.96E+08	2.49E+08	4.45E+08
2005	1.45	12.2	9.39E+06	7.24E+06	2.57E+08	1.98E+08	2.05E+08	2.66E+08	4.71E+08
Mean Year	1.39	11.07	7.95E+06	6.43E+06	2.17E+08	1.76E+08	1.82E+08	2.25E+08	4.07E+08

Appendix D: Table A.3: Monthly potential sediment transport rates

Month	Parameter		Transport rate (m^3 per month)						
	Wave Height	Wave Period	Bottom X	Bottom Y	Suspended X	Suspended Y	Longshore	Crosshore	Total
Jan	1.00	10.95	2.13E+05	2.41E+05	5.83E+06	6.58E+06	6.82E+06	6.04E+06	1.29E+07
Feb	1.05	11.7	2.41E+05	2.58E+05	6.60E+06	7.05E+06	7.30E+06	6.84E+06	1.41E+07
Mar	1.22	10.95	4.30E+05	3.97E+05	1.18E+07	1.08E+07	1.12E+07	1.22E+07	2.34E+07
Apr	1.39	11.7	6.54E+05	5.29E+05	1.79E+07	1.44E+07	1.50E+07	1.85E+07	3.35E+07
May	1.57	11.7	1.03E+06	7.36E+05	2.81E+07	2.01E+07	2.09E+07	2.91E+07	5.00E+07
Jun	1.66	12.12	1.20E+06	8.15E+05	3.29E+07	2.23E+07	2.31E+07	3.41E+07	5.72E+07
Jul	1.72	11.7	1.40E+06	9.17E+05	3.83E+07	2.51E+07	2.60E+07	3.97E+07	6.57E+07
Aug	1.73	11.7	1.44E+06	9.32E+05	3.92E+07	2.55E+07	2.64E+07	4.07E+07	6.71E+07
Sep	1.58	12.12	1.02E+06	7.27E+05	2.80E+07	1.99E+07	2.06E+07	2.90E+07	4.96E+07
Oct	1.40	9.93	6.85E+05	5.52E+05	1.87E+07	1.51E+07	1.56E+07	1.94E+07	3.50E+07
Nov	1.23	10.95	4.27E+05	3.91E+05	1.17E+07	1.07E+07	1.11E+07	1.21E+07	2.32E+07
Dec	1.10	10.95	2.97E+05	3.05E+05	8.12E+06	8.33E+06	8.64E+06	8.42E+06	1.71E+07
Mean Month	1.39	11.07	7.54E+05	5.67E+05	2.06E+07	1.55E+07	1.60E+07	2.13E+07	3.74E+07

Appendix E: Other Short-Term Analysis from Buoy

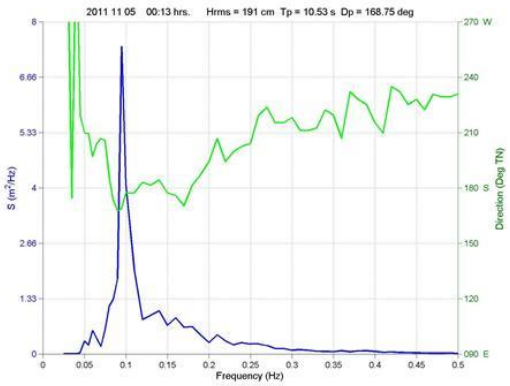

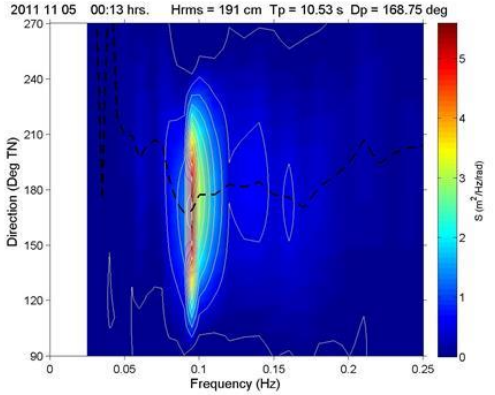

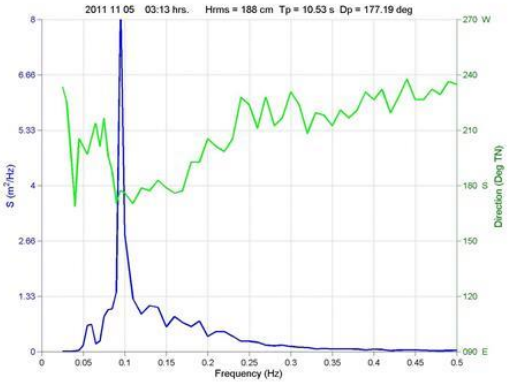

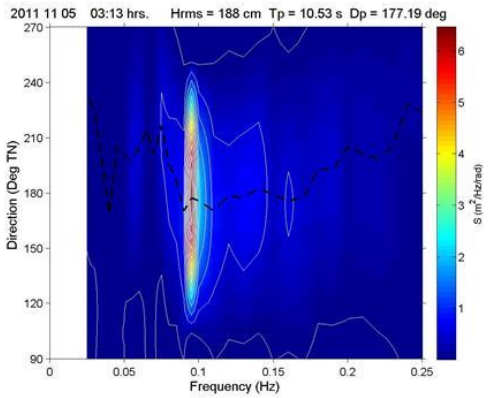

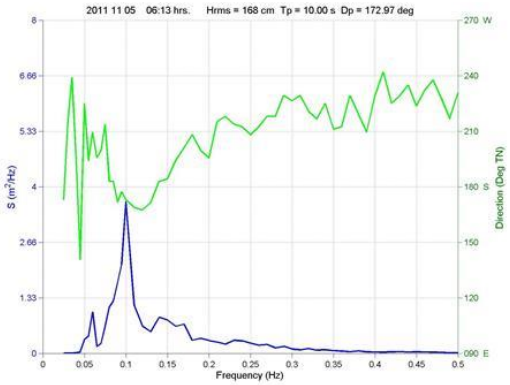

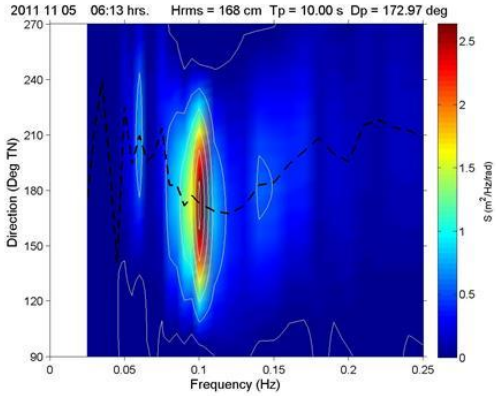

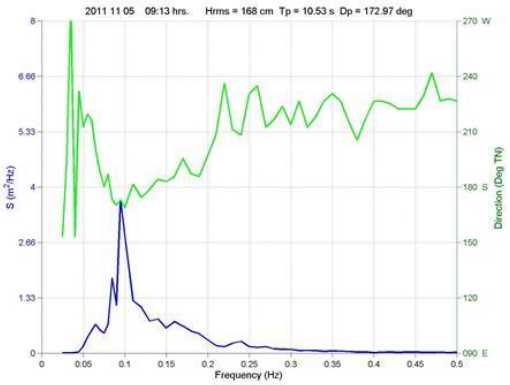

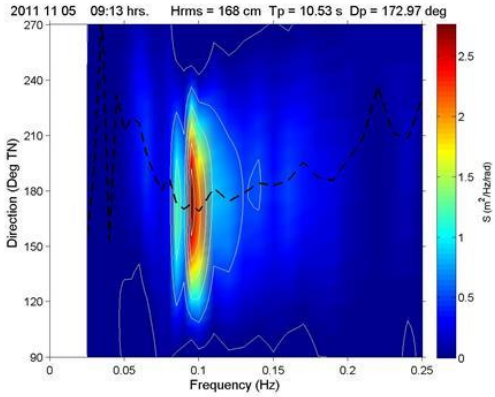

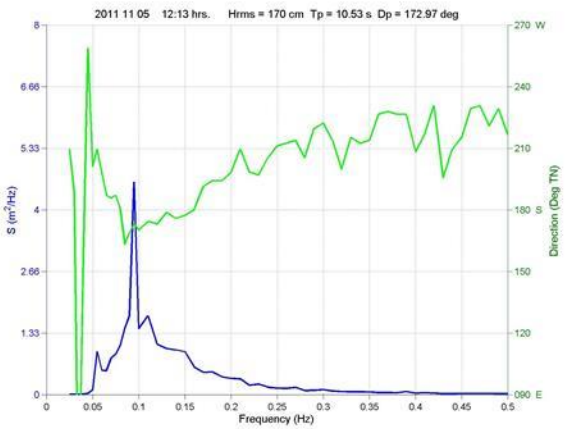
2011 11 05 12:13 hrs. Hrms = 170 cm Tp = 10.53 s Dp = 172.97 deg
S (m²/Hz)
Direction (Deg TN)
Frequency (Hz)

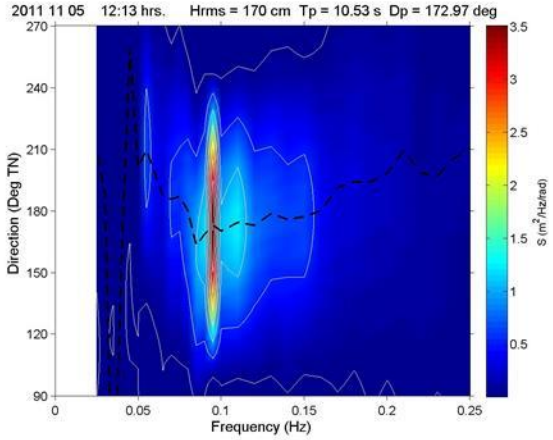
2011 11 05 12:13 hrs. Hrms = 170 cm Tp = 10.53 s Dp = 172.97 deg
Direction (Deg TN)
Frequency (Hz)
S (m²/Hz/rad)

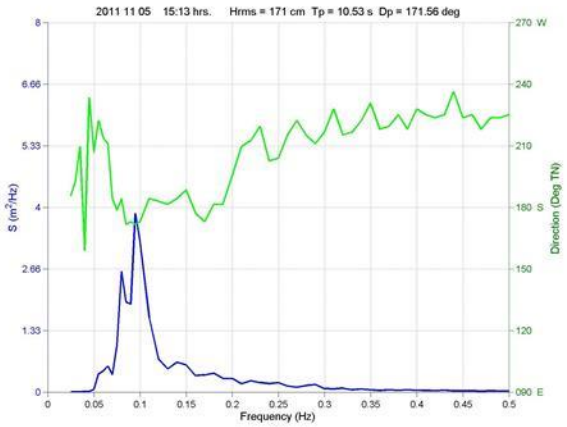
2011 11 05 15:13 hrs. Hrms = 171 cm Tp = 10.53 s Dp = 171.56 deg
S (m²/Hz)
Direction (Deg TN)
Frequency (Hz)

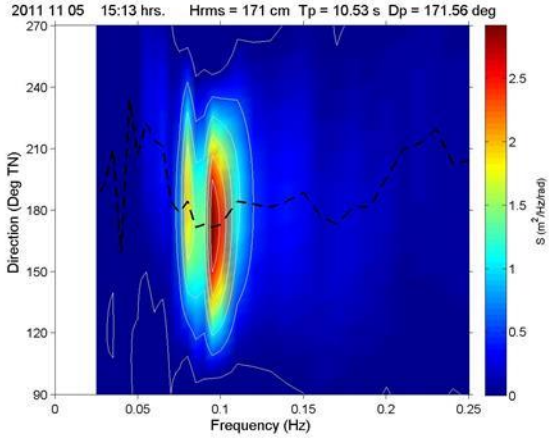
2011 11 05 15:13 hrs. Hrms = 171 cm Tp = 10.53 s Dp = 171.56 deg
Direction (Deg TN)
Frequency (Hz)
S (m²/Hz/rad)

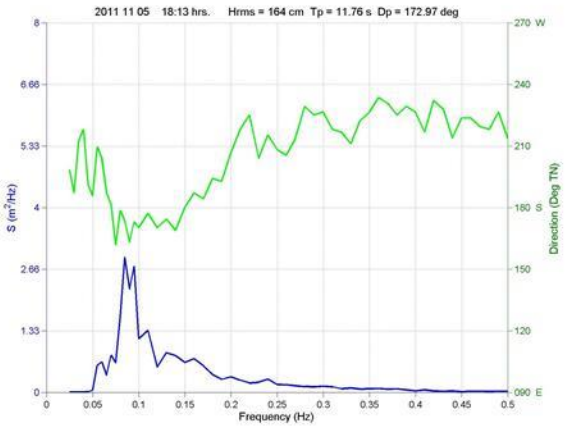
2011 11 05 18:13 hrs. Hrms = 164 cm Tp = 11.76 s Dp = 172.97 deg
S (m²/Hz)
Direction (Deg TN)
Frequency (Hz)

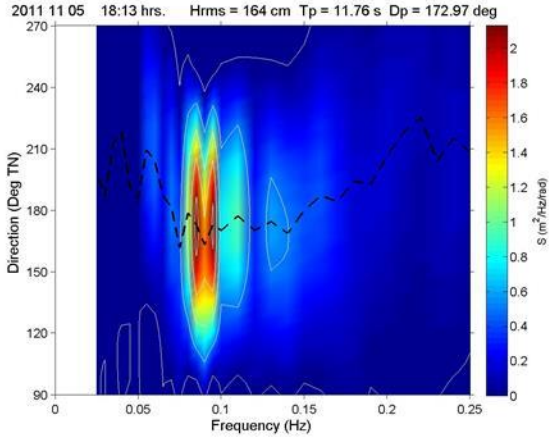
2011 11 05 18:13 hrs. Hrms = 164 cm Tp = 11.76 s Dp = 172.97 deg
Direction (Deg TN)
Frequency (Hz)
S (m²/Hz/rad)


2011 11 05 21:13 hrs. Hrms = 179 cm Tp = 10.00 s Dp = 178.59 deg
S (m²/Hz)
Direction (Deg TN)
Frequency (Hz)

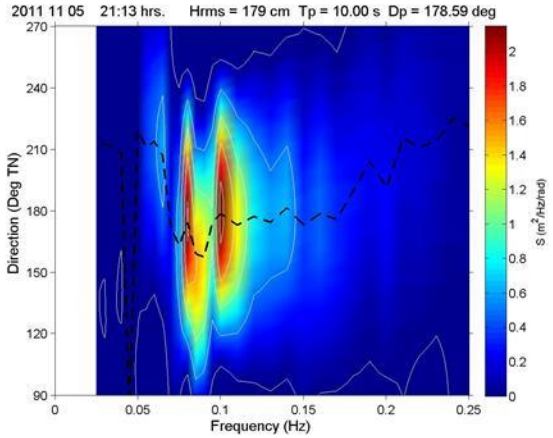
2011 11 05 21:13 hrs. Hrms = 179 cm Tp = 10.00 s Dp = 178.59 deg
Direction (Deg TN)
Frequency (Hz)
S (m²/Hz/rad)

X

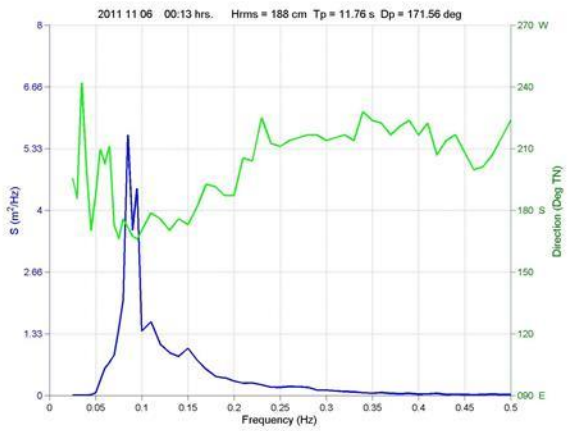
2011 11 06 00:13 hrs. Hrms = 188 cm Tp = 11.76 s Dp = 171.56 deg
S (m²/Hz)
Direction (Deg TN)
Frequency (Hz)

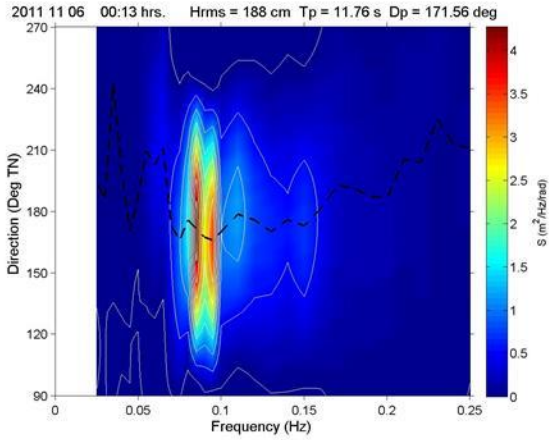
2011 11 06 00:13 hrs. Hrms = 188 cm Tp = 11.76 s Dp = 171.56 deg
Direction (Deg TN)
Frequency (Hz)
S (m²/Hz/rad)

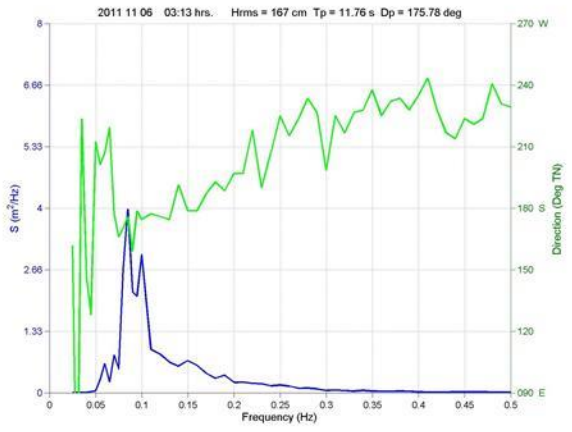
2011 11 06 03:13 hrs. Hrms = 167 cm Tp = 11.76 s Dp = 175.78 deg
S (m²/Hz)
Direction (Deg TN)
Frequency (Hz)

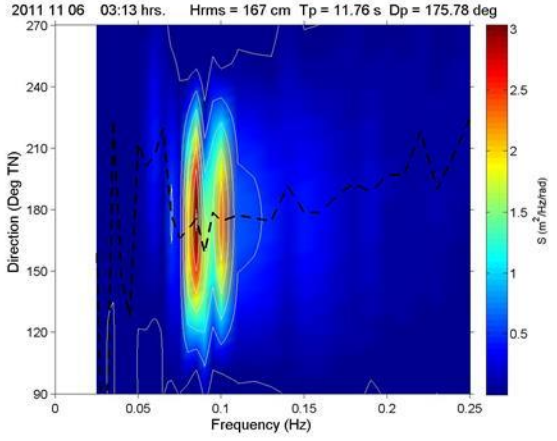
2011 11 06 03:13 hrs. Hrms = 167 cm Tp = 11.76 s Dp = 175.78 deg
Direction (Deg TN)
Frequency (Hz)
S (m²/Hz/rad)

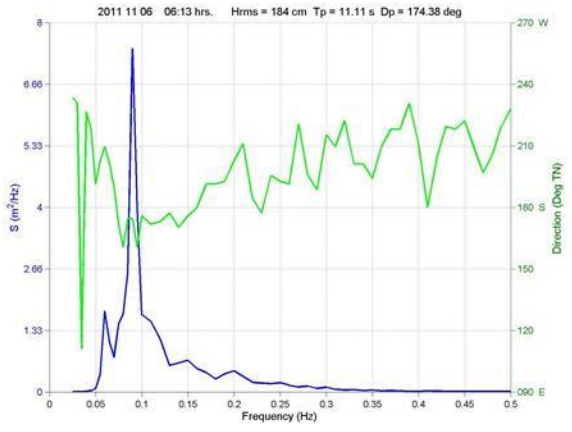
2011 11 06 06:13 hrs. Hrms = 184 cm Tp = 11.11 s Dp = 174.38 deg
S (m²/Hz)
Direction (Deg TN)
Frequency (Hz)

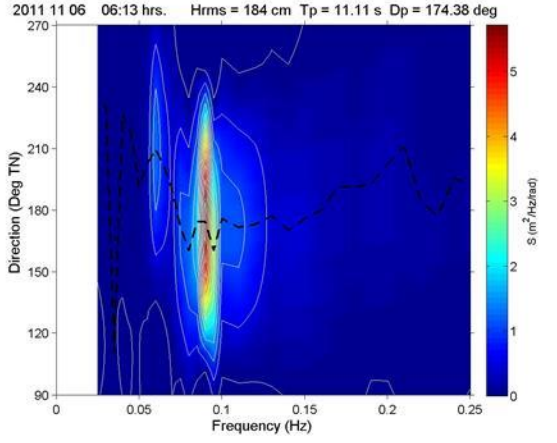
2011 11 06 06:13 hrs. Hrms = 184 cm Tp = 11.11 s Dp = 174.38 deg
Direction (Deg TN)
Frequency (Hz)
S (m²/Hz/rad)

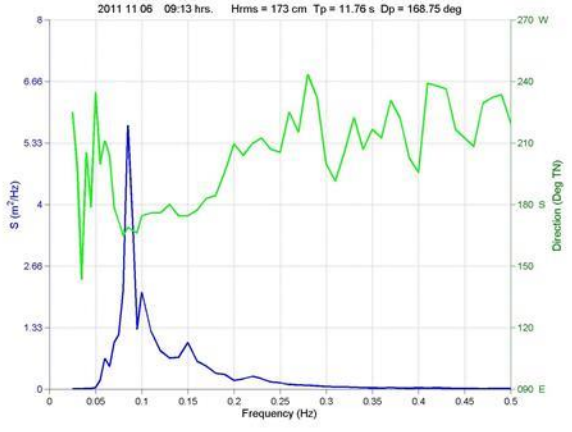
2011 11 06 09:13 hrs. Hrms = 173 cm Tp = 11.76 s Dp = 168.75 deg
S (m²/Hz)
Direction (Deg TN)
Frequency (Hz)

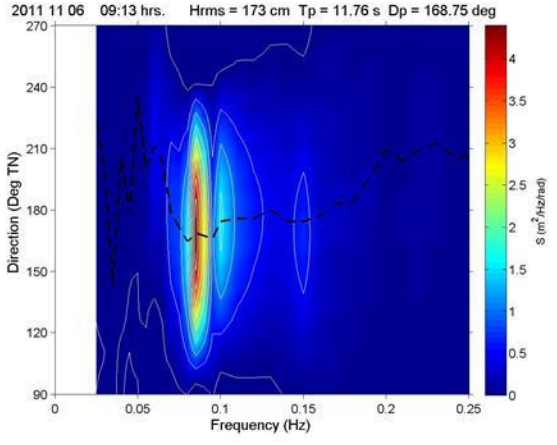
2011 11 06 09:13 hrs. Hrms = 173 cm Tp = 11.76 s Dp = 168.75 deg
Direction (Deg TN)
Frequency (Hz)
S (m²/Hz/rad)

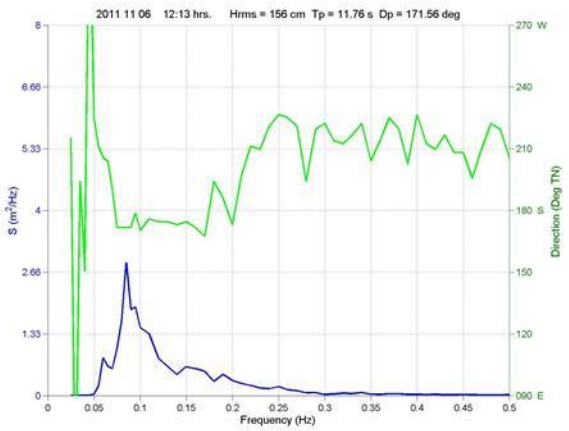
2011 11 06 12:13 hrs. Hrms = 156 cm Tp = 11.76 s Dp = 171.56 deg
S (m²/Hz)
Direction (Deg TN)
Frequency (Hz)

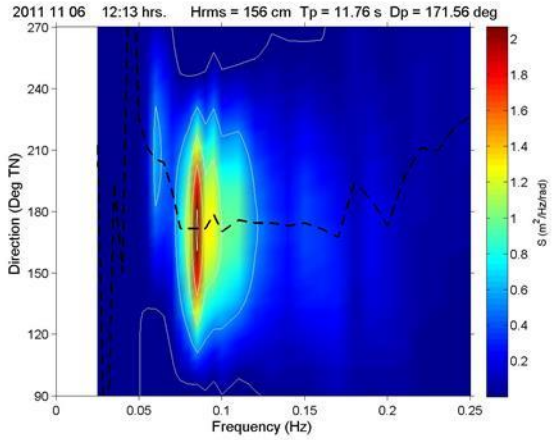
2011 11 06 12:13 hrs. Hrms = 156 cm Tp = 11.76 s Dp = 171.56 deg
Direction (Deg TN)
Frequency (Hz)
S (m²/Hz/rad)

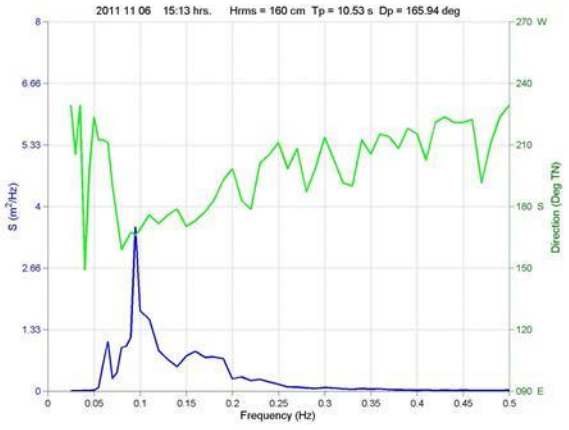
2011 11 06 15:13 hrs. Hrms = 160 cm Tp = 10.53 s Dp = 165.94 deg
S (m²/Hz)
Direction (Deg TN)
Frequency (Hz)

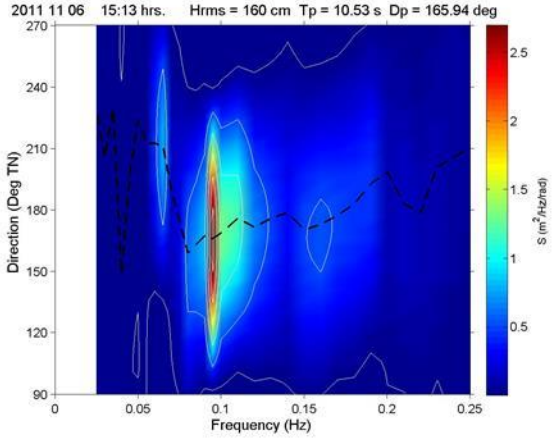
2011 11 06 15:13 hrs. Hrms = 160 cm Tp = 10.53 s Dp = 165.94 deg
Direction (Deg TN)
Frequency (Hz)
S (m²/Hz/rad)

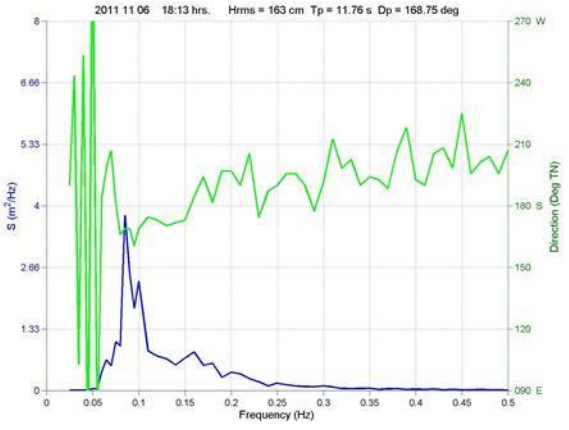
2011 11 06 18:13 hrs. Hrms = 163 cm Tp = 11.76 s Dp = 168.75 deg
S (m²/Hz)
Direction (Deg TN)
Frequency (Hz)

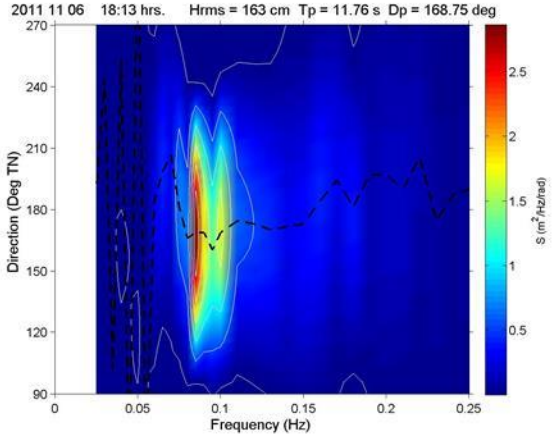
2011 11 06 18:13 hrs. Hrms = 163 cm Tp = 11.76 s Dp = 168.75 deg
Direction (Deg TN)
Frequency (Hz)
S (m²/Hz/rad)

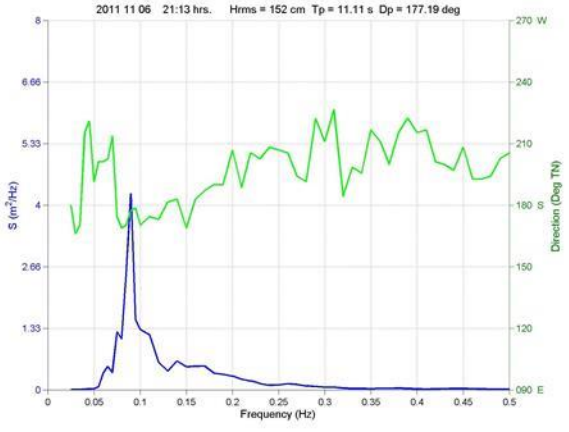
2011 11 06 21:13 hrs. Hrms = 152 cm Tp = 11.11 s Dp = 177.19 deg
S (m²/Hz)
Direction (Deg TN)
Frequency (Hz)

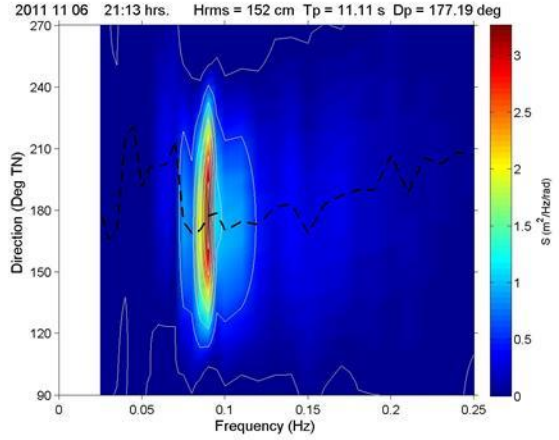
2011 11 06 21:13 hrs. Hrms = 152 cm Tp = 11.11 s Dp = 177.19 deg
Direction (Deg TN)
Frequency (Hz)
S (m²/Hz/rad)

Appendix F: Interpretation of Codes for Coastal Geological Map Legends

Dmag - Garnet-amphibolite gneiss; Dmgf - Felsic gneiss-granitoid terrain, mainly quartzo-feldspathic gneiss, some biotite gneiss; Tect - Arenaceous and argillaceous sediment, locally gravel (‘Continental terminal‘ sensu lato); Qa - Alluvial sand, silt, clay (Keta basin only); Tcq - Detrital sediment, mainly sandstone and conglomerate, undifferentiated; Tmmg - Granitoid gneiss, biotite gneiss; Gsb - Biotite (± hornblende, ± muscovite) granitoid, undifferentiated; Tpms - Mica schist (± chlorite), minor quartzite; Tpq - Quartzite, minor mica schist; Ackl - Sandstone, interbedded with shale ('Korle Lagoon Fm‘); Acks - Sandstone, thickly bedded, medium grained ('Kaneshie Fm‘); Amcs - Conglomerate, micaceous sandstone, arkose, mudstone; Bma - Amphibolite, partly of contact metamorphic origin; Bmb - Biotite gneiss, locally migmatitic, and minor biotite schist, ± garnet, ± amphibole, in parts gneissose rocks formed at periphery of granitoid plutons; Bsw - Wacke sediment dominant; Dmgq - Garnet quartzite, quartz-sericite (-garnet) schist, quartzo-feldspathic gneiss; Gsai - Biotite granite (with Archean continental signature) ('Winneba' type); Sek - Sandstone (5 formations) and interbedded shale (2 formations), undifferentiated; Ackb - Mudstone, finely laminated ('Korle Bu Fm‘); Bs - Sediment/volcaniclastic sediment, undifferentiated, locally mica schist; Bsv - volcaniclastics sediment dominant; Gvh - Horn'olende—biotite granitoid, undifferentiated; Gvhr - Hornblende-biotite granodiorite; Bsa - Argillitic/pelitic sediment dominant, ± kerogene ('graphite'); Bvi - Andesitic flow/subvolcanic rock and minor interbedded volcaniclastics; Bvm - Basaltic flow/subvolcanic rock and minor interbedded volcaniclastics; Cul - Limestone, marl, mudstone with intercalated sandy beds (includes minor Cenozoic clastic sediments in the Tano basin area); Gspx - Ultramafic and minor mafic igneous rock, undifferentiated; Gvht - Hornblende-biotite tonalite; Gvpx - Peridotite, pyroxenite, dunite, ± serpentinized; Sek - Sandstone (5 formations)

and interbedded shale (2 formations), undifferentiated; Tab - Conglomerate, mature, quartz pebble and quartzose sandstone ('Banket Fm').